THE EFFECT OF INTRAOCULAR SCATTERED LIGHT ON THE CONTRAST SENSITIVITY FUNCTION

STELLA NOELLE GRIFFITHS

Doctor of Philosophy

THE UNIVERSI

The University of Aston in Birmingham

THE EFFECT OF INTRAOCULAR SCATTERED LIGHT ON THE CONTRAST SENSITIVITY FUNCTION

Stella Noelle Griffiths

Ph.D Thesis

October 1986

SUMMARY

Intraocular light scatter is high in certain subject groups eg. the elderly, due to increased optical media turbidity, which scatters and attenuates light travelling towards the retina. This causes reduced retinal contrast especially in the presence of glare light. Such subjects have depressed Contrast Sensitivity Functions (CSF). Currently available clinical tests do not effectively reflect this visual disability. Intraocular light scatter may be quantified by measuring the CSF with and without glare light and calculating Light Scatter Factors (LSF).

To record the CSF on clinically available equipment (Nicolet CS2000), several psychophysical measurement techniques were investigated, and the 60 sec Method of Increasing Contrast was selected as the most appropriate. It was hypothesised that intraocular light scatter due to particles of different dimensions could be identified by glare sources at wide (30°) and narrow (3.5°) angles. CSFs and LSFs were determined for:

(i) Subjects in young, intermediate and old age groups.

(ii) Subjects during recovery from large amounts of induced corneal oedema.

(iii) A clinical sample of contact lens (CL) wearers with a group of matched controls.

The CSF was attenuated at all measured spatial frequencies with the intermediate and old group compared to the young group. High LSF values were found only in the old group (over 60 years). It was concluded that CSF attenuation in the intermediate group was due to reduced pupil size, media absorption and/or neural factors. In the old group, the additional factor was high intraocular light scatter levels of lenticular origin.

The rate of reduction of the LSF for the 3.5° glare angle was steeper than that for the 30° angle, following induced corneal oedema. This supported the hypothesis, as it was anticipated that epithelial oedema would recover more rapidly than stromal oedema.

CSFs and LSFs were markedly abnormal in the CL wearers. The analytical details and the value of these investigative techniques in contact lens research are discussed.

Key words: Psychophysical Technique - Contrast Sensitivity - Intraocular Light Scatter - Ageing - Corneal Oedema.

TO MY GRANDMOTHER,

JEAN ROBINSON C.B.E.

ACKNOWLEDGEMENTS

I am grateful to the following people for their help with this thesis:

Mr Neville Drasdo my supervisor, for all his help and advice at every stage. Mr Derek Barnes my associate supervisor, for his support particularly in the early days of the work. Mr Tony Sabell for assistance with the scleral lenses and Dr Christine Wright for help with the literature. To my colleagues in the Department, thank you for the useful discussions.

I want to thank all the people who willingly participated in the clinical studies and to Vision Sciences at Aston University for access to the facilities.

I am grateful to Dolland and Aitchison Ltd for the financial backing throughout, which has made this thesis possible.

Finally, my thanks to Paula Sliwinski for typing the thesis.

LIST OF CONTENTS Page

List of Tables

List of Figures

CHAPTER 1

INTRAOCULAR LIGHT SCATTER AND GLARE

1A Anatomy and Physiology of the Eye

1B Theory of Light Scattering, Turbidity and Transparency

1C Physiological Aspects of Intraocular Light Scatter

1.C.1 Cornea

1.C.2 Crystalline Lens

1D Intraocular Light Scatter in Relation to Ageing Processes

1.D.1 Cornea

1.D.2 Crystalline Lens and Cataractogenesis

1E Abnormal Intraocular Light Scatter

1.E.1 Effect of Corneal Oedema

1.E.2 Effect of Cataract

1F Clinical and in vivo Measures of Intraocular Light Scatter

1.F.1 Cornea

1.F.2 Crystalline Lens

1G Glare

1.G.1 Veiling (Disability) and Discomfort Glare

1.G.2 Relationship between Veiling Glare and Intraocular Light Scatter

1.A Anatomy and Physiology of the Eye

A complete description of the anatomy and physiology of the eye and visual system would be very complex and beyond the scope of this review. The aim of this summary is to provide a foundation for the topics covered in later sections of this project and will therefore be limited to a brief description of the human eye and the visual system.

The anatomy of the eye is represented in Fig. 1.1 and is explained in the following summary.[1,2,3]

Cornea

The cornea is the first and most powerful lens in the optical system of the eye. Production of a sharp image at the retinal receptors requires that the cornea be transparent and that it be of appropriate refractive power. The refractive index of the cornea is 1.376, which gives the average anterior central region a refractive power of 48.8D. The concave posterior surface of the cornea faces the aqueous, which has a lower refractive index (1.336), so that the refractive power of this surface is -5.8D, giving the entire cornea a refractive power of 43.0D, or about 70% of the total refractive power of the eye (see Fig 1.2).

Corneal Epithelium

The epithelium consists of five or six layers of cells. The most superficial cells are flat overlapping squamous cells, similar to superficial skin cells but lacking keratinisation. The middle layers consists of cells that become more columnar as the deeper layers are approached. The innermost (basal) layer is made up of columnar cells packed closely together. All the cells are held together by a cement substance. Also, the surfaces of the cells form processes that are fitted into corresponding indentations of adjacent cells and connected in places by attachment bodies (desmosomes).

Between the columnar epithelial cells and Bowman's membrane is a basement membrane from 60 to

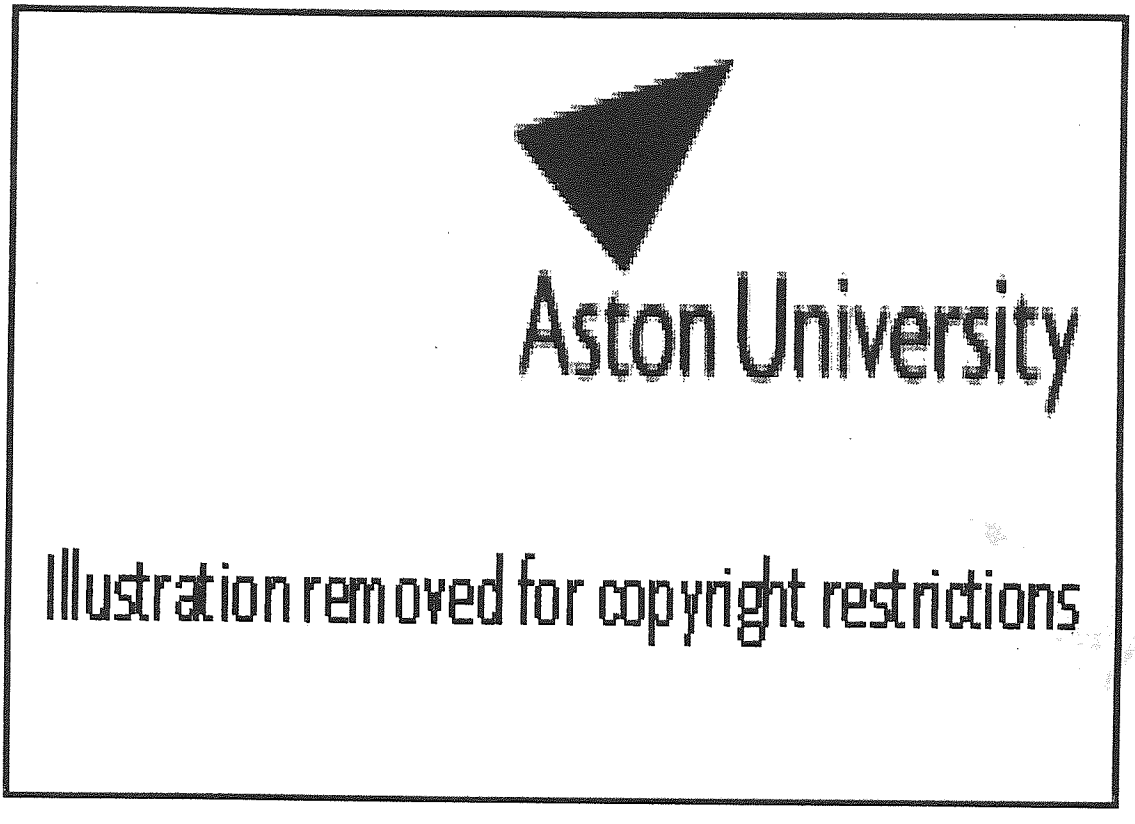
Aston University
Illustration removed for copyright restrictions

65nm thick. The basement membrane has been examined histochemically and found to be similar to other tissue basement membranes.[4] The epithelial cells form a layer of uniform thickness and regularity. The surface epithelial cells are uniform and smooth. Electron microscopy shows that the outer cell membranes of epithelial cells show the presence of microvilli[5]; these project into the tear film and may trap tear fluid, preventing drying of the epithelial cells.

Bowman's Layer or Membrane

Bowman's layer is a sheet of transparent tissue about 12μm thick, without structure as seen by light microscopy. With electron microscopy it is made of uniform fibrils, probably collagenous and running parallel to the surface. Bowman's layer is acellular, it may be considered as a modified superficial stromal layer found only in primates.

Stroma (substantia propria)

The stroma is composed of layers of collagen lamellae each of which runs the full length of the cornea; although the bundles interlace with one another, they are nearly parallel to the surface. The layered structure of the stroma makes corneal splitting, as in eye surgery, technically relatively easy. The cell bodies, called corneal corpuscles or keratocytes, are flattened so that they too are parallel to the surface, and their cell processes interface with one another. This arrangement of the fibres gives optical uniformity and transparency to the cornea. A subject discussed in detail in Section 1.C. The stroma comprises about 90% of the whole cornea.

Descemet's Membrane

Descemet's membrane is a structureless membrane by light microscopy bounding the inner surface of the stroma, it is about 10μm thick. It is considered to be the product of secretions of the endothelial cells. Electron microscopical examination shows that the anterior part of this membrane has a fine regular organisation. In tangential sections, it has a 2-dimensional lace network appearance with a

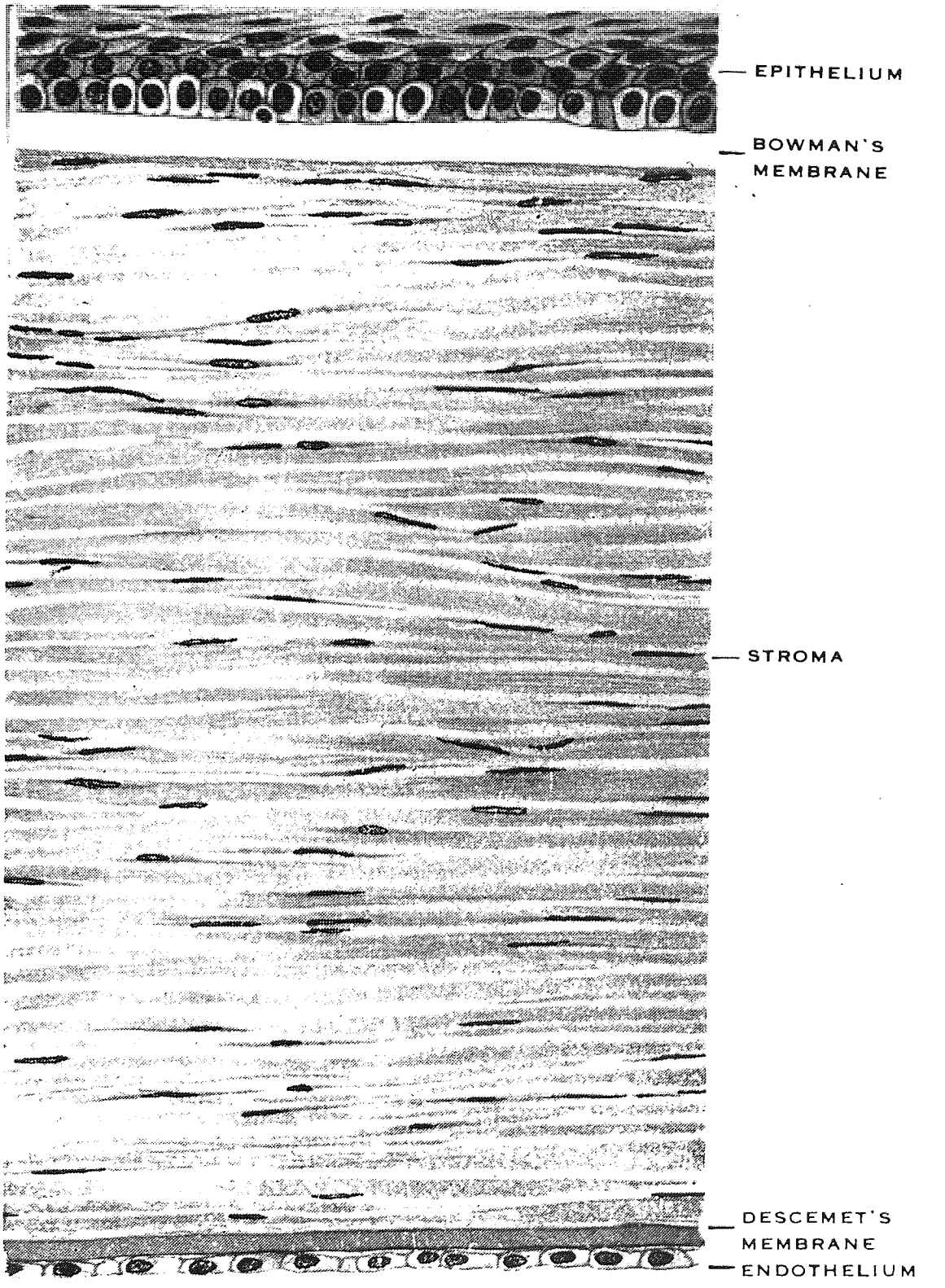

Fig. 1.2 Transverse Section of the Cornea.
After Wolff[1]

repeating hexagonal unit, seven dense nodes marking the angles; these are connected by fine filaments of equal length.[6]

Corneal Endothelium

The endothelium consists of a single thin layer of predominantly hexagonal cells which present a smooth surface to the anterior chamber. The nucleus may have an oval or a kidney shape and the cytoplasm often appears granular and vacuolated.[7] The cells are well stocked with organelles, especially mitochondria, the endoplasmic reticulum being especially prominent. Near the posterior border of this layer, the intercellular space is reduced to form a tight junction of 10nm width, this is thought to restrict the movement of substances in and out of the cornea between the endothelial cells.[8] Cells increase in size during growth of the eye and probably spread to cover damaged areas when injured. A thin polysaccharide coat on the posterior surface of the endothelium has been described.[9] In order to maintain its transparency and hydration, the cornea must be hypohydrated; an active transport system located in the endothelium has been postulated.[10] The endothelium functions as a barrier against an inflow of water and dissolved substances from the aqueous humour into the stroma, and therefore maintains the cornea in a dehydrated state.

Corneal Dehydration

When either the corneal epithelium or endothelium is damaged or a contact lens is placed on the cornea, the front surface is deprived of oxygen with a consequent reduction in aerobic glycolysis, swelling (oedema) of the epithelium and stroma follows.

Damaged to the endothelium is far more serious than epithelial damage. In the rabbit, removal of the epithelium produced an avarage increase of 200% in the corneal thickness in 24 hours, whereas, removal of the endothelium produced on increase of 500%.[11] The fact that endothelial damage results in much more corneal swelling and more rapid swelling than epithelial damage supports the premise that the endothelium is of great importance in maintaining dehydration. Harris[12] suggested that the

major cause of hydration of the cornea following endothelial damage was influx of water from the aqueous humour rather than decreased transport of water out of the cornea. Accordingly, the endothelium provides a barrier to the influx of water from the anterior chamber, and Descemet's membrane is the barrier across which outflow occurs.

A contact lens presents a barrier between the cornea and the atmosphere; and oxygen uptake by the cornea is reduced. This effect is minimised by the circulation of oxygenated tears under a contact lens. Tear exchange is at a minimum with sealed scleral lenses, and even with fenestrated sclerals, tear exchange is half of that obtained with hard corneal lenses.[13] Interference with normal metabolism due to contact lens wear produces corneal oedema with thickening and reduction in transparency. The thickening which is observed with corneal lens wear varies with individuals between 4%[14] and about 8%.[15] The increase usually takes more than 1 hr to reach after inserting a hard corneal lens and within 2 hrs of removing the lens normal thickness is recovered. It is worth noting that corneal thickening approximately equal in amount to that induced by contact lenses occurs normally during sleep, on awakening, the cornea gradually thins over a period of 1 to 2 hrs.[16]

The Aqueous

The normal aqueous humour, as it is found in the anterior chamber is a crystal clear fluid, having an osmolarity slightly higher than that of blood plasma. The chief differences between aqueous humour and blood plasma in humans are as follows: there is a very low concentration of protein in aqueous ie. 0.02mg per 100ml and a low concentration of sugar and urea. In the case of anions the concentration of bicarbonate is less than that in plama, while the concentrations of ascorbate, lactate and chloride are in excess. The concentrations of cations, such as sodium, are in excess in the aqueous. The osmotic pressure of the aqueous is higher than that of blood.

The aqueous is formed chiefly from the ciliary processes of the ciliary muscle and the fluid reaches the anterior chamber from the posterior chamber by passing between the back surface of the iris and the

anterior surface of the lens through the filtration angle and into Schlemm's canal. It leaves Schlemm's canal through aqueous veins containing both blood and aqueous. The blood aqueous barrier function is not fully understood. It is thought that small molecules such as water, sugar and urea are constantly passing in and out across the capillary beds of the ciliary processes. Such substances, therefore enter and leave the anterior chamber by diffusion. Active transport is thought to be responsible for removing other substances from the aqueous to the blood against the osmotic gradient. Aqueous humour is formed therefore by secretion and filtration, and under normal conditions the rate of production and the rate of loss from the eye are balanced so that only slight variations in intraocular pressure (IOP) occur. Any pathological condition that upsets this balance will lead to a change in IOP.

Clinically, a patient with a consistent rise in IOP above the upper normal limit is regarded as ocular hypertensive; when raised IOP is associated with visual field loss this is called glaucoma. Examination of the anterior chamber of a patient with a normal aqueous should be optically empty, and the slit-lamp beam will not be seen. Increased protein content in the aqueous as in anterior uveitis can be recognised clinically by the visibility of the slit-lamp beam as it traverses the anterior chamber. When such a light beam is seen, it is called aqueous flare. Detailed descriptions of the aqueous are available in the literature.[1,2,3]

Crystalline Lens

The lens is positioned behind the iris, refracts the light entering through the pupil and focuses it on to the retina. The function of the lens is to provide refractive power by contributing to the optical system of the eye. The lens is avascular but obtains nutrition from the surrounding fluids; the aqueous and vitreous. Glucose from these fluids provides the lens with chemical energy required to continue growth and maintain transparency. Fig 1.3 shows the lens anatomy.

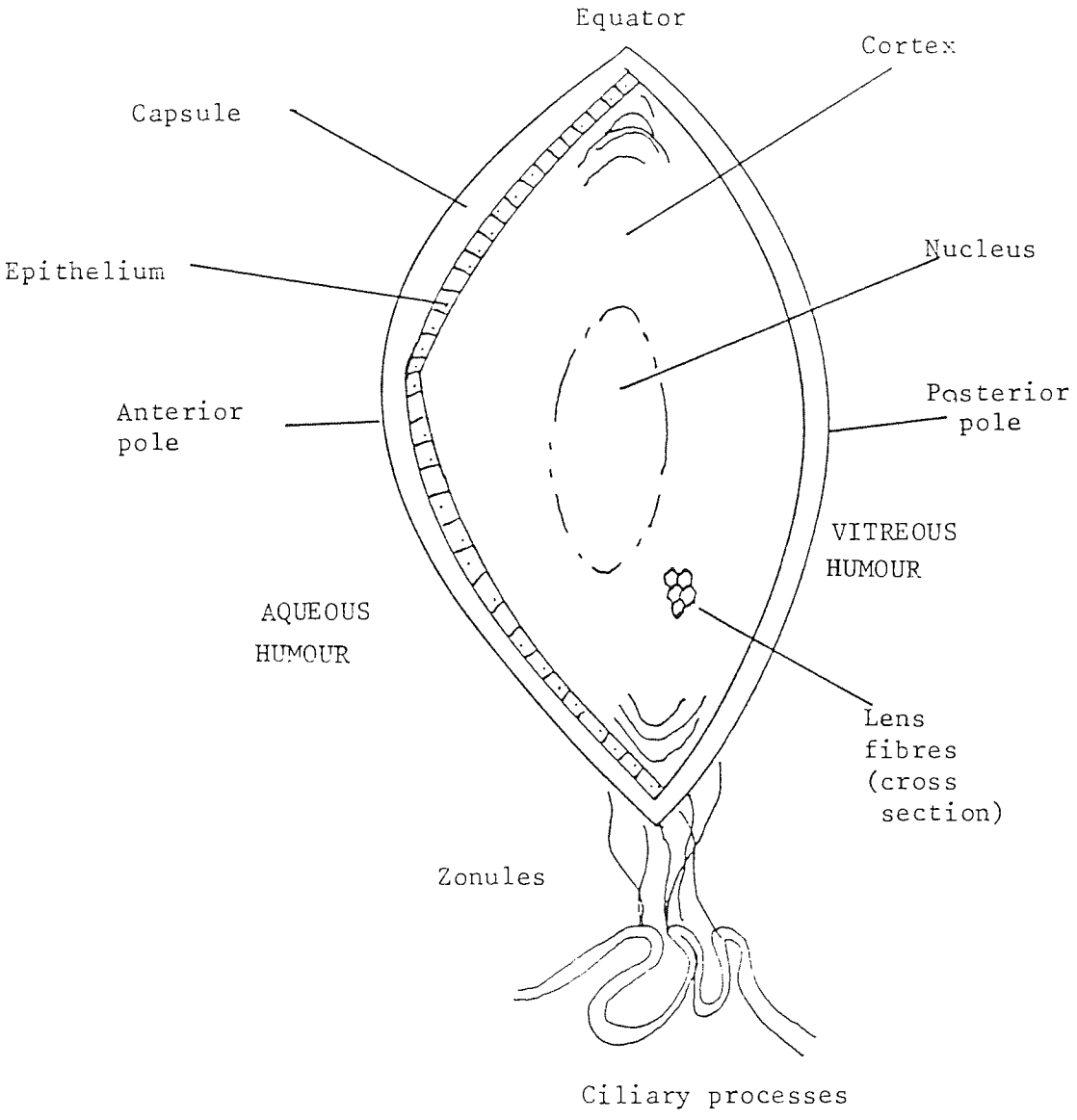

Fig. 1.3 Crystalline lens and Zonular Ligaments
After Adler[2]

Lens Capsule

An elastic capsule surrounds the lens and maintains its structural integrity. The capsule is secreted at the embryonic stage by the lens epithelium. The capsule is 2 to 20μm thick (thinnest at the poles and equator) and homogenous by light microscopy. With electron microscopy, many lamellae measuring 300 to 400nm in thickness are found, each lamellae contains fine filaments. The capsule is made up of collagen-like glycoprotein material, but is not considered to have independent metabolism, it depends on contact with lens epithelium and fibres for metabolic supplies.

Lens Epithelium

The epithelial cells of the lens are firmly attached to the anterior capsule and loosely attached to the underlying fibres, and form a monolayer. Cells are more densely packed in the equatorial areas. Most of the miotic cells are found in the pre-equatorial region. The epithelium is the area of the lens with the highest metabolic rate. Glucose and oxygen are utilised by the lens epithelium and the content of ATP and enzymes is the highest in the area. Chemical energy is needed for the epithelium to transport carbohydrates, electrolytes and amino acids into the lens. Energy is also needed for protein synthesis in the newly formed lens fibres at the lens equator. Mechanical trauma to the epithelium results in miotic stimulation; "repair" epithelial cells are elongated, resemble fibroblasts and can pile up to 10 layers thick under the lens capsule. Heaping up of epithelial cells is found in the anterior pole of the lens in many human and experimental cataracts.

Lens Fibres

The fibres make up the bulk of the lens cortex and nucleus. A rabbit lens cortex alone contains approximately 800,000 lens fibres. Each fibre, hexagonal in cross section, represents an elongated cell with a membrane. The areas in which the fibres meet anteriorly and posteriorly are the sutures of the lens. These are the two Y- shaped sutures in human lenses. The lens fibres lose their nuclei as they grow old; nuclei are found near the equator in the younger fibres. The membranes of the fibres have side digitations that result in fibres interlocking. Such a system results in the elasticity needed

for the fibres to change shape during accommodation. The spaces between the lens fibres (extracellular spaces) are very small and account for only about 5% of the lens volume. These spaces are enlarged in human and experimental cataracts. Fluid collection between the fibres and destruction of many lens fibres result in the vacuoles or clefts seen by slit lamp observation. The theory of lens transparency and cataract formation is considered in Section 1.B and 1.D.

Vitreous

The vitreous is adjacent to the lens, the zonular fibres, the pars plana of the ciliary body, the retina and the optic disc. Its shape is not only determined by the tissue surrounding it but also by its own framework, elasticity and turgescence. The structure of the vitreous is most probably maintained by a framework of branching vitrosin fibrils of collagen, in the meshes of which the watery solution of crystalloids, hyaluronic acid and soluble proteins are trapped. The concentration of residual protein is so small (0.01%) that the fibrils must be very fine, and the meshwork relatively coarse, if such a small amount of material is to form a coherent jelly. The anterior surface of the vitreous is condensed to form the hyaloid membrane, which tends to hold the lens in place after partial dislocation and also helps to prevent the escape of vitreous during cataract extraction.

Both the collagen and the mucopolyscaccharide hyaluronic acid contribute to the stability of the gel structure. The hyaluronic acid exists in the form of a variety of different sized molecules ie different degrees of polymerisation. The molecules probably exist as a randomly kinked coil, entraining relatively large quantities of water in its framework so that in solution it occupies some 1000 times the volume it occupies in the dried state. The individual molecules probably entangle with each other to form a continuous 3-dimensional network. In the vitreous, such a network stabilises the primary network formed by the vitrosin fibrils.

A clinically important structure is the posterior hyaloid membrane, and can be seen biomicroscopically after a vitreous detachment. The vitreous is important in the support it gives to

the interior of the eye and maintenance of transparency. The presence of solid fibrils in the vitreous does not impair transparency, probably because the fibrils are thin and their concentration is low. Pathological aggregates of colloidal material would cause opacities. With increasing age, the vitreous becomes more liquefied. Small opacities can form and then float up and down and can cause annoyance to a patient by getting in the line of sight. These are often called vitreous floaters (muscae volitantes).

Retina

The retina is a complex nervous structure made up of a total of 10 layers; from the vitreous to the choroid these are:

(i) Inner limiting membrane (next to vitreous)

(ii) Optic nerve fibres

(iii) Ganglion cell layer

(iv) Inner plexiform layer

(v) Inner nuclear layer

(vi) Outer plexiform layer

(vii) Outer limiting membrane

(ix) Bacillary layer

(x) Pigment epithelium (next to choroid)

The retina can thus be differentiated into a layer of receptors (layer of rods and cones), a layer of bipolar cell bodies (inner nuclear layer) and a layer of ganglion cell bodies (ganglion layer). The rods and cones are highly differentiated cells, and their orderly arrangement gives rise to a bacillary layer consisting of their outer segments; an outer nuclear layer containing their cell bodies and nuclei; and an outer plexiform layer made up of their fibres and synapses with the bipolar cells, the region of synapse between bipolar and ganglion cells is the inner plexiform layer. Two other types of nerve cell are present in the retina namely the horizontal and amacrine cells, with their bodies in the inner

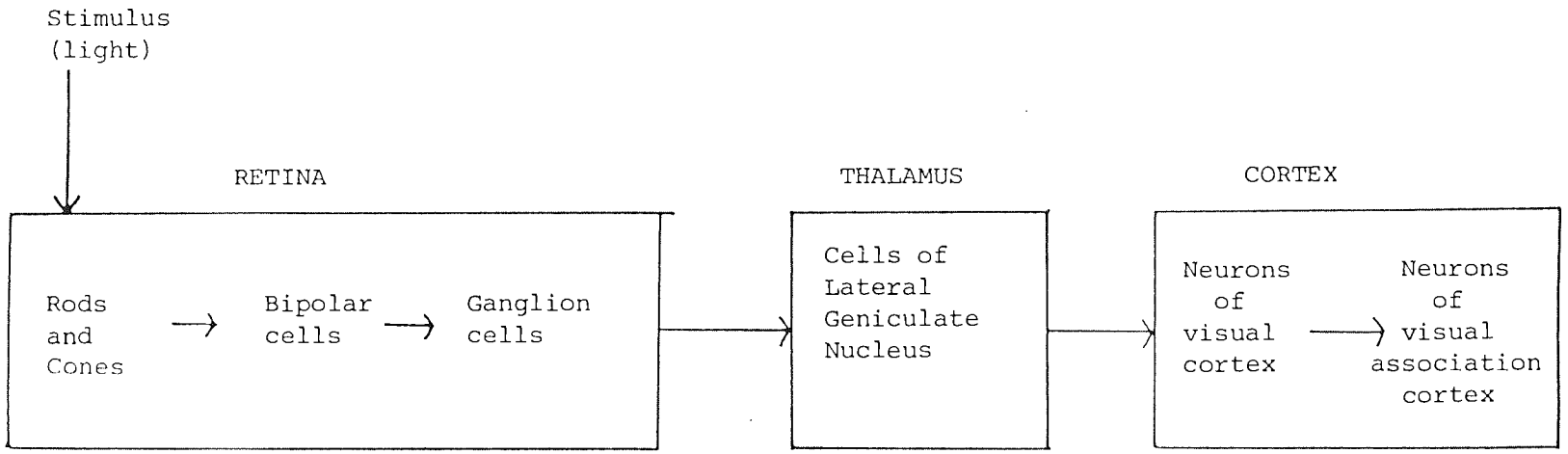

Fig. 1.4 Diagrammatic representation of the cells and neurons of the visual pathway

nuclear layer. The ramifications of their dendritic and axonal processes contribute to the outer and inner plexiform layers respectively; their largely horizontal organisations permits them to mediate connections between receptors, bipolars and ganglion cells. Besides the nerve cells there are numerous neuroglial cells giving rise to the radial fibres of Muller, which act as supporting and insulating structures, filling the intercellular spaces and possibly reducing fluctuations in the refractive index. Fig 1.4 shows the pathway of visual processing from the light stimulus reaching the rods and cones of the retina to the final destination in the visual cortex.

Apart from the possibility of some yellow pigment at the macular region, the tissue anterior to the retinal receptors is non-pigmented and does not absorb light. This region of the retina is transparent. According to the present theory of transparency, there is very little fluctuation in the refractive index over dimensions comparable with the light wavelength. Vos and Bouman[17] found experimentally that the retina may scatter as much light as the normal cornea.

In certain retinal pathologies the normally transparent retina will scatter light and will lose transparency eg retinal oedema. In a case of occlusion of a branch of the central retinal artery, a portion of the retina normally fed by the occluded arteriole has a milky grey appearance by ophthalmoscopy. This area of the retina is oedematous, the oedema fluid probably leaking from the occluded vessel. The fluid accumulates in the nerve fibre layer, thereby spreading the nerve fibres apart. Because the oedema fluid has a different index of refraction from that of the nerve fibres, the area loses transparency and scatters light. The back scattered light gives the area a milky look as compared to the surrounding retina which simply reflects back the red/orange light from the underlying choroid.

1.B Theory of Light Scattering, Turbidity and Transparency

Introduction

The eye transmits and focuses light from the environment onto the retina. For this to occur, the ocular media must be transparent, allowing light to pass through with no apparent interaction. In reality, the structure of the ocular tissues is such that the proportion of light scattered within them is at an inconsequential level in the normal young eye.[18,19] In order to understand ocular transparency and turbidity it is necessary to explain some basic physical properties of light.

Light may be considered to be propagated by means of a transverse wave motion, when light interacts with a particle (ie. light transmitted through ocular tissues or a beam of light passing through dusty air) a diopole moment is induced in the particle. This is because the particle (eg an atom, a molecule or an aggregate of molecules) in the electric field is subjected to polarization, ie the nuclei and electrons move in opposite directions. Since electromagnetic radiation such as light carries an oscillating field, the induced dipole in the particle will also oscillate. However, an oscillating dipole is a source of electromagnetic radiation, that is, the scattered light that is propagated in all directions. An observer's eye sees a shaft of light because of the sideways scattered light from each of the particles is detected. In the absence of the scattering particles the primary light beam would be invisible to the observer. This is the principle on which a slit-lamp functions. The cornea and lens can be observed because these media scatter part of an incident beam into the objective of the microscope. As the primary beam passes through the aqueous where scattering is very weak, nothing of the primary beam is normally seen.

A turbid medium is one that attenuates the light passing through it. Hence as a result of the scattering process the primary light beam loses energy and therefore grows progressively weaker as it passes through more scattering medium. The level of turbidity can serve as a characterisation of the

transparency or opacity of a scattering medium. Turbidity and transparency of any medium eg cornea and lens are related to the microscopic structure of the tissues. The essence of transparency is in the superposition of the phases of scattered waves.

A detailed rigorous and mathematical description of the theories of light scattering is beyond the scope of this section, and is inappropriate to the clinical nature of this project. The review that follows is designed to summarise in simple terms basic types of light scattering, turbidity and transparency and how it applies to the ocular tissues. Analytical and mathematical descriptions regarding light scattering can be found in textbooks ie Tanford[20] and Kerker. [21]

Interference and Superposition of Scattered Light Waves

Scattering from each particle is produced as the electric field in the incident light wave excites electrons. Each particle radiates out an electric field in synchrony with the exciting wave. To find the resultant field at any observation point in space, the radiating fields are added together. Each of the scattered wavelets will be at a different point in an oscillation cycle at any particular observation point. The resultant electric field is the superposition of each of these waves and the size of the result, depends on whether the constituent waves interfere constructively or destructively with one another. The phase of each wave is directly proportional to the position of the scattering particle; the difference in phase between waves depends on the spacings of the scattering particles in comparison to the wavelength of light.

If two scattering particles are spaced by distances comparable to the wavelength of light, the two scattered waves may be 180° out of phase and the waves will then cancel each other out giving no scattered light at the observation point (see Fig 1.5). Conversely, if two scattering particles are spaced by distances small compared to the light wavelength, the phases of the two waves will be nearly the same and the scattered electric field will have an amplitude twice as large as the amplitude of each individually. ie maximum light scattering (see Fig 1.6). The final summation of all scattered waves

Fig. 1.5 Destructive interference of waves

Top wave is 180^{o} out of phase with 2nd wave. Resultant of both waves is complete cancellation.

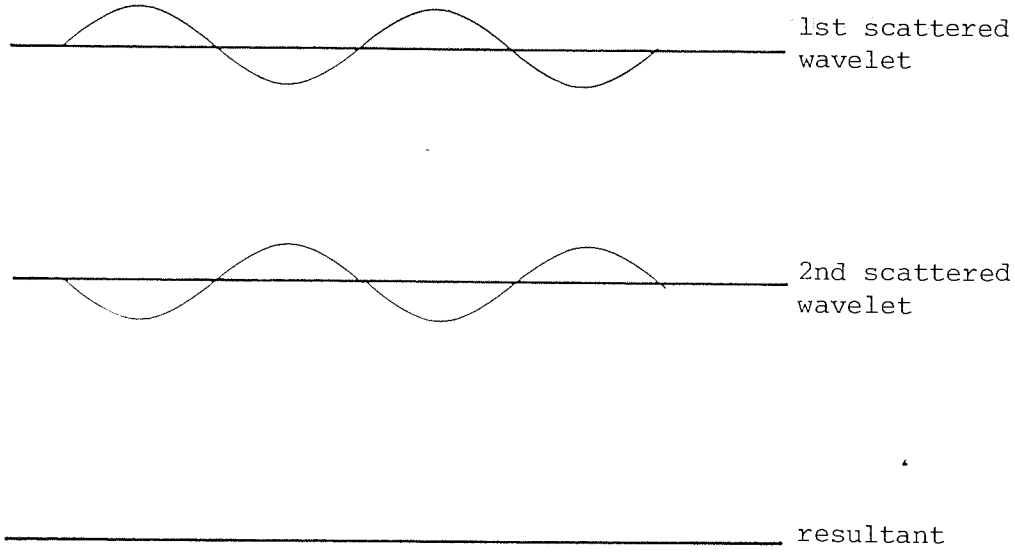

Fig. 1.6. Constructive interference of waves

Top and middle waves are in phase. Resultant wave is summation of both and twice as large in amplitude as each individually.

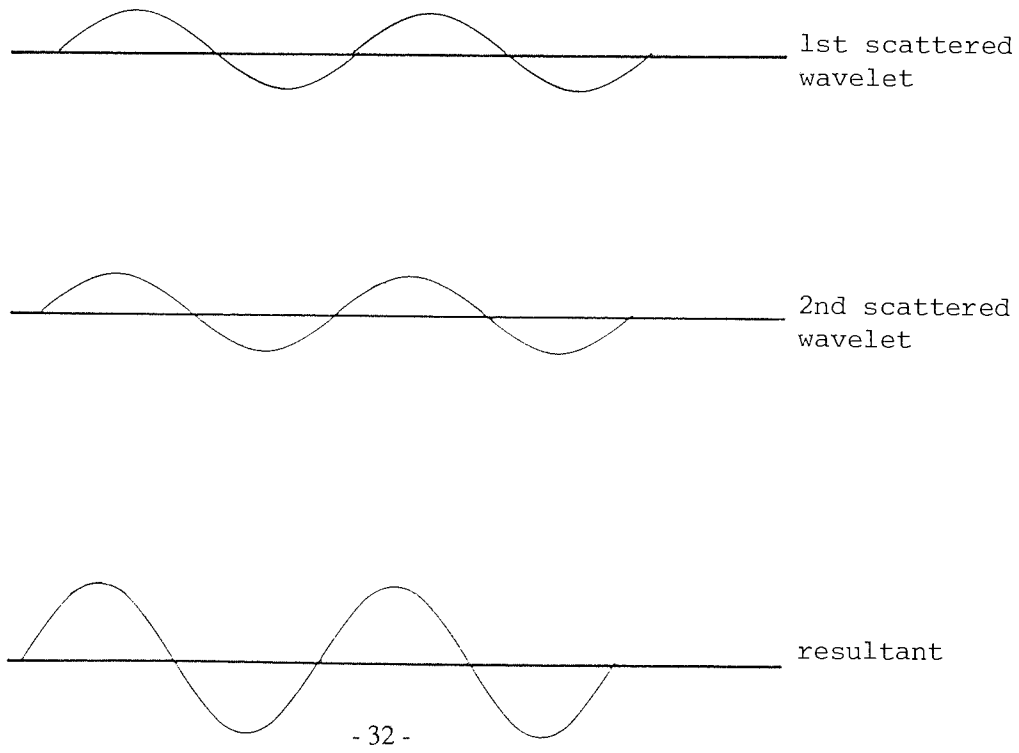

will depend on the relative positions of the particles and the light wavelength. The intensity of scattered light is proportional to the square of the total electric field. In the two examples described, scattered intensity can be four times the intensity of light scattered from each particle, or it can be zero depending on the phase of the individual waves.

Einstein[22] (1910) and Debye[23] (1944) recognised that the question of transparency and turbidity could be regarded as due to fluctuations in density (ie concentration). Mathematical techniques were developed to describe particle distributions that ranged continuously from the perfectly random eg gases to the perfectly ordered eg crystals including quasi-random distributions. They concluded that only a limited degree of particle correlation was needed to produce transparency. Furthermore, the light scattering theories show that when light is scattered by a density fluctuation, only those Fourier components whose wavelength is larger than half the light wavelengths contribute to scattering. Thus if a medium contains periodic fluctuations in density which have wavelength smaller than half the light wavelength, these will not contribute to light scattering.

With a medium which is said to have independent scatterers eg gases, there is no correlation in the relative positions of any of the scattering particles. However, if the density of the particles is increased to the point where the particles are comparable in size to the light wavelength, then some scattering may occur. In contrast to the random position of gas molecules within a scattering volume, the atoms in a crystal are rigidly fixed in a geometric array (lattice). Since the wavelength of light is much larger than the individual scatterers (atoms) there are always a pair of atoms (equal scatterers) which scatter out of phase from the point of view of the observer (or the detector) at any particular scattering angle. Thus the destructive interference of a pair of scatterers is complete and no scattered light will be observed ie transparency results.

Scattering from pure liquids is intermediate between crystals and gases. A pair of small volume elements (ie smaller than $\lambda/20$) would be independent scatterers that are out of phase, resulting in

destructive interference. However, since liquids are not orderly, the packing of particles in each member of a pair of volume elements may not be the same, therefore, the intensity of the scattered light from volume element (A) may be different from volume element (B); destructive interference is not complete as a consequence, and some scattering will occur.

As regards the tissues of the eye, transparency of the cornea is due to an imperfect lattice arrangement, similar to a crystal. Perfect lattice periodicy is not needed theoretically, nor is it found experimentally[24] in order that the cornea is still essentially transparent. The lens is less transparent than the cornea; but in the young eye is generally regarded as a liquid in terms of its light scattering properties. The scattering molecules are not in a lattice arrangement, they produce little scattering because there are many particles within one wavelength of light and the density changes little from one region to another. The following sections of this chapter deal in detail with the changes in transparency of the ocular tissues; which may be explained theoretically by the above principles.

I.C Physiological Aspects of Intraocular Light Scatter

I.C.1 Cornea

Section 1.A described the anatomy of the cornea and should be referred to for the background to this description of corneal transparency.

Corneal Epithelium

The cells of the corneal epithelium are held tightly together by desmosomes resulting in minimal spacing. There is normally only slight variation in refractive index between and within these cells. As a consequence, the epithelium scatters almost no light and transmits light as would a fluid. (see Section 1.B) Clinically, this can be confirmed by looking at the epithelial layer in the slit lamp. If a drop of fluorescein is added to the tear film, the optically empty layer between the green tears and the most anterior portion of the stroma is the epithelium.

Stroma

The stroma constitutes 90% of corneal thickness and gives the cornea its strength. It is remarkable for its regular structure and the absence of blood vessels, the two basic features upon which transparency rests. The stroma consists of about 200 lamellae of collagen fibrils (n = 1.555) embedded in a matrix of mucopolysaccharides (n = 1.345). The fibril diameters are of a regular size at any given depth in the stroma; but they vary between an average of 19nm in the anterior layers and 34nm in the posterior layers in man.[25]

In 1957, Maurice[26] produced an analysis of the transparency of the corneal stroma. Electron micrographs had already revealed the long fibres of collagen surrounded by mucopolysaccharide.[24] Maurice calculated that if each collagen fibre scattered light independently of any other fibres, more than 90% of incident light would be scattered, hence the stroma would be opaque. In order to account

for stromal transparency, it was necessary to take into account phases of waves scattered from each fibre. To this end, Maurice considered the position of each collagen fibre as being on a perfect rectangular lattice, similar to a crystal. (see Section 1.B) If the fibres were so arranged, the position of each particle would be precisely known, and the relative phases of each of the scattered waves could be computed; as could the sum of the scattered fields and the intensity. When Maurice carried out this calculation, it was concluded that the scattered light intensity would be essentially zero in all directions, if each collagen fibre was spaced from the the next by a distance equivalent to smaller than the light wavelength, (see Fig 1.7).

Goldman and Benedek[24] observed that the collagen fibres of the shark stroma were arranged in complete disorder, their axes being randomly orientated in every direction. If the fibres were to be treated as independent scatterers, the shark cornea would be opaque. Clearly, even in this disordered array, the phase relations of scattered waves substantially reduced the intensity of scattered light. Hart and Farrell[27] computed detailed probability distribution functions for the relative positions of fibres taken from photographs of corneal stroma. They concluded that the position of pairs of collagen fibres remained correlated only over two near neighbours at most, ie far from a perfect lattice, but their precise mathematical summations of the phases of waves scattered by such a partially ordered array was in good agreement both in magnitude and wavelength dependence with that found experimentally. Benedek[28] simplified these complex mathematical results obtaining similar conclusions.

In 1971 Feuk and McQueen[29] following work from earlier studies[30] examined the angular dependence of light scattered from normal rabbit corneas, they estimated that the loss of intensity of the primary beam on passing through the cornea was about 10% of incident intensity. Hence clinically, the stroma can be seen in the beam of a slit-lamp. The authors further showed a decrease in light scattered with increasing scattering angle. Feuk and McQueen's[29] work is further examined concerning oedema in Section 1.E.1.

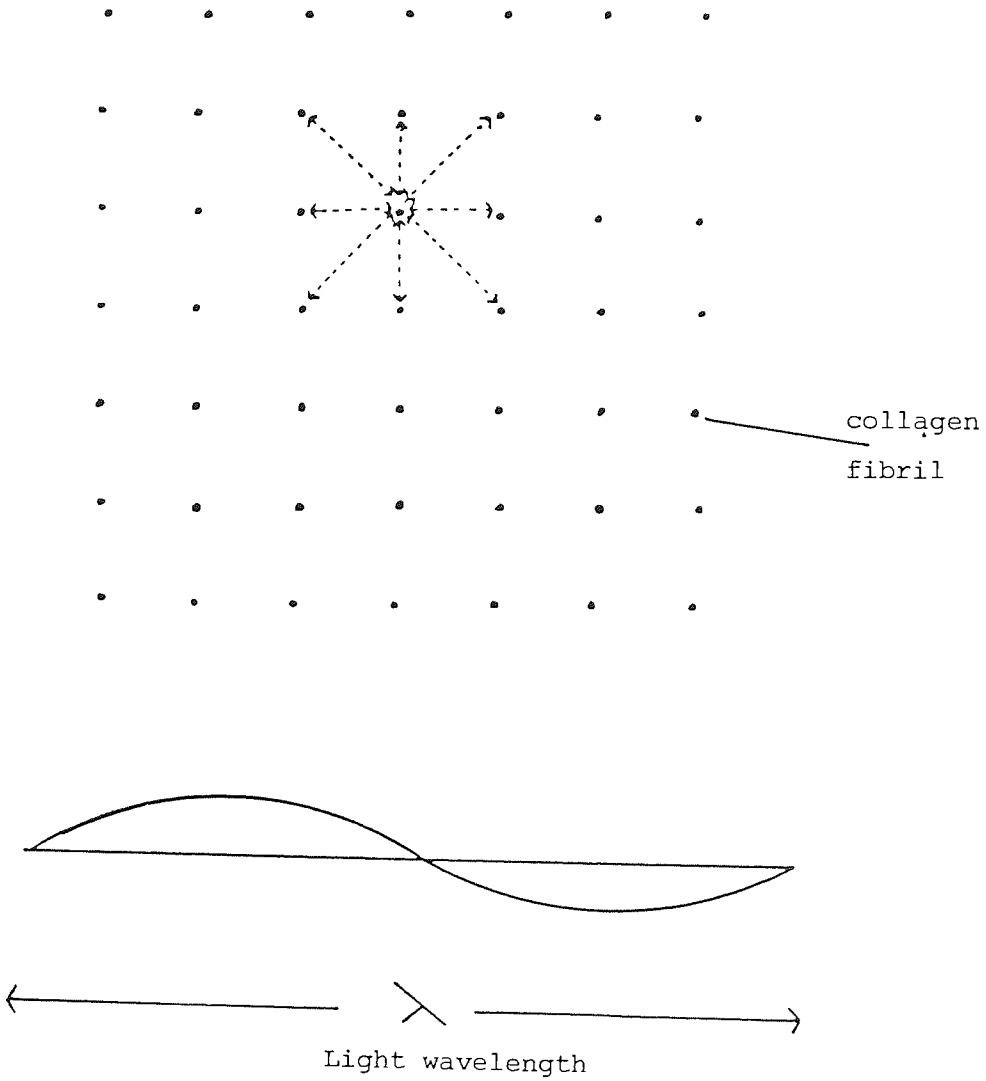

Fig. 1.7 Cross-sectional view of lattice arrangement of collagen fibrils as proposed by Maurice[26] along with the wavelength of light for comparison

McCally and Farrell[31] following work by Lindstrom, Feuk and Tengroth[32] examined normal rabbit cornea with a slit lamp and recorded the non-scattering epithelium, the stroma which scatters light relatively uniformly, and the bright band of the endothelium. They also measured scattering vs depth into the cornea mounted in Ringers solution. By use of a slit-lamp, photocell and X-Y recorder, at a series of scattering angles between 20° -145°, as the scattering angle increase, they found that the amount of light scattered decreased. It was concluded that the stromal region accounts for more than 60% of total scattering over the range of angles studied. Lindstrom et al[32] had recorded greater than 70% of scattered light from the stromal region. Endothelial light scattering properties have never been considered in isolation; only as part of the total cornea. However, the clear visibility of the endothelium in a slit-lamp beam has been commented on.[30]

In conclusion, the research cited in this section indicates that the corneal stroma is responsible for the vast majority of light scattering from the cornea. However, all the studies considered have been theoretical and/or animal research conducted in vitro. What conclusions may be drawn regarding the human in vivo condition? And what clinical considerations should be accounted for? It is well known that the physiological properties of the cornea changed rapidly in excised eyes, hence it is essential to consider the in vivo situation. Section 1.F.1 details research carried out in this area along with clinical considerations.

1.C.2 Crystalline Lens

The structure of the crystalline lens is such that more light is scattered in the lens than in the cornea. This section considers aspects of light scatter in the 'young' lens and discusses relevant research (human and animal) completed in the area. Theoretical considerations have been discussed in Section 1.B and a brief review of the anatomy in Section 1.A.

Lens Membranes

Simpson[33] attributed ocular haloes to the diffraction of light by the fibre cells of the lens which are aligned geometrically. With the use of lasers, sharp diffraction patterns were demonstrated from thin sections of bovine lenses.[34] The calculations made from laser diffraction patterns corresponded well to the membrane-to-membrane distances in fibre cells observable in electron micrographs. By the use of polarised and unpolarised light, membranes causing diffraction were shown to demonstrate only periodic density fluctuations and no optical anisotropy. The diffraction patterns were found to become progressively weaker when proceding from the cortical region to the nucleus. Philipson[35] produced similar diffraction patterns using thin sections of human lenses and calculated that the spacings from such patterns corresponded well to the thickness of cortical fibre cells ie about 7μm. More recent studies[36,37] showed that the intensity of lens diffraction patterns increased with cold cataract and salt cataract fomation in calf lenses, although the positions of the diffraction spots did not change. Scanning electron microscopic observations showed that in these cataracts, patches occured on the surface of the cell membrane which increased the refractive index fluctuation and therefore could account for the increase in intensity of the diffracted laser beam.

In conclusion, observations of the studies of diffraction patterns from human and animal lenses suggest that diffraction in the lens is derived from membrane sites. Fig 1.8 demonstrates the principle of lens diffraction.

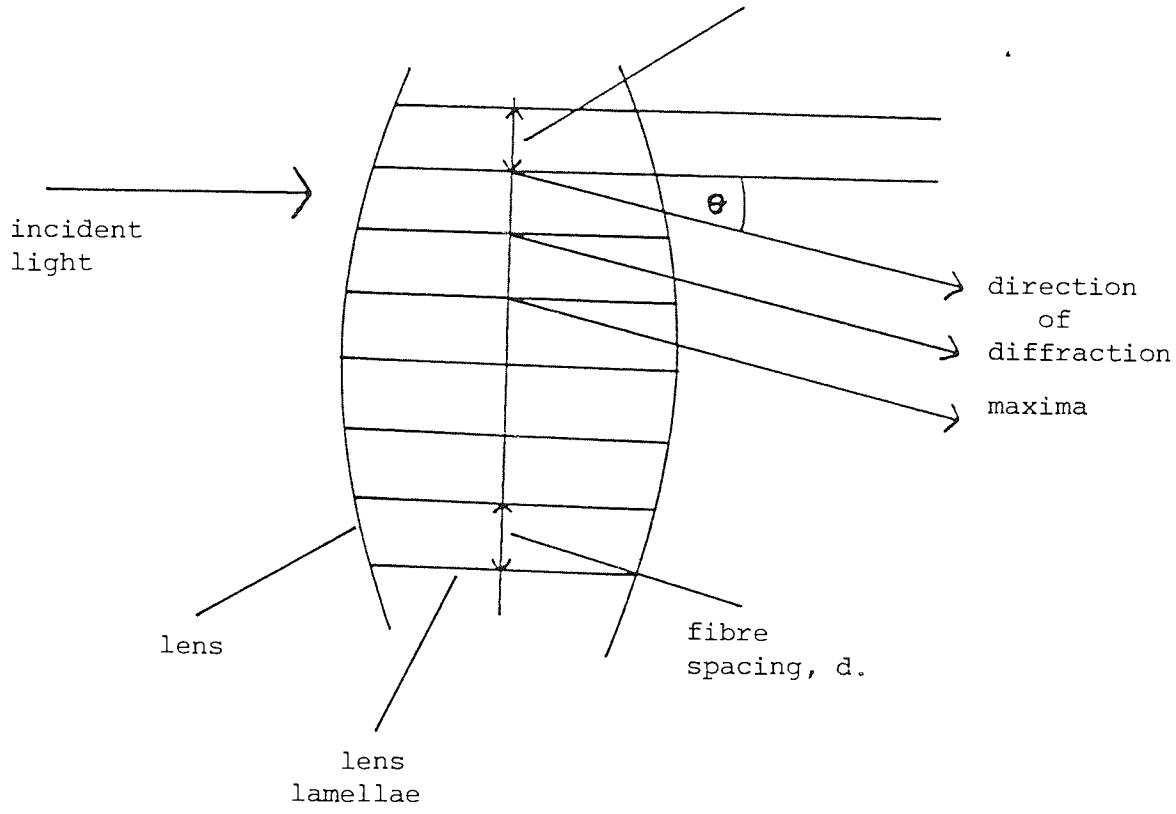

$$d \sin \theta = \lambda \quad \text{(1st order diffraction)}$$

Fig. 1.8. Lamellae of lens acting as a diffraction grating. d represents the spacing between the lamellae, θ the angle between diffracted and incident waves, λ is the light wavelength. After Simpson[33]

Lens Cytoplasm

Trokel[38] proposed the first theory of lens transparency by studying the tissue cultured lenses of albino rabbits. Absorption and scattering of light was measured with spectrophotometers. The major conclusions were as follows; the reduction in intensity of the transmitted beam (visible spectrum) was due to light scattering. Back scattering from the lens increased with age. The soluble proteins comprising most of the interior of lens fibres acted as small particles scattering light. Trokel calculated the turbidity of the normal rabbit lens assuming the lens proteins were independent scatterers and found that 69% of incident light would be scattered and only 31% transmitted. Trokel therefore concluded that a paracrystalline state with a high degree of spatial order was necessary in lens proteins in the intact fibres to explain transparency. Philipson[39] reached the same conclusion regarding a relatively even protein distribution within lens fibres accounting for transparency.

From Section 1.B it may be concluded that turbidity is due to fluctuations in lens density (ie concentration) over spatial domains comparable to the light wavelength. There are two contributions to density fluctuations.[40]

(i) fluctuations in refractive index

(ii) fluctuations in optical anisotropy

(i) Fluctuations in Refractive Index

Fluctuations in refractive index occur from the fact that solvent and solute molecules have different densities. The thermal motion of the molecules makes these fluctuations random. If the solvent molecules are small compared to the light wavelength, little light scattering will occur and the lens is transparent. When the size of high molecular weight (HMW) proteins becomes very large, comparable to the light wavelength or larger, the scattering intensity decreases with scattering angle and particles of this size in dilute solution may be treated by the 1908 Mie Theory[41] of scattering. Benedek[28] predicted an increase in turbidity with an increase in HMW proteins.

Bettelheim and Siew[42] used a condensed-phase model of light scattering namely, the Debye and Bueche theory[43] to calculated turbidity in normal lens cytoplasm. They showed that both the size of HMW proteins and interprotein seperations were important when considering turbidity. Hence both an increase in the size and number of HMW proteins and a dilution of the interparticle distances so that the order of the light wavelength is reached, can increase turbidity. Another process that occurs in the normal lens and leads to an increase in turbidity is syneresis,[44] this is the process where hydrated molecules and aggregates exude water into the immediate environment, hence aggregates will acquire a higher refractive index and the surrounding a lower refractive index. The increase in light scattered from lens cytoplasm has been shown to be proportional to the increase in refractive index difference.

(ii) Fluctuations in Optical Anisotropy

Extensive studies carried out by Bettelheim and associates[45,46] considered another aspect of normal lens scattering, namely, optical anisotropy, where the refractive index is a function of orientation. The optical anisotropy of a body can be measured by its birefringence (ie double refraction) and this can be recorded by the use of polarisation. A body with optical anisotropy has 2 refractive indices in 2 mutually perpendicular directions, both of which are perpendicular to the propagation of light in the sample. The total birefringence of an optically anisotropic body will be a sum of 'form' and 'intrisic' birefringence. The total birefringence of the lens was found to be very small, of the order of 10^{-6} to 10^{-7}. Form birefringence was estimated in the order of 10^{-4}. Further studies applying mathematical and theoretical calculations and studies on the polarisation patterns of excised human lenses concluded that the minimal total birefringence of the lens was due to cancellation of intrisic birefringence by form birefringence. This must be provided by the onion-like layers of fibre cells that make up the lens. Any disturbance in the delicate balance between form and intrinsic birefringence will inevitably lead to turbidity.

Wavelength Dependence of Normal Lens Light Scattering

Considering normal light scattering from lens cytoplasm, it is generally thought that the proportion of light scattered is directly proportional to the inverse 4th power of the light wavelength a type of Rayleigh scattering called the Mie (Dilute solutions) theory.[41] However, Hemenger[47] using the data of several previous studies of light transmission through lenses[48,49,50] concluded that the light scattered was proportional to the inverse 2nd power of the wavelength.

The most recent publication on this subject is that of Bettelheim and Siew[51] who conducted a comparison, based on theoretical calculations to predict how light scattering intensity would change with changes in lens density. They concluded that their Random Fluctuation Theory provides a description that is in agreement with observed behaviour both in the 'dilute solution' and in the 'gel' range of light scattering; and that the Random Fluctuation Theory should be applied to mathematical/ theoretical considerations of light scattering rather than approximations arising from the application of the 2 other light scattering behaviour theories. Further investigations regarding the theoretical considerations of lens light scattering can be found in full from the references cited in this Section.

In summary, transparency of the normal lens is accounted for by 3 factors:

(1) Relative absence of HMW aggregates

(2) A degree of hydration of supramolecular aggregates that minimises the refractive index between them and their surroundings.

(3) Very low amounts of optical anisotropy fluctuations due to the opposite effects of intrinsic and form birefringences.

Consequently, any process leading to changes in the above conditions will initiate opacity and cataract formation.

Lens Fluorescence in the 'Young' Eye

When light is absorbed by a molecule it is converted from a resting state into an excited state ie there is an increase in the level of rotational and vibrational energy. When a photon is absorbed, an obital electron is raised from its ground state, any remaining energy can increase the vibrational state of the molecule. Return to the ground state (de-excitation) can occur by molecular collision (dissipation as heat) or by a photon of light being re-emitted (at longer wavelength) resulting in fluorescence as the molecule returns from the excited to the ground state. Fluorescence is independent of the wavelength of the absorbed light.

The proteins of the lens are endowed with an intrinsic Ultra-Violet (UV) fluorescence because they contain the aromatic amino acids phenylalanine, tyrosine and tryptophan. Phenylalanine has the lowest fluorescence quantum yield and tryptophan the greatest.[52] Fluorescence spectroscopy on the intact human lens demonstrates an intrinsic protein fluorescence due to tryptophan with a maximum at 332 $\pm$ 2nm and a band width of approximately 47nm, (see Fig 1.9). Tryptophan masks the fluorescence effect of the other fluorescent lens compounds.

It is generally accepted that the yellow pigmentation in the lens serves as an intraocular filter for blue light[53,54] and that the yellow colour reduces the effects of chromatic aberration. These pigments protect the underlying vitreous and retina from UV radiation by absorbing most of the UV (longer than 295 nm) transmitted by the cornea. In addition to the fluorescence due to tryptophan, these pigments contain one or more fluorescent compounds called fluorogens with activations wavelengths of approximately 340 to 360nm and 420 to 435 nm and emission maxima at 420 to 440 nm and 500 to 520 nm respectively.[55,56] This type of fluorescence is present in the soluble HMW proteins and increases with age.

Clinically, the phenomenom of lens fluorescence has been utilised by ophthalmic surgeons in estimating the amount of lens matter remaining in an eye following extracapsular cataract extraction.

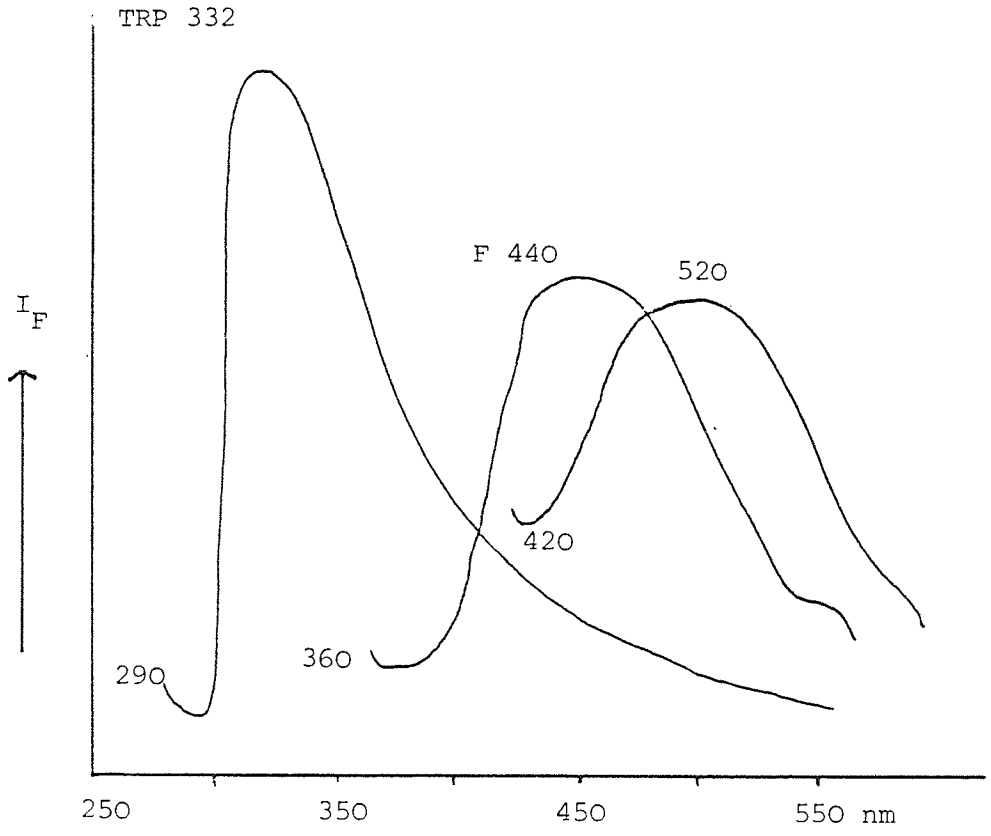

Fig. 1.9 Fluorescence spectra of a normal human lens showing TRP 332 fluorescence and 440 nm fluorescence (FL440). Also demonstrated in 2nd spectral region with 420 nm excitation resulting in 520 nm emission due to a 2nd fluorescent region that develops with age. After Lerman[52]

During such a procedure lens proteins may leak into the interior of the eye. By the use of a UV light and a darkened operating theatre it is possible to see the fluorescent lens matter within the eye. The increase of lens fluorescence with ageing will be considered in Section 1.D.2.

1.D Intraocular Light Scatter in Relation to Ageing Processes

1.D.1 Cornea

The optical properties of the cornea can be observed in the beam of a slit lamp. As age advances the normal cornea scatters more and more light,[19,57] up to about 1% at the age of 80 years (see Fig 1.10), although 10% scattered has been cited from animal studies[29] Boetter and Woltner[58] showed that the spectral transmissivity dropped with age (see Fig 1.11) whether or not the increase in light scatter and decrease in transmissivity are connected, is still a subject of controversy.

The hydration of the cornea is higher than the sclera and changes in the water content alter the refractive index of both tissues.[59] Laing, Sandstom and Leibowitz[60] examined the endothelial mosaic with a specular microscope. In young subjects, the cells in this unicellular layer are approximately equal in size and normally distributed around a mean of about 20μm. Their size increases to 30μm at age 70 years. In order for this to happen, either the cornea has increased hydration or, if there is no change in tissue volume, there must be cell loss. The regular hexagonal shape of the young cells is replaced by more irregular units in the old, this could cause on increase in scatter.[61]

The density of the corneal stroma increases with age. This too, may increase light scatter and slow down protein transport through the cornea.[62] This is accompanied by a reduction in permeability to much smaller ions. The increase in stromal density is preceded by a rise in corneal fluorescence.[63] The fluorogen pteridine has been identified in the cornea, and Klangs curve (see Fig 1.12) expresses corneal fluorescence in terms of sensory (luminance) units rather than in those of quanta. Weale[61] notes that in vivo measurements of corneal fluorescence may be contaminated by lenticular fluorescence. With increasing age, is increasing cholesterol content, both for the sclera and the cornea.[64] Corneal lipids have been studied with reference to arcus senilis, a fatty light scattering annulus on the inner side of the limbus. It has been found to be strongly associated with serum

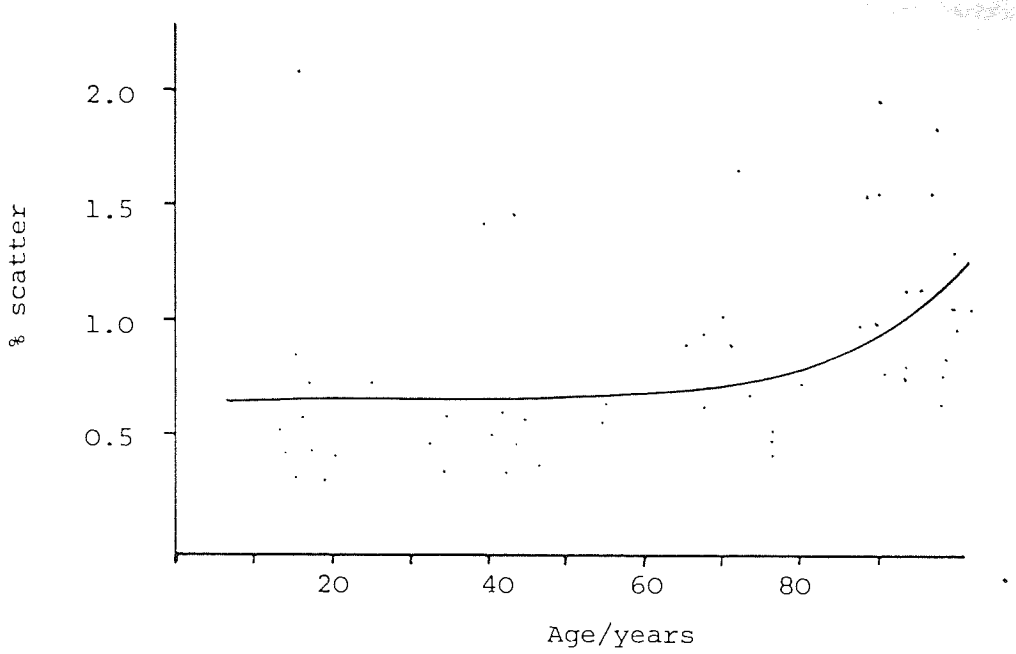

Fig. 1.10 Relative amount of light back scattered by the human cornea as a function of age. After Allen and Vos[19]

Fig. 1.11 Percent transmittance of the cornea. After Boettner and Woltner[58]

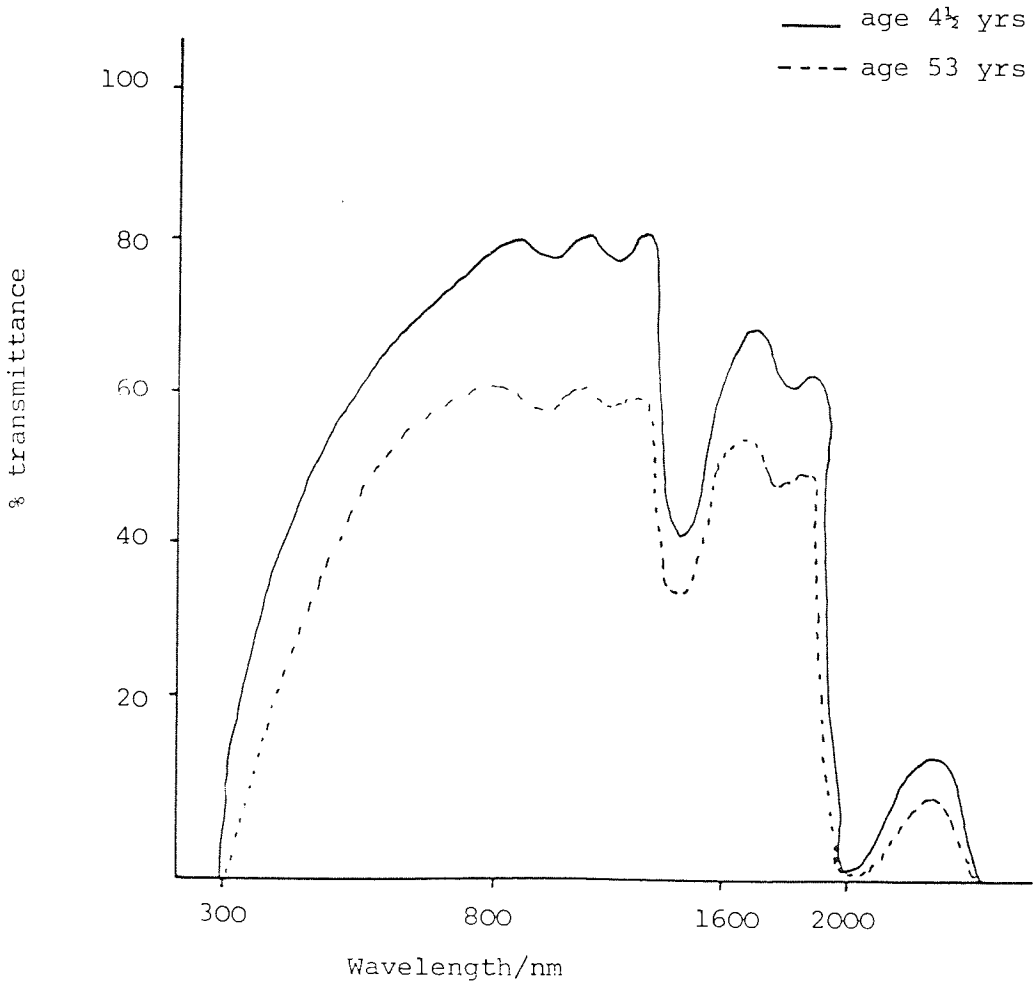

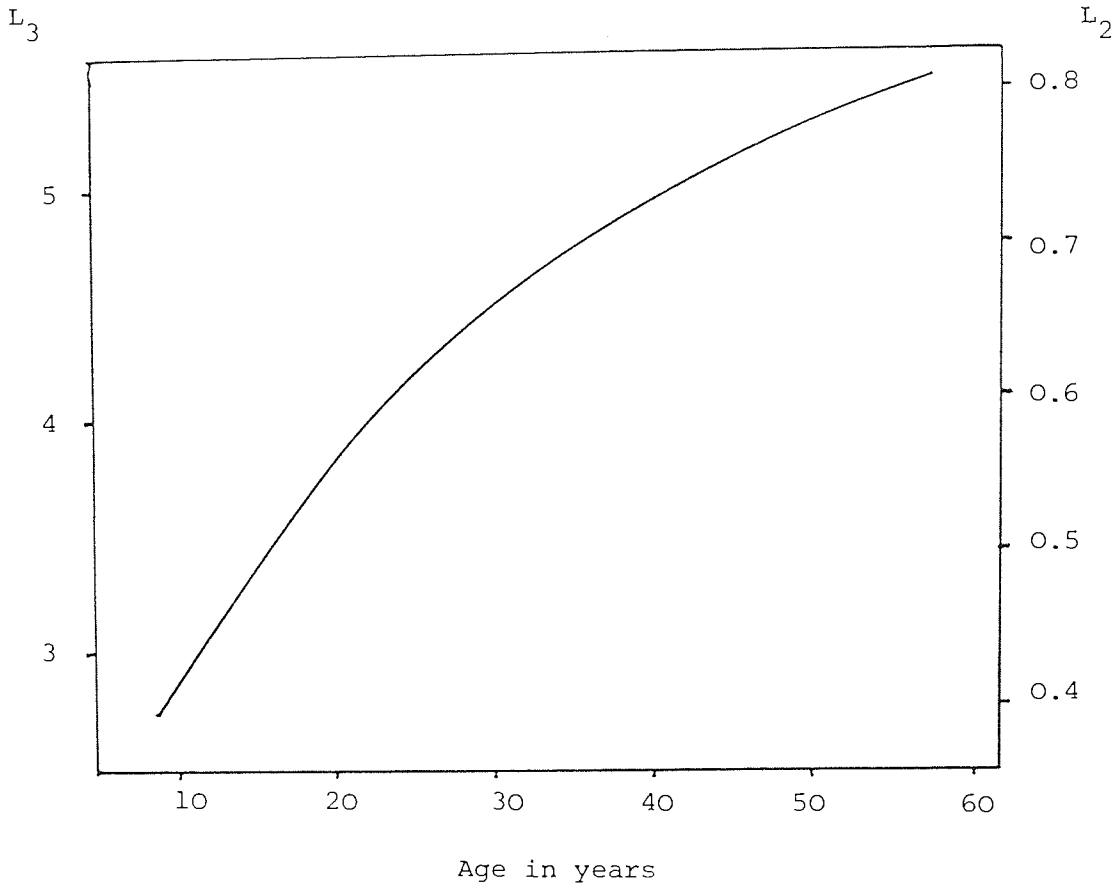

Fig. 1.12 Fluorescence of the Human Cornea

The same curve describes results obtained with green (L_2) and with violet (L_3) radiation; hence only one flurogen is likely to be involved. After Klang[63]

cholesterol and in pronounced form, it is found in those suffering from hypercholesterolaemia.[64] However although McAndrew and Ogstom[65] found the typical increase in arcus with age, they found no statistically significant difference between healthy and post cardiac-infarction patients matched for age. The association of cholesterol with the presence of arcus is still in much dispute.

Clinical studies of corneal light scattering are considered in Section 1.F.1. However, two studies deserve mention at this point due to their specific references to ageing. The work of Allen and Vos[19] shown in Fig 1.10, examines the increase in back scattered light from the in vivo human cornea as a function of age, up to 1% of light is back scattered at age 80. Olsen[66] using similar techniques also found an increase in back scatter with age and concluded that it was due to the increasing irregularity of collagen fibril spacing with ageing.

1.D.2 Crystalline Lens and Cataractogenesis

A continuation of the ageing process is eventually likely to lead to the production of cataract. There is a very fine dividing line between increased physiological scattering with age and actual cataract formation. Cinotti and Patti[67] estimated that 65% of the normal population in the age group 50-59 years would have some form of early cataract. (see Table 1.1) Wolf[68] and Wolf and Gardiner[18] found that with advancing age and therefore with cataract development, glare sensitivity increased as did the amount of light back scattered from the lens, both these effects are due to increased intraocular light scattering. From the patient's point of view, the major complaints are of a veil or fog that interferes with clear vision, and dazzle from bright lights. The first effect is due to decreased luminance transmission and reduced contrast sensitivity,[69] the second is due to increased light scattering increasing glare susceptibility. In more severe cases, visual acuity is obviously also effected. Section 1.C.2 summarised the factors that accounted for the initiation of lens opacity and cataract, the 2 main causes were:

(1) The presence of HMW aggregates

(2) An increase in refractive index between supramolecular aggregates and their surroundings (Syneresis)

This Section will discuss in more detail the factors influencing lens aging and cataractogenesis. While Section 1.E.2 describes clinical investigations on this subject.

(1) HMW Aggregates

Goldmann[70] measured the increased light back scattered by the lens in vivo and attrributed this to aggregated proteins about to form water insoluble particles. The fact that HMW protein aggregates increase with age in bovine and human lenses is widely documented.[71,72,73] (see Fig 1.13). The insoluble protein fraction of the lens also increases with age and it is proposed that HMW protein is

Age Group (yrs)	40-49	50-59	60-69	70-70	80-89
	Percentage of eyes				
Anterior subcapsular vacuoles	26.6	27.6	22.7	36.3	16.0
Cortical Spots/ spokes	0	6.9	24.4	25.3	72.0
Posterior Subcapsular opacities	26.7	20.7	17.6	20.9	12.0
Nuclear sclerosis	3.3	10.3	10.1	26.4	32.0
Clear Lenses	36.7	41.4	16.8	8.8	0

Table1.1 Most Common Changes in 327 Eyes as a Function of Age.

After Cinotti and Patti[67]

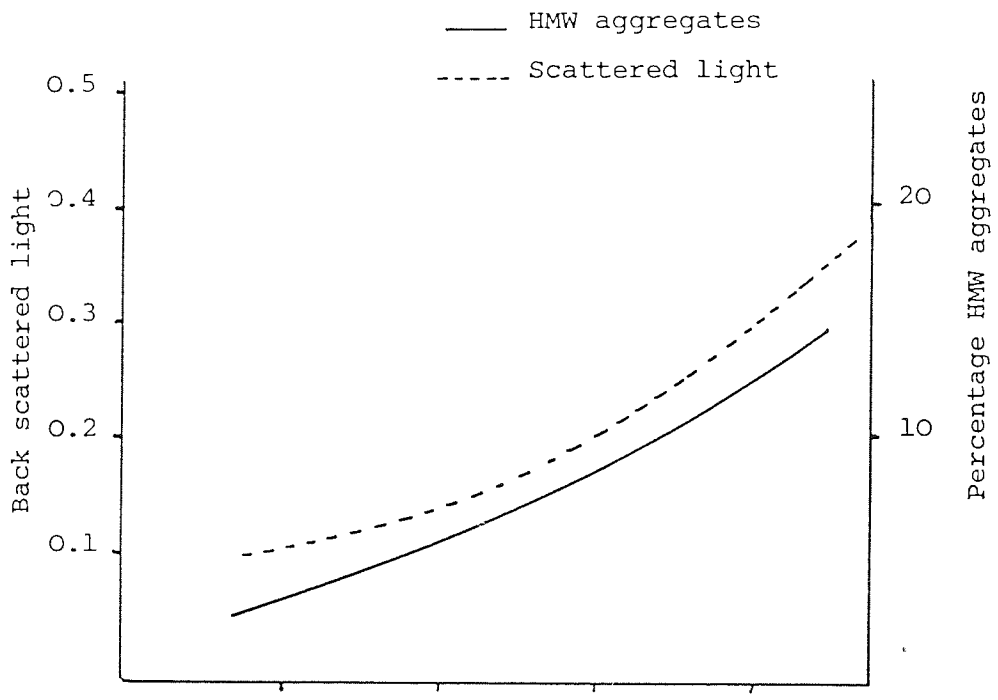

Fig. 1.13. Back scattered light in the human lens and the abundance of HMW protein.

After Spector et al[72]

the precursor of insoluble protein aggregates. Harding and Dilley[74] have written an extensive review of this subject. Kramps, Stols, Hoenders and deGroot[75] viewed these aggregates under the electron microscope and recorded them as being irregular shaped and up to 500 nm in diameter. HMW proteins, mainly from the central region of the lens of molecular weight greater thant 10^6 and up to molecular weight 3×10^8 have been reported.[74]

Tanaka, Ishimoto and Chylack[76] used a 'cold cataract' model to explain ageing and opacity formation. When the temperature of the lens was lowered to 5°C, an opacity started to form in a similar way to that occuring in a protein-water binary mixture, in which the aggregation of protein molecules forms microphases of a size comparable to the light wavelength. The result was light scattering rather than transmission. When the temperature was raised again, the opacity disappears, both in the binary solution and in mammalian lenses. In conclusion, the argument for ageing and cataractogenesis based on the phase seperation cold cataract hypothesis, is that it is a thermodynamic concept, based on reversibility. Ageing and cataractogenesis, as is known, are irreversible, moreover, it has been shown that cold cataract formation is irreversible in fish lenses.[77] Obviously, this model is too simple.

(2) Syneresis

A 2nd cause of increasing turbidity with age in the lens is due to an increase in the amplitude of density fluctuations. This reflects the refractive index difference between aggregates and their surroundings. Age related changes in the primary structure of lens crystallins is well documented. Furthermore, a number of fluorescent components were found in the insoluble yellow protein of human cataractous lenses, this has been reviewed by Harding and Dilley.[74] The majority of the literature indicates that cataractogenesis, especially the nuclear type, may occur via the unfolding of protein chains and the formation of HMW aggregates and water-insoluble proteins.

In Sugar cataracts, Kinoshita[78] described the effect of a galactose diet on cataract formation by attributing an increase in water up-take in the cortical region to an accumulation of galactitol in the

cortex. Eventually, small vacuoles appear in the cortex and lake-formation results causing turbidity. Although sugar cataracts largely involve imbibition of water from the surroundings, due to the development of an osmotic pressure gradient across the membranes, they are also partly the result of a syneretic effect.

Philipson[79] using an electron microscope found uniform distributions of protein masses in normal lenses. Sudden changes in density and correspondingly in the refractive index were reported at points where opacities occurred in the lens of cortical cataracts. Such changes coresponded to refractive index fluctuations of 0.02 to 0.04 over domains larger than 1μm. However, further measurements of refractive index fluctuations with nuclear cataracts found that these ranged over domains smaller than 1μm. This reinforces arguments that cortical turbidity in the final stages is due to large (greater than 1μm) lake formations, while nuclear turbidities are due to density fluctuations over smaller domains.

Lens Fluorescence and Ageing

Fluorescence studies on normal human lenses (see review in Lerman[52]) ranging in age from 1 day to 90 years have demonstrated that the 420-440nm fluorescence is not present in the first year of life. It then becomes manifest and increases in intensity with age (see Fig 1.14). The progressive increase in this fluorescence is paralleled by an increase in the relative concentration of HMW protein aggregates with age. A second fluorescent region (approximately 420-435nm activation and 500-520 nm emission) becomes apparent in human lenses after the 1st decade of life and increases slowly as the lens ages. The longer wavelength fluorogen becomes much more pronounced in the brown nuclear cataract.

UV and visible light transmission studies on normal human lenses ranging from 6 months to 82 years shows that over 75% of UV (300-400nm) is transmitted by lenses under 10 years of age, while above 25 years this drops markedly to 20% (see Fig 1.15). These data are consistent with lack of fluorogens in the young lens and increasing fluorogen concentration with ageing, which is accompanied by

Fig. 1.14 I_F 440/332 ratios representing whole lens fluorescence intensity at 440nm (360nm excitation) divided by tryptophan intensity (in whole lens) at 332nm (290nm excitation) After Lerman[52]

• = normal lens, ˅ = cortical cataract,
o = nuclear brown cataract, + cortical/nuclear mixed cataract.

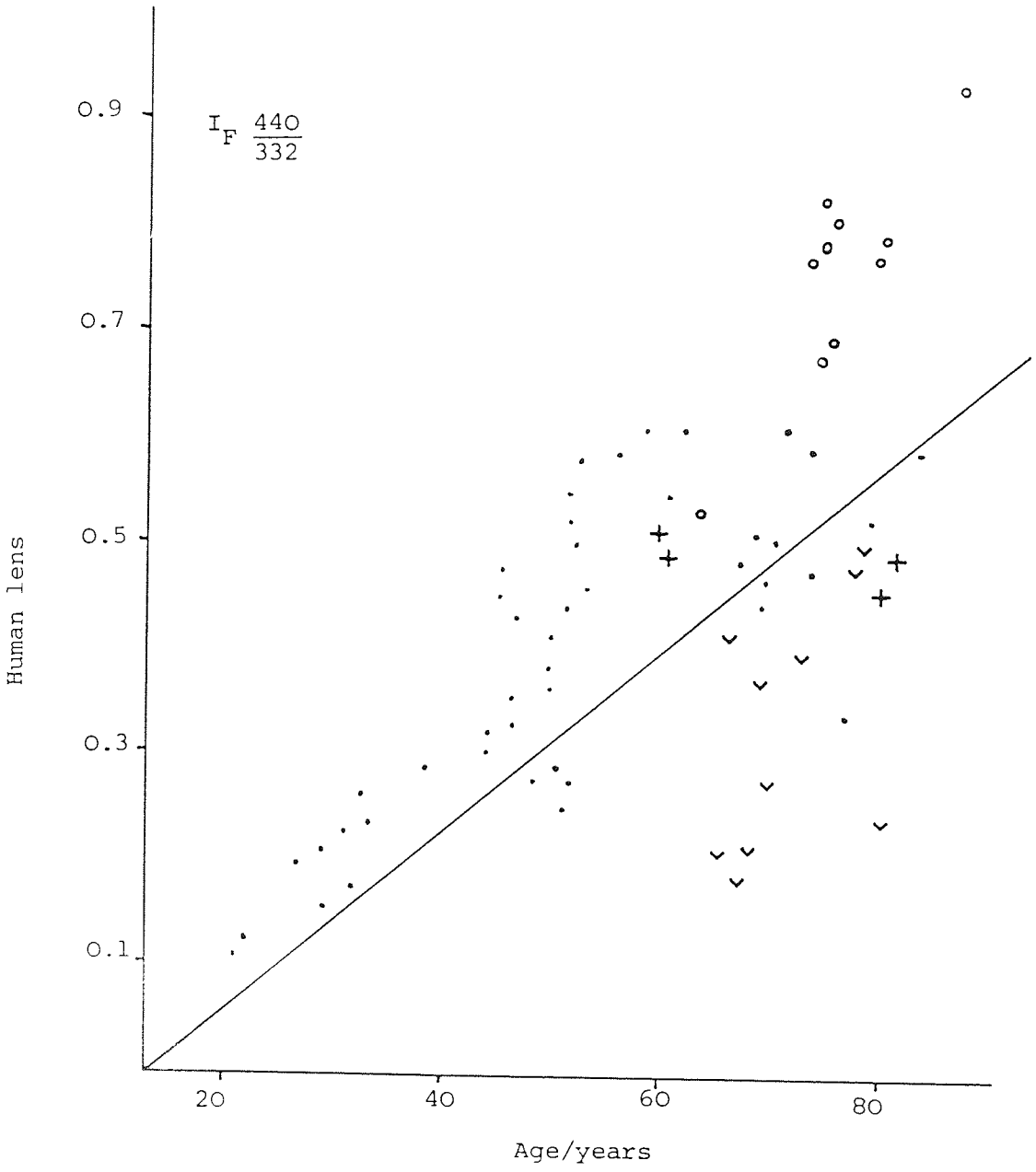

Fig. 1.15 Percent UV and visible light transmission of normal human lenses 6 months to 82 years. After Lerman[52]

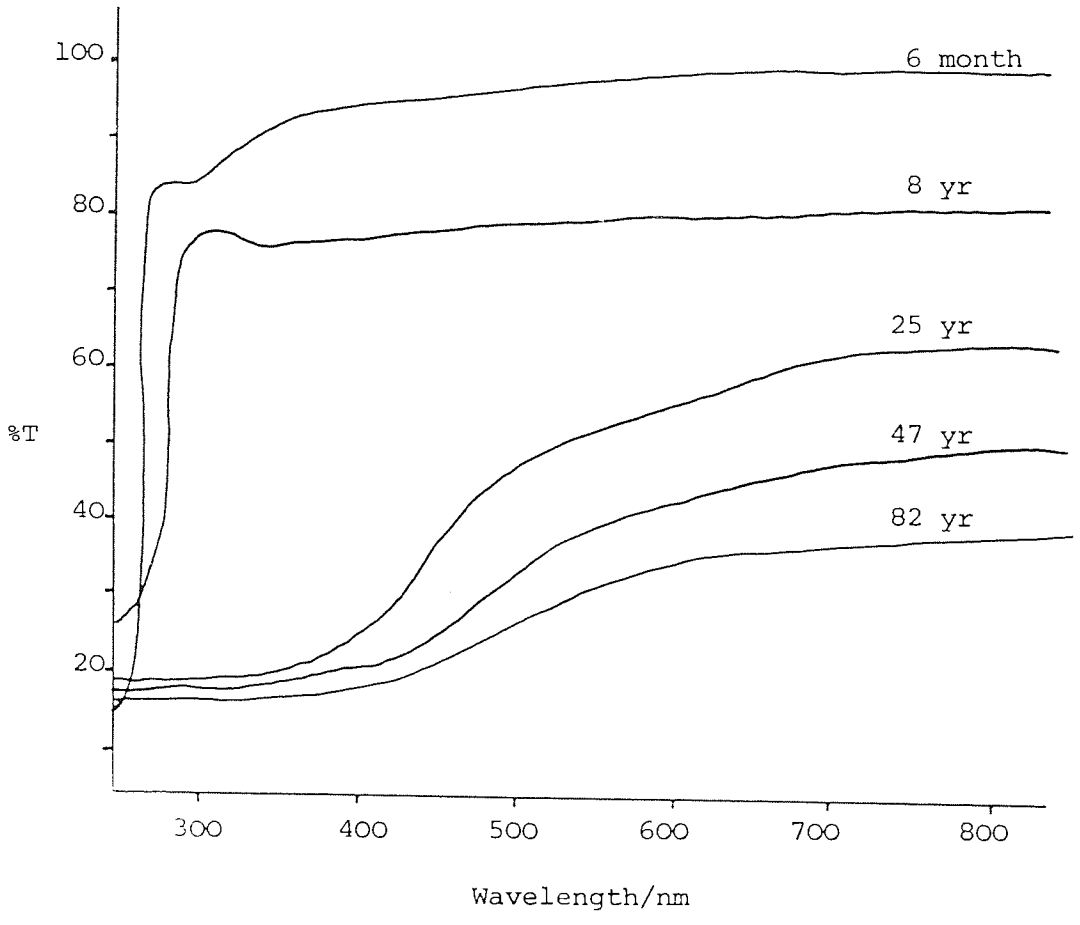

decreased light tranmission and increase in yellow colouring of the lens as it ages. These pigments, which are mainly confined to the nucleus, lead to an increasing yellow colour of this tissue and can also account for decreased light transmission. Their role in the cross-linking and insolubilisation of previously soluble lens crystallins may also be a significant factor in the development of nuclear sclerosis.

1.E Abnormal Intraocular Light Scatter

1.E.1 The Effect of Corneal Oedema

Corneal Epithelium

The anatomy of the normal corneal epithelium is described in Section 1.A and should be referred to in connection with this section. When the epithelium becomes oedematous, fluid fills the intercellular spaces of the basal epithelium. In doing so, an intricate three dimensional meshwork is produced around the cells. In this mesh, the index of refraction is different from the average index of the surrounding cells. If this fluctuation in the index of refraction has sufficient spatial regularity, they serve as a diffraction grating which produced a diffraction pattern[80,81] Fig 1.16 shows a schematic representation of the appearance of the diffraction grating produced by the intercellular oedema fluid. Such an arrangement of cells distributed in the epithelium will produce a circular diffraction pattern or halo.

It is possible to estimate the angular radius of the halo produced by the epithelial oedematous cells; and Finkelstein[81] was among the first to calculate this after inducing epithelial oedema with scleral contact lenses. The index of refraction fluctuates in the manner shown in Fig 1.16. This is equivalent to a set of diffraction apertures whose spacings (d) are equal to the average cell diameter. The direction (θ) in which this line of apertures will produce diffraction maxima is given by:

$$n\lambda = d\sin\theta$$

where $n = 1,2...$

λ = Light wavelength

d = cell size

The meshwork distribution of index of refraction fluctuation can be represented by a sum of plane fluctuation waves of principal wavelength equal to the cell diameter. These plane waves are orientated

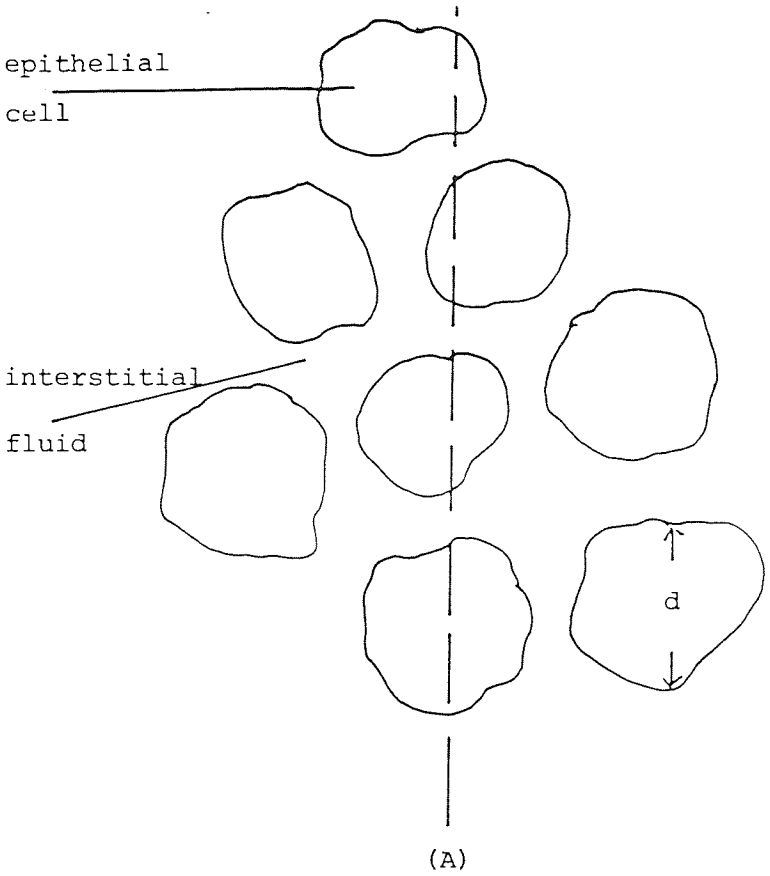

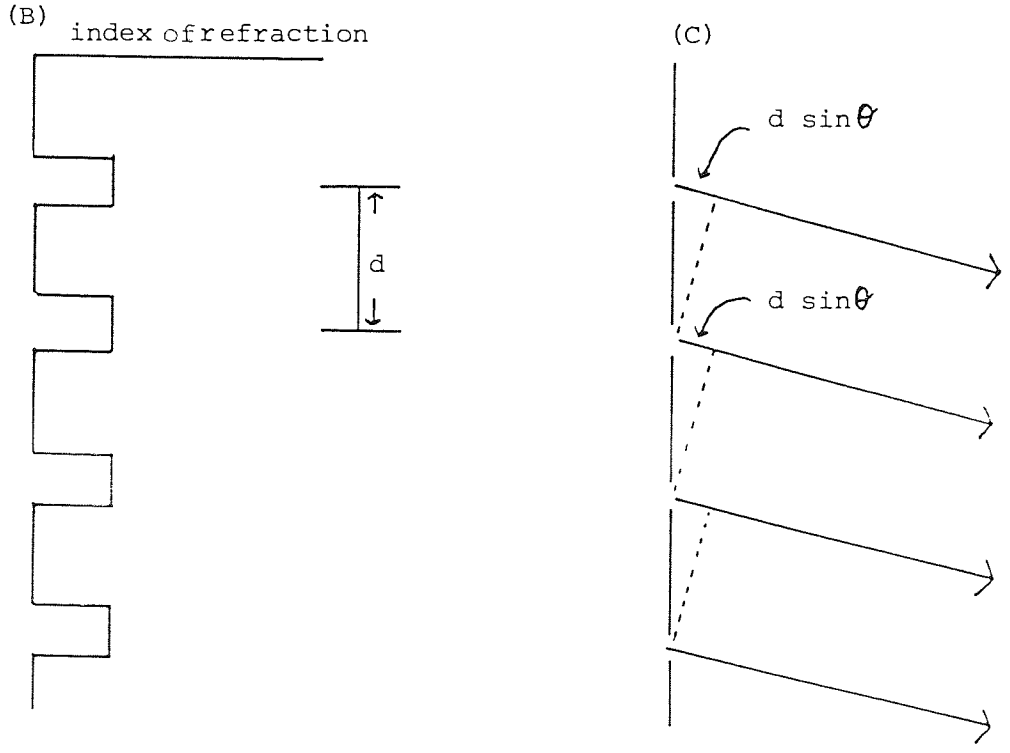

Fig. 1.16 Theoretical representation. (A) A flat section of corneal epithelial cells surrounded by oedema fluid forming a diffraction grating. (B) Distribution of refractive index on traversing an oedematous corneal epithelium. (C) A typical diffraction grating. After Miller and Benedek[80]

in all directions in the plane of the figure. The superposition of such plane waves makes up the meshwork, and the diffraction pattern produced by all the waves will produce a circular diffraction pattern whose angular radius is given by the above equation. The first order ring coresponds to n=1, and the second order corresponds to n=2. Finkelstein[81] measured epithelial cell diameter (d) as about 10μm. This is in good agreement with other authors[80] who measured d at 9.8μm. Subsequently, corneal epithelial haloes have been recorded as a means of monitoring corneal epithelial oedema[82,83] with obvious clinical implications particularly regarding contact lens practice.

In conclusion, the corneal epithelial cells with desmosomal connections are very tightly packed. Haloes will present themselves only when epithelial oedema forces fluid into the cellular interstices. Various authors have measured the diffraction maxima as angular radii; 3.18°[81] and 2.8°[80] Fig 1.17 shows a densitometric trace of an oedematous excised rabbit cornea demonstrating the average angular subtense of the halo as about 2.8° from the central light.[80]

Corneal Stroma

In 1957, Maurice[26] proposed a theory, based on a lattice which would account for increased light scattering in the stroma on swelling, mechanical straining or cooling. Under such conditions, the collagen fibrils seperate from each other and cease to be in the same order and straightness (see Fig 1.18). The result is decreased transparency and increased light scattering. Hart and Farrell[27] following Maurice's work reported that the ordering of collagen fibrils was short-ranged ie the regularity of spacing did not extend over many wavelengths in any given region. When the cornea becomes even more inhomogenous stromal scattering light wavelength dependence changed from λ^3 to λ^2. Twersky[84] considered stromal oedematous light transmission as through pair correlated random distributions of small scatterers, and considered that loss of transparency was due to increased spacing between particles. This would decrease the destructive interference effect, and Twersky's model predicted a transmissivity at 500nm which was in good agreement with experiments on excised corneas swollen to 1.5 times initial thickness. Several authors (see Farrell and McCally[85] for review)

Fig. 1.17 Densitometric trace of oedematous rabbit cornea, showing angular position of haloes which are represented as 1st order maxima. After Miller and Benedek[80]

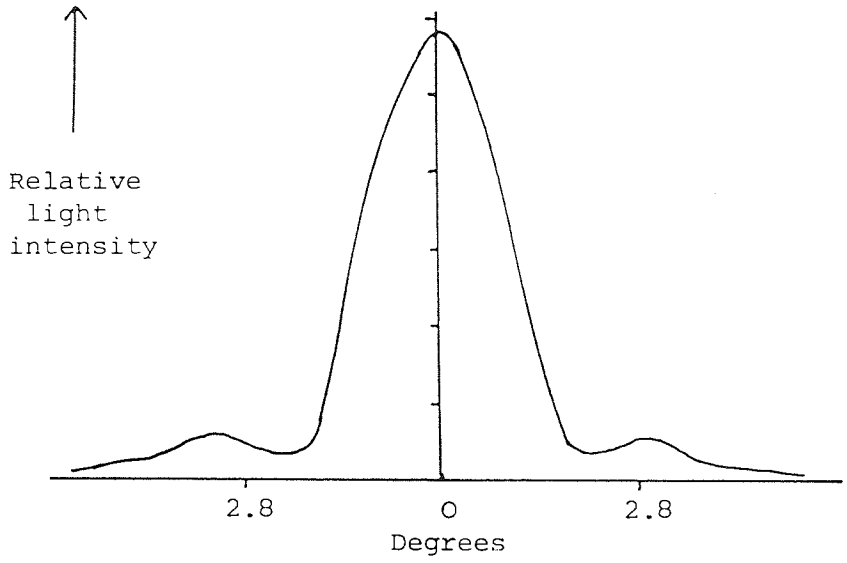

Fig. 1.18 Cross-sectional view of collagen fibrils showing disorder of fibril rows due to weakening alignment forces from neighbouring rows. eg due to oedema. After Maurice[26]

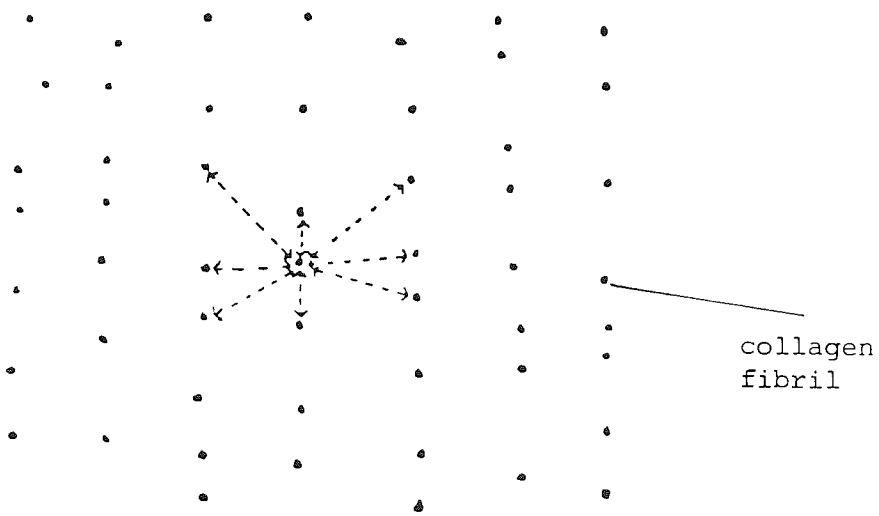

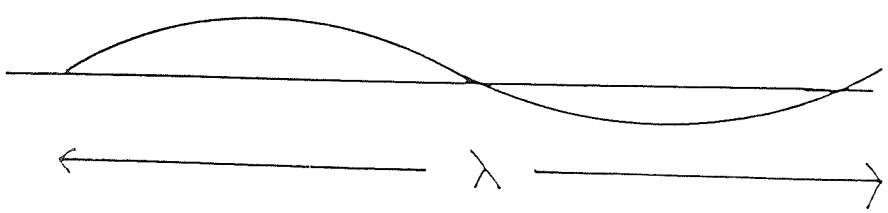

have examined electron micrographs of swollen stromas and concluded that there is little change in fibril diameter, but that the spatial arrangement of fibrils is disturbed. In between stromal fibrils large areas called 'lakes' have been identified and these could account for increased scattering. Farrell and McCally[85] considered two factors concerning stromal oedema ie the disruption in ordering of fibrils and the increasing difference in refractive index between fibrils and the surrounding medium. They concluded that the disorientation of fibrils was the most significant effect. Although the explanation of Maurice[26] concerning stromal transparency and its loss during swelling has subsequently been questioned, the basic principle of the ordered arrangement of collagen fibres appears to be an adequate explanation. The endothelium plays a large part in the active transport of the cornea and is responsible for the maintainence of corneal hydration. It can be viewed with a slit lamp as a thin bright line on the inner edge of the cornea. Clinical and in vivo measures of corneal light scattering are reviewed in Section 1.F.1.

1.E.2 The Effect of Cataract

Ageing and cataractogenesis of the crystalline lens with reference to light scatter have been examined in detail in Section 1.D.2. The development of a cataract has 3 effects on light reaching the retina.

(1) Reduces the amount of light reaching the retina.

(2) Reduces the contrast of light reaching the retina.

(3) Alters the filtered properties of light reaching the retina.

The human lens is yellow in white light. As a result of increasing absorption with age, particularly at shorter wavelengths the transmittance of the lens changes both quantitatively and qualitatively, it is reduced overall but more so for violet and blue light than for longer wavelengths (see Fig 1.15). This means that as age advances, relatively more red light reaches the retina. A review of mechanisms of cataract formation may be found in Duncan.[86]

Classifying Cataractous Lenses

Human cataractous lenses vary in colour from pale yellow to deep brown and in sodium concentration from 20mM to 200mM and in total protein content from 20mg to 90mg.[86] Pirie[87] was the first to try and catalogue cataracts, relating lens brunescence to water insoluble protein content (see Table 1.2(a)). The scheme had some basic inadequacies eg although the mean concentration of insoluble protein in the various Pirie colour groups increased with increasing colour, the insoluble content of individual lenses varied widely within any one group as did sodium and calcium content. Accordingly, Marcantonio, Duncan, Bushell and Davies[88] developed classification systems that will produce more homogenous groups of lenses. (see Table 1.2(b)). Whatever system is finally adopted, it must be decided on between clinicians and scientists.

Plate 1.1 taken from Duncan[86] shows typical examples of senile cataractous lenses photographed first in vivo, prior to operation and then, shortly afterwards in vitro. Although there is good agreement on

Table 1.2

Classification of Human Cataracts (Refer to Plate 1.1)

Group	Characteristics of Lens	Frequency(%)
(a) Pirie (1968)[87]		
I	Uniform pale yellow	45
II	Pale cortex with visible nucleus	42
III	Pale cortex with hazel brown nucleus	11
IV	Pale cortex with deep brown nucleus	2
(b) Marcantonio et al (1980)[88]		
I	Uniform pale yellow	17
II	Slight nuclear involvement (Significant light scatter but minimal absorption)	14
III	Nucleus deeper yellow than cortex (both scatter and absorption)	25
IV	Amber nucleus, pale or amber cortex	27
V	Brown nucleus, pale or brown cortex	17

Plate 1.1 Shows in vivo and in vitro Photographs of Typical Senile Cataractous Lenses. Taken from Duncan[86]

(a) In vivo and in vitro lenses classified both in terms of nuclear colour (I to V) and sodium concentration (A to E). The class description is given below the in vivo photographs and the experimental number of the same lens is given below the in vitro photographs.

(b) Examples of lenses where it was found difficult to assess osmotic involvement (ie electrolyte imbalance) from photographic evidence alone. Lens IIA shows evidence of cortical scatter here, but the sodium levels were normal. Lens IIC showed clear evidence of cortical scatter and slight nuclear involvement when photographed in vivo, but it is difficult to obtain much evidence of either of these from the in vitro potograph of the same lens (1119). Photograph IVD again shows nuclear and osmotic involvement, but the in vitro photograph of the same lens (1001) does not reveal the osmotic involvement to the same extent (compare with IVD lens in (a)). Lens 1044 was included as it shows that brunescence is not always restricted to the nuclear regions (see also lens 1013 in (a)).

The classification is after Mancantonio et al.[88]

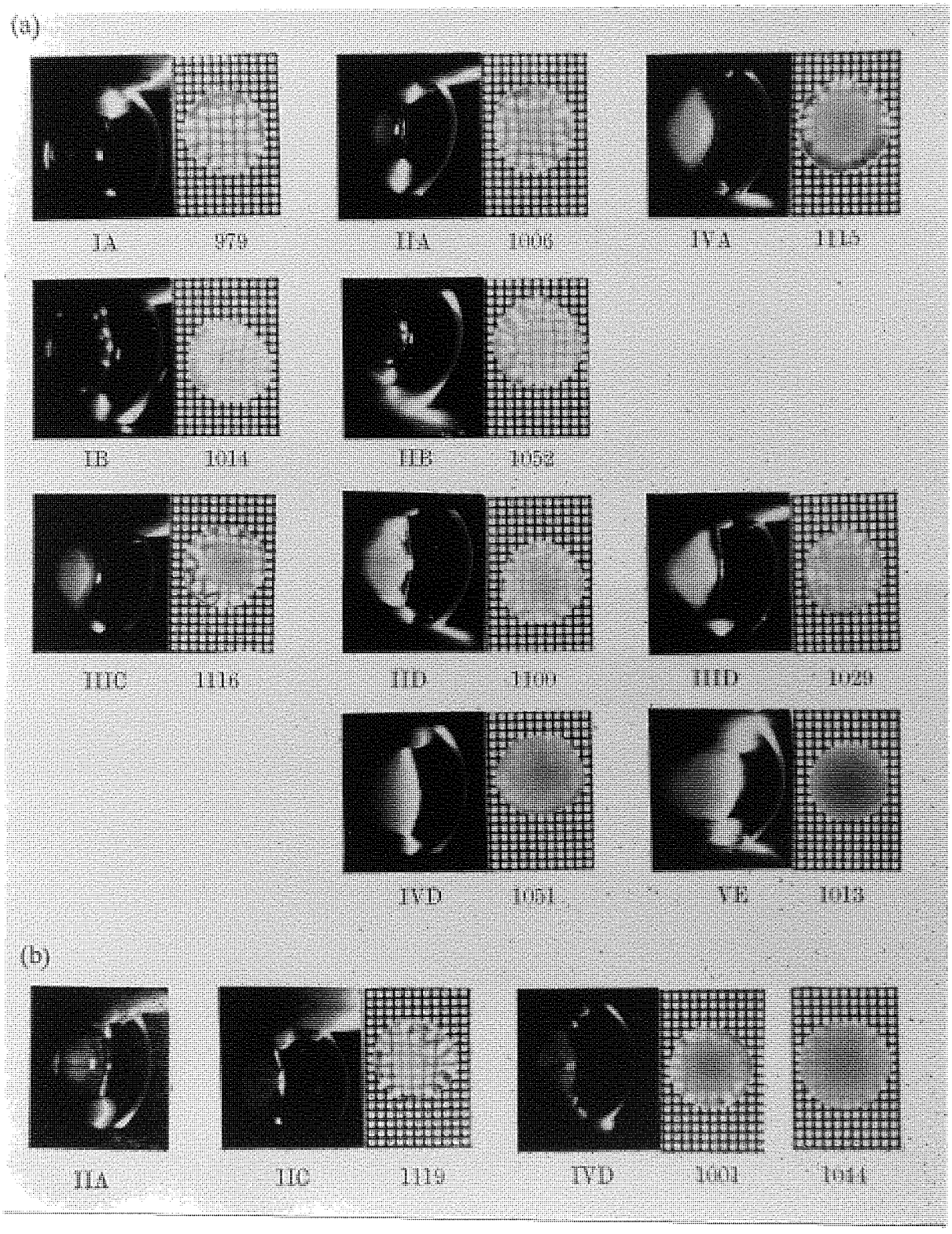
(a)
IA 979
IIA 1006
IVA 1115
IB 1014
IIB 1052
IIIC 1116
IID 1100
IIID 1029
IVD 1051
VE 1013
(b)
IIA
IIC 1119
IVD 1001
1044

Plate 1.1

basic colour of the nucleus between the two photographic methods, the slit-lamp camera system is greatly superior for revealing small polor cataracts (eg lens IA) and also, cortical cataracts in general (eg IB, IIB, IID etc), the classification is after Marcantonio et al[88]

An important distinction must be made between any changes in spectral transmission and changes in light scattering in association with cataracts. The direct use of the Contrast Sensitivity Function (CSF) using sine wave gratings in the non-cataractous eye does not alter the modulation, even though the spectrum may absorb light differentially; spectral and spatial frequencies do not interact. The situation is radically different in the presence of scattering nuclei, they do interfere with the contrast transfer of spatial frequences, and as regard to the spectral effect, this depends on the radiation wavelength and the size of scattering nuclei, but generally radiation of short wavelength are scattered more strongly than those of long wavelengths (eg Rayleigh scattering).

The experiments in this project use sine wave contrast threshold targets. Any changes in modulation that occur will be due to the scattering particles in the corneas or/and lenses of the subject groups. The use of glare sources in the experiments enhances the effects of the scattering particles. It is hoped that such experiments may lead to a more appropriate understanding and classification of the effects of ageing and cataracts on a patient's vision. Such an emphasis is particularly directed at the clinical situation.

1.F Clinical and in Vivo Measures of Intraocular Light Scatter

Many studies citing the light scattering and changing spectral properties of cornea and lens have been examined in the preceding sections with regard to ageing and cataract formation. For the clinician, the priority is to relate these theoretical animal and in vitro studies to the "in vivo" clinical situation. What concerns clinician and patient alike is a realistic and appropriate assessment of their present and future vision. This section reviews these studies and will mention in vitro studies where appropriate.

1.F.1 Cornea

Allen and Vos[19] were the first to attempt to quantify ocular scattered light in vivo. They related an objective measure of scattered light from a slit-lamp with the same subjects visual performance on a variable contrast Visual Acuity target. The assumption was that light back scattered from the tissues of the eye was related to and thus representative of forward scattering towards the retina. Fig 1.19 shows the experimental set-up that was used to record slit-lamp photographs. Similar arrangements have been used by various authors subsequently, Fig 1.10 shows that the graphs of results for back scattered light from the cornea against age, up to the age of 80 years, less than 1% of incident light was found to be back scattered.

Hess and Garner[89] induced corneal oedema in subjects by the use of atmospheric induced anoxia. The effect on vision was assessed both by a conventional high contrast Visual Acuity chart and with contrast sensitivity measurements. For the amount of oedema that was produced, contrast thresholds were only depressed at high spatial frequencies, a greater degree of oedema was simulated with a diffuser, where upon low spatial frequencies were also affected. Hess and Garner concluded that visual acuity measurements alone were inadequate to monitor visual function in conditions of corneal light scattering.

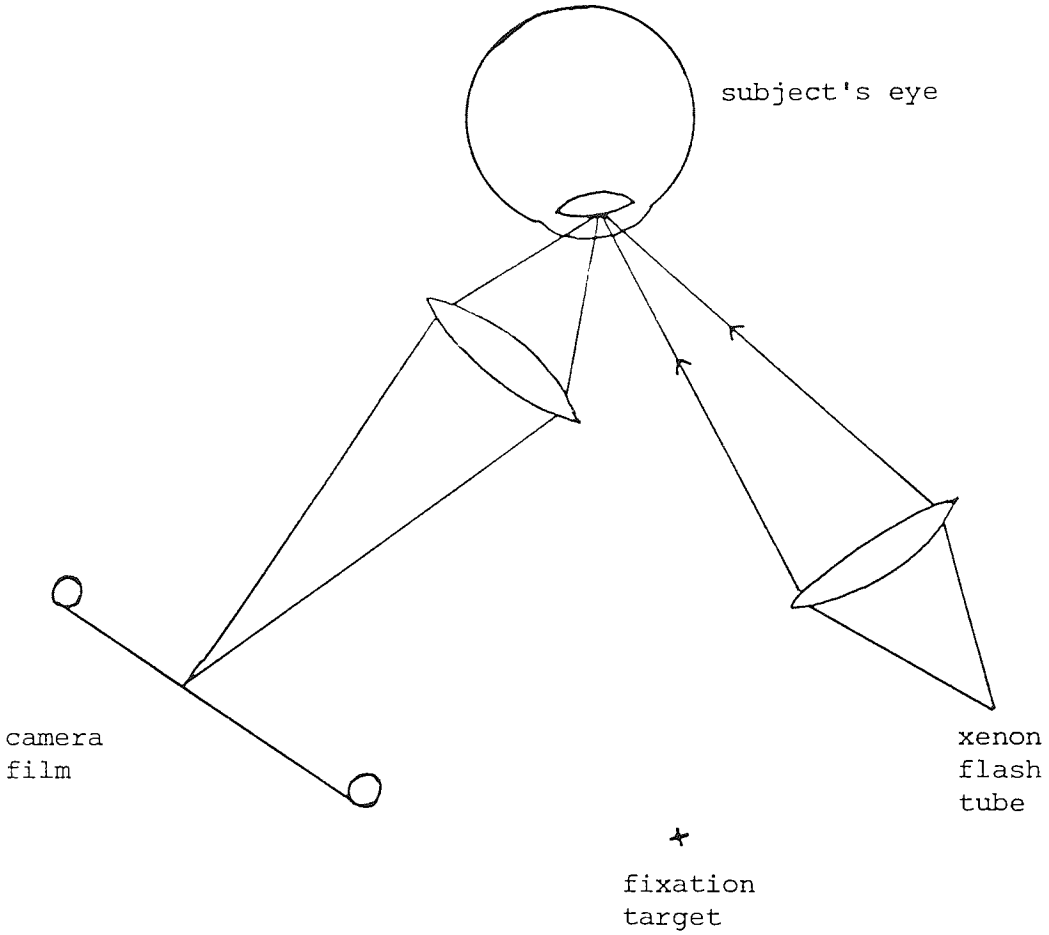

Fig. 1.19 Experimental arrangement (simplified) to record slit-lamp photographs of back scattered light from the eye. After Allen and Vos[19]

Hess and Carney [90] in a similar study induced both corneal oedema with a tightly fitting scleral contact lens containing distilled water, and also 'distortion' by passing 100% oxygen over the cornea by means of a scleral lens. Visual function was measured by means of V/A and contrast sensitivity. Distortion produced contrast attenuation at high and medium spatial frequences whereas oedema (with 11% thickness change) attenuated contrast thresholds at low and medium-high frequencies. Although Hess and Carney acknowledged that it was virtually impossible to totally seperate 'distortion' and oedema they felt that, in general terms the two different effects could be shown by contrast sensitivity measurements.

In 1981, Remole[83] measured the light scattering characteristics of the cornea in vivo after immersion in hypo and hypertonic saline solutions. Forward scattering was monitored in terms of contrast thresholds, which are more sensitive than visual acuity measurements, for this purpose. Scattering changes (reduced contrast thresholds) were recorded during an immersion period of one hour and during a recovery of 30 mins. As expected, scattering increased with hypotonicity. Remole concluded that individual differences in results prevent his methods being used as an absolute index of scattering of the retinal image and the draw back of the method included distortion from the goggles used. It is commented that readings are easier to take during recovery, when the goggle is absent.

Stevenson, Vaja and Jackson[82] in a similar method to Remole [83] bathed the cornea in hypotonic saline solutions. Corneal thickness was measured with a pachometer and increase in light scatter was recorded by the presence and brightness of a halo. A 9% increase in corneal thickness and maximum halo brightness was recorded with the use of distilled water. As the halo diminished and disappeared (during recovery) no significant decrease in corneal thickness could be monitored. Since pachometry records changes in stromal thickness, halos were epithelial in origin. Other authors have also noted this effect eg. Lambert and Klyce,[91] Lovasik and Remole. [92]

Finally in 1983, Lovasik and Remole[92] measured the forward light scattering profile of excised corneas and recorded the angular dependence of scattered intensity over 140° angle within a time of 9 secs. Corneas were bathed in saline solutions ranging from 0.9% NaCl (isotonic) to 0.5% NaCl (hypotonic), corneal thickness was also recorded. The method used was quick and cheap and confirmed previous studies[29,30] showing decrease in corneal light scatter with increasing scatter angle. Moreover, if used to measure back scatter in vivo, the method had obvious clinical implications and was believed more sensitive than pachometry.

1.F.2 Crystalline Lens

In 1965, Wolf and Gardiner[18] measured a patient's sensitivity to glare, (the subjective result of intraocular light scatter) by recording the increase in contrast required to recognise Landolt 'C' rings. The results (see Fig 1.20) showed a high correlation between glare, age and scattered light in the dioptric media indicating that glare is an entoptic phenomenon in its influence on visual efficiency. Up to 40 years, there was little change in glare sensitivity while above that age there was a linear relationship between lens opacity and glare sensitivity.

Allen and Vos[19] (see Section 1.D.1) measured lens back scattered light as a function of age, assuming back scattered light is representative of forward scattered light. An index of scatter was calculated as the percentage of light scattered out from the slit beam. Fig 1.21 shows an increase in light back scattered from the lens. Glare sensitivity also rose as recorded by more contrast being required to see the visual acuity target.

Siegelman, Trokel and Spector[93] using a slit-lamp camera recorded in vivo back scatter by tracing the photographs with a microdensitometer. They examined groups of normal patients and those with nuclear sclerosis and senile cataracts. They concluded the following:

(1) Back scattered light from the lens increases with age.

(2) Nuclear region of the lens shows significant back scatter but this increases with age.

(3) Cortical lens region causes appreciable back scatter in young lenses and there is a slight increase with age due to growth of the cortical region.

(4) No loss of visual acuity with considerable back scatter.

(5) In nuclear senile cataracts there is a large increase in back scatter from the nuclear region.

Fig. 1.20 Luminance of scattered light from the lens
After Wolf and Gardiner[18]

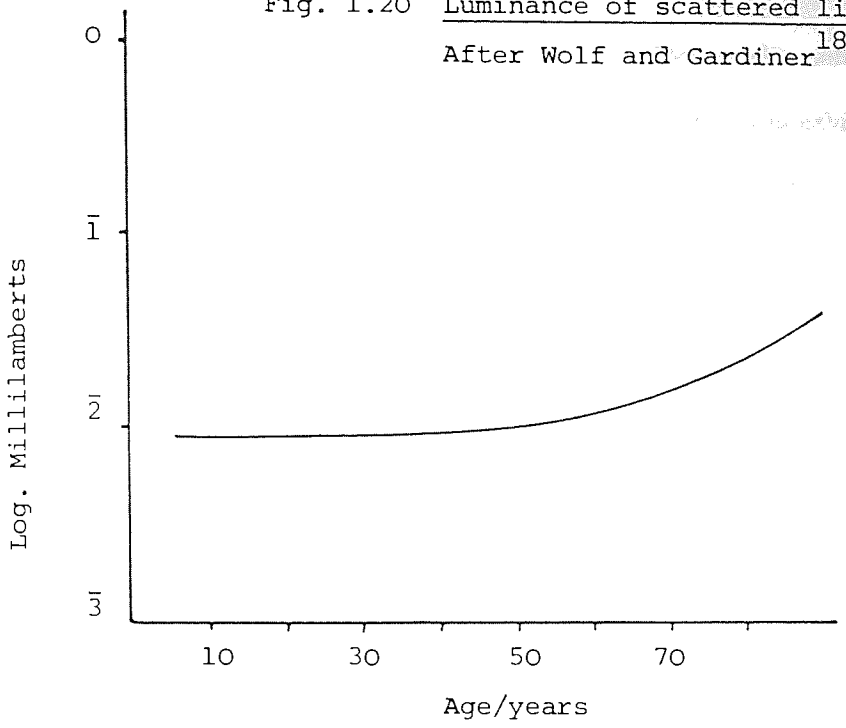

Fig. 1.21 Scatter indices for various parts of the lens. (a) ant. cortex, (b) post. cortex, (c) nucleus. After Allen and Vos[19]

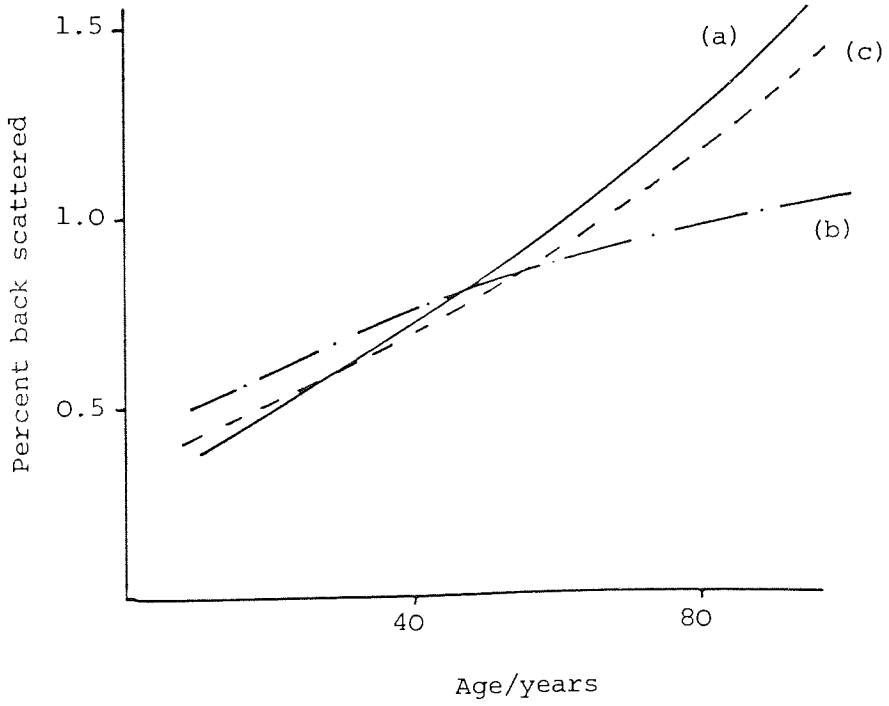

Ben-Sira, Weinberger, Bodenheiner and Yassur[94] repeated the work of Siegman et al[93] in a clinical environment using apparatus resembling that of Goldmann.[70] Their results confirm that the cortex scatters a significant amount of light in young eyes and also that the nucleus exhibits a sharp rise in scattered light after age 40. A more quantitative clinical characterisation of lens opacity has been attempted with stereoscopic photographing of lenses and their classification.[95] Further improvements in this technique were elicited using rotating slit-lamp photography employing Scheimpflug principles.[96]

In 1978, Hess and Woo[69] compared contrast thresholds for a range of spatial frequencies to visual acuity tests for 10 patients with uniocular senile cataract. The results indicated that the magnitude and extent of the intra-resolution limit abnormality varied dramatically in cataract patients and for some, vision was abnormal for objects of all sizes. They concluded that present acuity evaluations of vision with cataracts was inadequate because it would over estimate the nature of the visual world of the cataract patient. This paper was an important advance in clinical research as it firmly established the use of contrast sensitivity measurements in the in vivo assessment of forward light scatter in the eye.

Since veiling glare has been established as being the result of intraocular light scatter.[97] The use of glare sources during measurements of light scatter could enhance contrast sensitivity attenuation. In 1980, Paulsson and Sjostrand[98] combined contrast sensitivity measurement with a quantitative assessment of intraocular light scatter using glare lights. They derived an expression for a Light Scattering Factor (LSF) where

$$\text{LSF} = \frac{L}{E}\left(\frac{M_2}{M_1} - 1\right)$$

where L = luminance of target screen

E = direct illuminance onto the eye of the glare light

M_2 = detection contrast threshold with glare light

M_1 = detection contrast threshold without glare light

The LSF was a direct measure of intraocular light scattering. The patient's Contrast Sensitivity Function (CSF) was measured using a TV display system. A bright light source was introduced into the field of vision and the resulting decrease in the CSF was measured. The LSF was then calculated from the results. Five normal controls (age 30-61 years) and six patients with posterior subcapsular cataract (age 46-68 years) were used. Results showed a loss of contrast sensitivity at low and medium spatial frequencies in patients with cataract compared to controls. With the addition of a glare light, the normal subjects showed on insignificant decrease in contrast sensitivity, whereas this was markedly decreased in cataract patients. Depression in the CSF was most distinct at low and medium spatial frequencies. A single value of a LSF was calculated as a convenient measure of intraocular light scattering, and was found to vary between cataract patients with the same visual acuity. Most patients used in the study performed well on a visual acuity test and met the requirements for a driving license.

Paulsson and Sjostrand[98] conclude that their method of measuring contrast thresholds with added glare light gives a LSF which was a quantitative measure of a patient's intraocular light scatter and that this may prove useful as a clinical vision test. In the experimental section of this project, Paulsson and Sjostand's LSF was used in the assessment of intraocular light scatter.

1.G Glare

1.G.1 Veiling (Disability) and Discomfort Glare

In lighting terms, glare is taken to be the expression of the undesirable visual effects which result from the presence within the visual field of areas of excessively high brightness. Two distinct forms of glare are recognised. These are referred to as veiling (disability) and discomfort glare.

Veiling glare is the direct reduction in the ability to discriminate objects or surfaces in the visual field due to the presence of a bright light source eg the sky, or a light bulb, the light from which becomes scattered in the optic media. This scattered light reduces the contrast sensitivity of the eye and can also reduce visual acuity. A haze will also appear around the retinal image impairing the visibility of nearby objects. Veiling glare is caused and is the subjective result of intraocular light scatter, the subject of this project.

Discomfort glare is the sensation of distraction, annoyance, dazzle and acute discomfort which can result from large areas of bright light being directly visible from points within a room, it appears to be a compound effect of contrast and saturation. Excessive brightness causes the pupillary muscles to close the pupil more tightly. The resulting muscular fatigue causes instability of the pupil itself and is believed to be partly responsible for discomfort glare. Instability arises from contradictory indications from highly stimulated parts of the retina, receiving illumination from the glare sources and from the less fully stimulated parts of the retina, receiving illumination from a low luminance surround.

The basic studies on glare discomfort have employed forms of apparatus in which the glare source can be varied in size and brightness, while the rest of the visual field remains exactly the same, although apparently lit by the source. The method of evaluating glare discomfort has been to ask observers for

their direct subjective impressions, hence the observer is asked to think about the situation, evaluate it, and make a setting of a control variable, such as the source luminance, until the glare sensation corresponds to a criterion which has been described and which the observer believes can be reproduced. No successful studies have been made using specific visual tasks and the performance of them as the basis for evalution. Such experiments that have been carried out in this way and this work is reviewed in Hopkinson and Collins[99], have found that acute subjective discomfort arises from situations which give rise to little or no decrement in visual performance, as measured. Any such decrement that may exist, may be in part due to the culmulative effect of ciliary instability, phototropism and mental fatigue over days, weeks or months in a glaring situation. Some types of glare may be a matter of annoyance and distress rather than direct reduction in visual performance.

The results of various investigations into the glare discomfort phenomenon all agree that the magnitude of glare sensation is related directly to the luminance of the glaring source and its apparent size as seen by the observer, and that the discomfort is reduced if the source is seen in surroundings of high luminance. The glare sensation is also reduced the further the glare source is off the line of sight. Over a limited range of conditions, this finding can be expressed by a Glare Constant, and has been found to correspond as follows:

Glare Constant	Criterion for Glare Discomfort
600	Just intolerable
150	Just uncomfortable
35	Just acceptable
8	Just perceptible

Thus, if the glare constant for a given situation was evaluated as 60, the degree of glare, for the average observer, would be between, 'just uncomfortable' and 'just acceptable'.

1.G.2 Relationship Between Veiling Glare and Intraocular Light Scatter

Ordinary vision involves the act of recognising the presence of objects against a background or details within an object. Vision is concerned with discriminating the light intensity of one object as opposed to another ie contrast. There are 2 basic ways in which contrast is interferred with in the normal eye:

(i) Optical System - Uncorrected myopia, hyperopia and astigmatism all throw an image out of focus. Optical defects inherent in the eye's system ie spherical and chromatic aberration, also tend to interfer with sharp focus. Moreover, the process of diffraction tends to bend light around the edge of the pupil and reduce the sharpness at the edge of the image.

(ii) Image Detection Process - Although a scene may be sharply focussed on the retina the presence of an additional light source flooding the retina makes it difficult to detect the contrast of the scene. Veiling glare is the term used to describe the contrast lowering effect of intraocular scattered light on a visual scene. In 1927, Holladay[100] published the first quantitative data on the masking effect of the visible halo around glare sources. This was expressed in terms of an equivalent veiling luminance (Leq), that would produce the same masking effect. Vos and co-workers[97,101,102] realised that the equivalent veil was a real light veil produced by intraocular light scatter, and was able to quantify the equivalent veil effect using glare sources from 1° to 100° from fixation. This was used as the basis of calculation for the Light Scatter Factors of Paulsson and Sjostrand.[98] Studies carried out from theoretical[27] and psychophysical methods[94,97] and with the use of excised eyes[103,104] can be summarised with the following conclusions:

(a) Glare is due to light scattering in the eye and unwanted stray light is present in the normal eye.

(b) This unwanted stray light interferes with the contrast of the foveal image and increases the background light level.

(c) Two principle sources of intraocular light scatter within the eye are the cornea and the crystalline lens.

(d) The intensity of stray light decreases with distance from the visual axis.

Obviously any pathology of the eye eg epithelial or stromal oedema (in dystrophies) aqueous flare (in anterior uveitis), cataracts, vitreous floaters and retinal oedema (in retinopathies for example) will dramatically increase the amount of light scattered onto the retina, due to changes in the microstructure of the eye, and thereby produce glare conditions. Over the last 5 years a group of authors have specifically addressed themselves to the measurement of glare in the clinical environment, in order for the clinician to make more accurate assessment of a patient ability to drive for example[105] or following surgury[106,107,108] or in the presence of cataract[109] or as a result of the normal ageing process.[110]

The results, not surprisingly echo those of studies of intraocular light scatter cited in Section 1.F. In summary surgical procedures such as radial keratotomy and implant surgury, ageing processes and cataractogenesis all increase glare susceptibility, reduce contrast sensitivity and in some cases also reduces visual acuity.

CHAPTER 2

THE CONTRAST SENSITIVITY FUNCTION (CSF)

Chapter 2

The Contrast Sensitivity Function (CSF)

2.A The Visual Pathway and Image Processing

As the visual signals pass through the visual system a very large amount of information is compressed into a form the cortex can analyse, and important information is enhanced at the expense of less relevant information. The sites for these stages in the visual processing are the synapses, at which the nature of the signal transmitted is determined by the number of nerve fibres converging on a single cell, and the distribution of excitatory and inhibitory endings.[111]

The retina is designed to enhance images falling on the central 2° - the fovea - by means of a high concentration of cones in this area. In addition, the high number of ganglion cells means that almost every ganglion cell with receptive fields in the fovea receives the output of one cone, in comparison to the peripheral retina where many cones converge onto each ganglion cell. The area of receptor mosaic feeding into each ganglion cell is known as the receptive field, the size of which increases with increasing distance from the fovea, with a consequent reduction in visual acuity. Barlow, Fitzhugh and Kuffler[112] reported that receptive fields give a maximum response when stimulated by neighbouring areas of contrasting luminance but hardly respond at all to overall changes in luminance. This is due to the differentiation of the receptive field into a circular centre and concentric surround. Such receptive fields can have a maximum response from the centre when stimulated by light (excitatory or 'ON' centre) while the response of the surround is decreased by light stimulation and responds maximally when the light is switched off (inhibitory or 'OFF' surround). The reverse arrangement ('OFF' centre and 'ON' surround) is also found.

The signals transmitted along the optic nerve fibres are now each representing units of the visual field in topographical arrangement with the central field having the major representation. About a quarter of the fibres project to the superior colliculus which seems to be concerned with aspects of visual attention centering of the visual image on the retina.[113] The remaining fibres synapse in the LGB where the retinotopic arrangement of the fibres is maintained. From the LGB these fibres project to the visual cortex, where the signal is finally processed by 'simple' and 'complex' cortical cells (Area 17). Visual pathway and image processing has been thoroughly reviewed recently by Hubel[114] and by Wiesel[115] and should be referred to for a detailed account.

Parallel Neural Channels

One further phenomenon connected with visual processing deserves seperate attention and that is the evidence that parallel processing also plays an important part in the transmission of information through the visual pathway, and the connection with the contrast sensitivity function (CSF). Three channels have been proposed, named the X, Y and W systems. Although there are still some differences in the reported characteristics of these systems, the general properties have been recognised.

X and Y ganglion cells were first identified in the retina on the basis of their receptive field characteristics. The X cells have a clearly defined centre and surround which shows linear interaction. They comprise 40-50% of cat ganglion cells and predominate in the central retina. The Y cells comprise 5-10% of cat ganglion cells (ie 50 - 140 min for Y cells compared to 20 - 70 min for X cells). The Y cells are relatively more numerous in the retinal periphery with large less well defined receptive fields which are non linear. Y cells respond to a stimulus with a transient burst of activity while the X cells show a sustained response and the conduction velocity of the Y cells is much faster. W cells[116] have been found with large receptive fields and slow conducting fibres and can constitute as many as 55% of the ganglion cells of the cat.

Separate X, Y and W fibres are found in the LGB[117] and at the imput to the visual cortex.[118] Psychophysical evidence suggests that the X system forms the basis for spatial vision as suggested by the small dimensions and sharp differentiation between centre and surrounds of the X cell receptive fields[116] and the predominance in the central retina.[119] The large, less well defined receptive field of the Y cell make them poor spatial discriminators and it is thought that they signal temporal changes.[116,120] Psychophysical evidence indicates that directional (movement) and non directional (flicker) temporal information is transmitted by the same system, which is believed to be the correlate of the Y cells.[120]

These characteristics would be consistent with psychophysical evidence for two independent systems - a 'pattern detecting mechanism' which is most sensitive to stimuli of high spatial frequency which are stationary or presented at low temporal frequency, and a 'movement detecting mechanism' which is most sensitive to low spatial and high temporal frequences.[120,121,119] Evidence for these two systems includes the observation that the contrast sensitivity of the visual system to low spatial frequency stimuli is enhanced by temporal modulation.[122] Estimates of the relative contributions of the two systems vary, with estimates of a Y cell contribution up to 30 cpd[121] or alternatively, a Y cell contribution up to 3 - 4 cpd with temporal information at higher spatial frequencies transmitted by the X system [120] (see Fig 2.1). The low spatial frequency cut off of the X system is estimated at about 3 cpd.[120]

If the X and Y cells terminate in area 17 and 18 in the cat visual cortex, it seems that area 17 is predominantly associated with spatial processing and area 18 with temporal processing. In primates, all cells terminate in area 17. This being so, separate aspects of visual information are undergoing serial processing in parallel channels.[113] The higher mechanisms by which the brain combines the visual information signals from different parts of the visual field into the final visual image are yet to be understood.

Fig. 2.1 Two possible schematic representations of the spatial frequency tuning of the sustained and transient systems.

Note similarity of 'sustained' curve to the CSF. After Green[120]

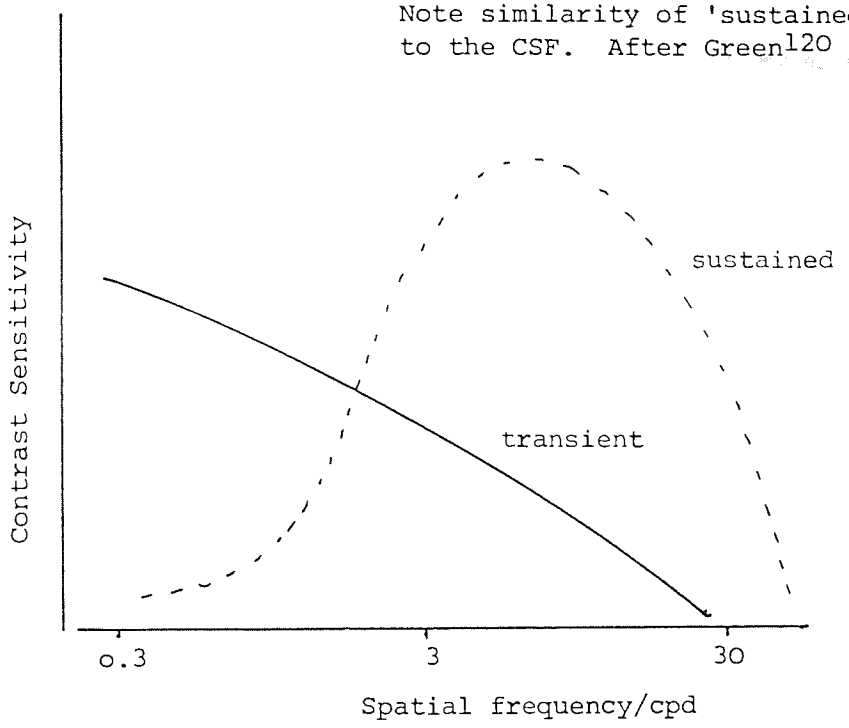

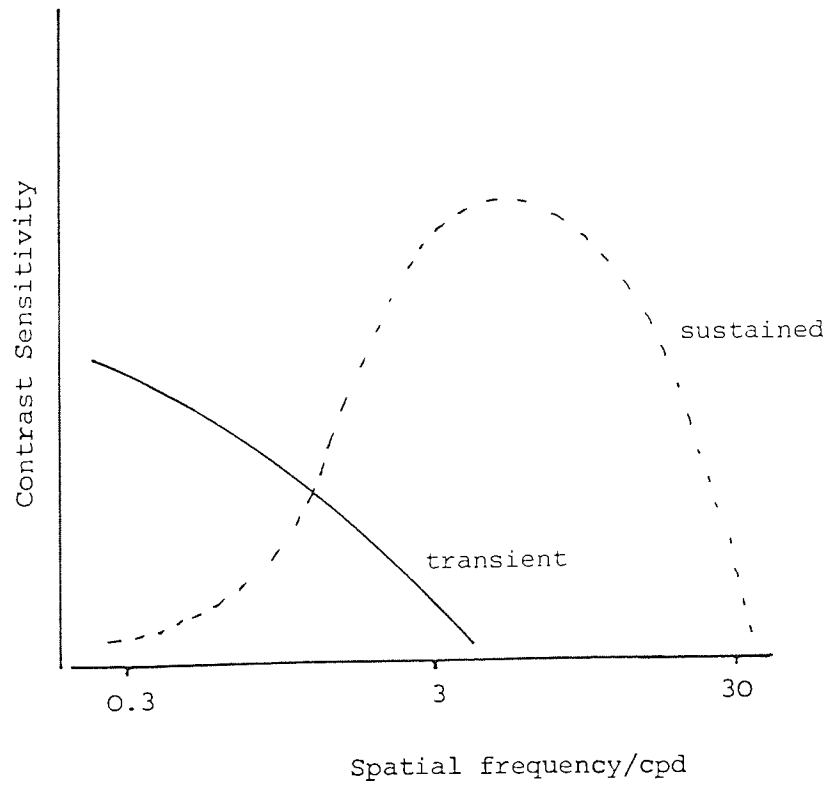

2.B Basic Concepts of Contrast Sensitivity

Introduction

The measurement of the spatial and temporal properties[123] of the visual system have developed considerably over the past 25 years since Schade's[124] early work using electronic principles. The performance of an electronic system can be assessed by comparing phase and amplitude of the output signal to that of the known input signal. Fourier analysis says that any complex waveform can be represented as the sum of a number of sine waves of specific phase and amplitude. The form of a sine wave passing through a linear system remains unchanged even though the phase and amplitude might be altered. However, a non-linear system will distort the wave. The output form of a sine wave will therefore show whether an unknown system is linear or non-linear.[123]

In the measurement of the spatial properties of the visual system, the input signal consists of a grating with a sinusoidal luminance profile. The number of bars per degree of visual angle is determined by the modulation of the sine wave. Sinusoidal variation is superimposed on a steady luminance value. This determines the mean luminance of the input signal and remains constant whatever the sinusoidal modulation. Constant mean luminance ensures constant adaptation of the retina enabling linear assumptions to be made.[125]

Modulation is defined by the following equation[126] which is independent of the mean luminance.

$$\text{Modulation} = \frac{(L_{max} - L_{min})}{(L_{max} + L_{min})} \qquad L = \text{Luminance}$$

The output signal amplitude of the human visual system is usually determined subjectively by measurement of the threshold, which is assumed to be of constant amplitude. This represents the value at which the spatial and temporal modulation are just percieve; and is therefore inversely proportional to the sensitivity of the visual system.

2.B.1 Psychophysical Aspects of the CSF

Visual acuity records the ability of a subject's visual system to see small targets of very high contrast, it does not give any information on the ability to see larger targets of lower contrast, this being a much more realistic assessment of the visual world. The CSF measures the relationship between different values of size and contrast and therefore gives a much more complete description of the visual system.

The CSF is an inverted 'U' shape with a peak at intermediate spatial frequencies (Fig 2.2). If the CSF is plotted on a linear spatial frequency axis, the extrapolation of the CSF plot to the high frequency limit of the visual system is at roughly 100% contrast, and corresponds to visual acuity. This is usually between 30 and 40 cpd,[127] each bar of a 30 cpd grating subtending 1 min of arc at the eye. A log/log plot of CSF (Fig. 2.3) will have the effect of contracting the high frequency portion and extending the low frequency section. Sine wave gratings for CSF measurement can be produced on oscilloscopes, T.V displays or using printed gratings for clinical screening[127] (See Section 2.C.1)

The Peak of the CSF Curve

Contrast sensitivity is maximum for gratings of about 4 cpd when a field size of 3° to 6° is used.[128-132] However, with a 1° foveal field size, a peak as high as 10 cpd has been reported,[133,134] and as low as 1 cpd when a target 30° from fixation was used,[135] this indicates that the peak depends on the area of retina stimulated.

Rovamo and Virsu[136] studied the change in peak sensitivity. Using a constant target size, they demonstrated a progressive decrease in contrast sensitivity and shift of the peak to lower spatial frequencies with increasing retinal eccentricity. (Fig. 2.4). When the target size was increased at each eccentricity to stimulate an equal number of ganglion cells; contrast sensitivity no longer decreased with retinal eccentricity, although the peak of the curve still shifted to lower frequences.

Fig. 2.2 The Contrast Sensitivity Function plotted on a log/linear scale (Luminance = 5 cd/m^2) After Abadi[128]

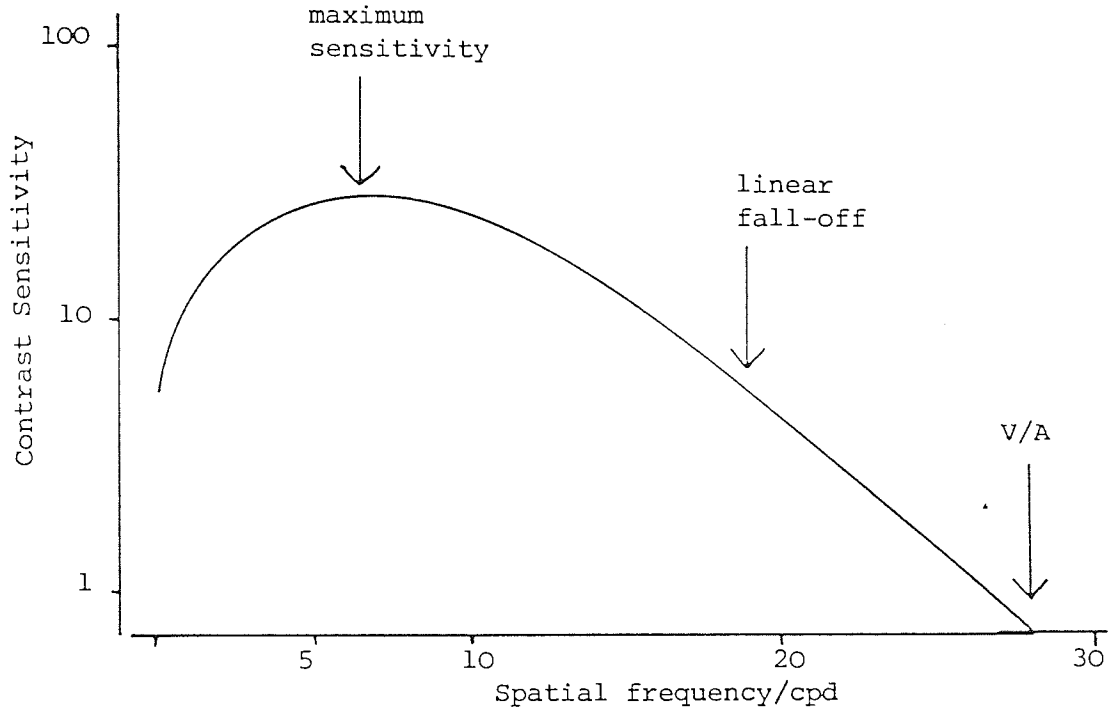

Fig. 2.3 The Contrast Sensitivity Function plotted on a log/log scale (Luminance = 500 cd/m^2) After Campbell and Robson[129]

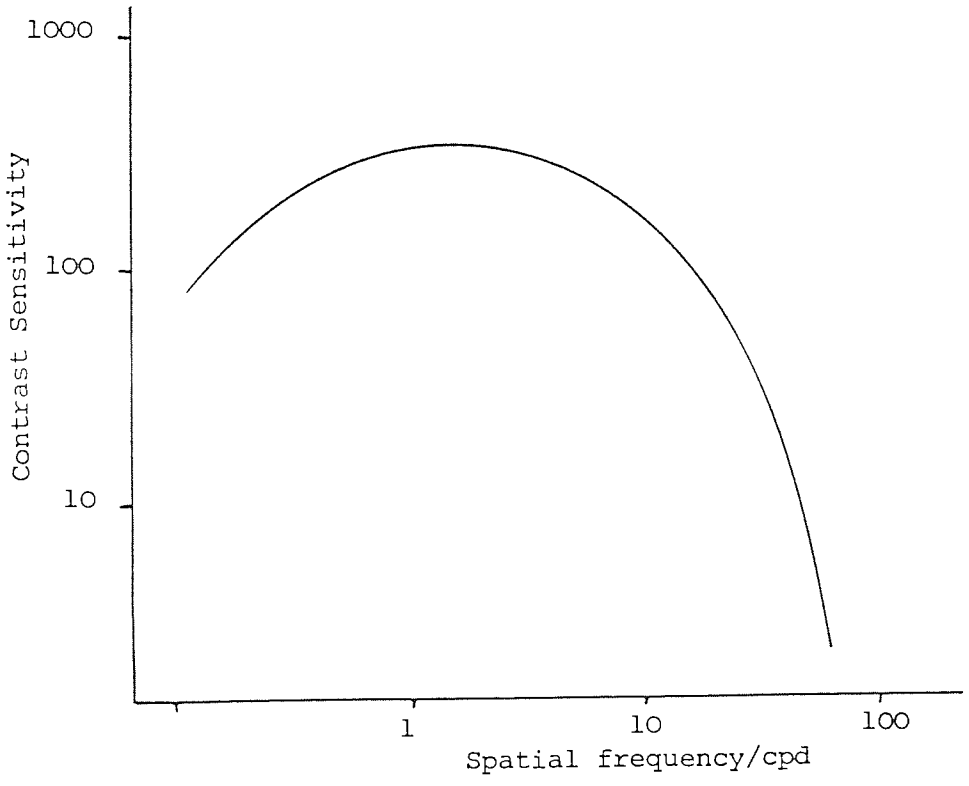

Fig. 2.4 Contrast Sensitivity as a function of retinal spatial frequency and eccentricity, showing progressive decrease in sensitivity and shift of peak to lower spatial frequencies. After Rovamo and Virsu[136]

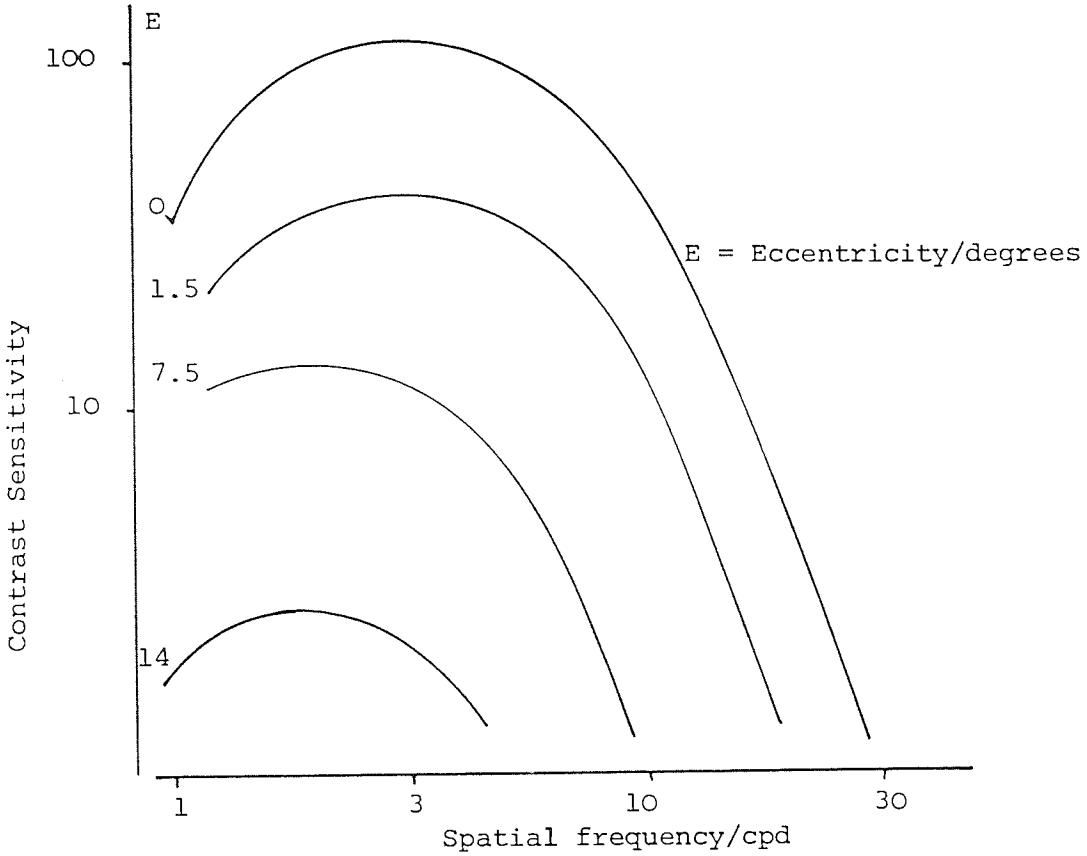

Fig. 2.5 The CSF curve for different temporal frequencies After Robson[143]

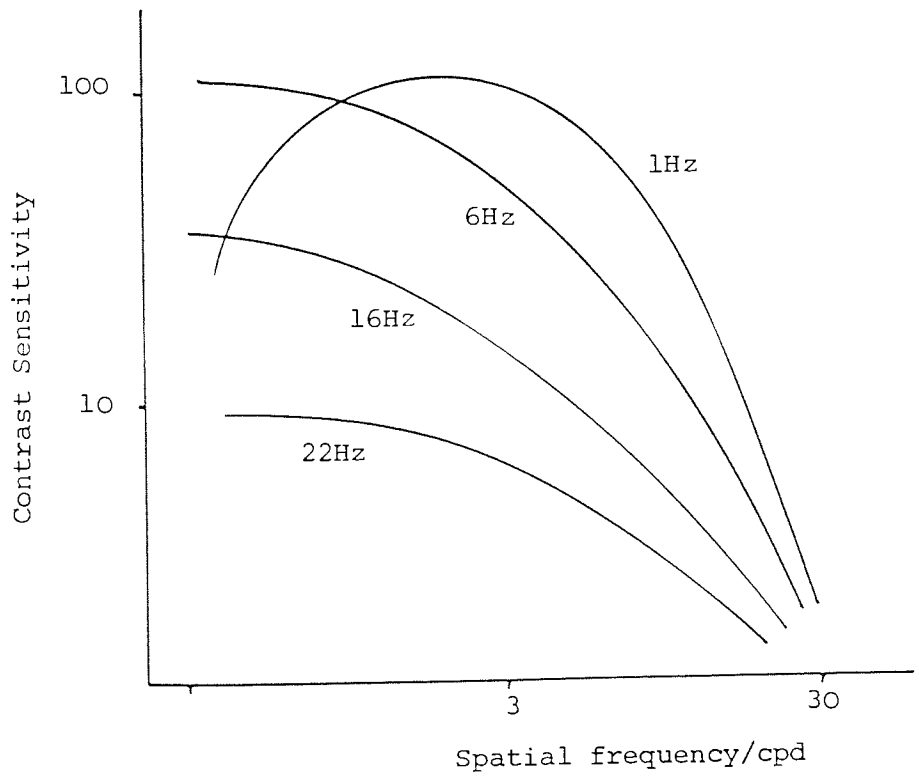

Rovamo and Virsu stated that "contrast sensitivity depends on the number of visual cells stimulated by a grating". The peak of the CSF curve is also shifted towards lower spatial frequencies with decreasing luminance due to the use of larger receptive fields at lower adaptation levels.[137,138]

High Spatial Frequency Attenuation

Contrast sensitivity decreases exponentially with increasing spatial frequency[130] and is attenuated by optical blur (see Section 2.B.3). When optical effects are bypassed with the use of laser interferometry to generate gratings on the retina, the CSF shows less high frequency attenuation. Comparison of these results with the CSF curve obtained by viewing a grating under normal conditions shows that the eye's optics account for 1/3 of the attenuation in the 30 - 40 cpd range with a 2mm pupil.[130] (see Section 2.B.4 and 2.C.2). The remaining attenuation is due to the limitations of the retinal mosaic. An additional neural factor affecting high frequency sensitivity is the level of light adaptation.[137] High frequency sensitivity has been shown to be proportional to the square root of the average luminance in the mesopic range (up to 24 cd/m^2) but becomes less dependent at higher luminance levels.[138]

Low Spatial Frequency Attenuation

Low spatial frequency attenuation of the CSF has been attributed to neural properties of the visual system, such as lateral inhibition.[139,140]The attenuation decreases with increasing stimulus area. This can be partly attributed to the increase in receptive field size with eccentricity. The number of cycles present in the viewing field is another factor. Contrast sensitivity is dependent on the number of cycles in the field.[134,141] Estimates for the critical number of cycles that must be present in the viewing field have been quoted at eight[134] six[143] five[141] and four.[129] The critical number has been found to be proportional to luminance.[134] Low spatial frequency is also progressively improved with increasing temporal modulation of the stimulus.[125,143] When the bars of the grating are modulated in counterphase at temporal frequencies of 6Hz and above there is no low frequency attenuation (See Fig. 2.5).

2.B.2 CSF and Spatial Processing

Campbell[144] has reviewed the work of recent years that suggests that the CSF curve represents the combined response of a wide range of independent spatial frequency channels. The basis of the theory is that the visual system acts according to Fourier principles, with information about the constituent sinusoidal components of the image transmitted separately through the neural channels. Such a theory is in turn based on evidence that the visual system is capable of linear behaviour, which is provided by the study of the X cell system.[145]

Campbell and Robson[129] provided evidence that the behaviour of the CSF can be predicted by Fourier principles. The thresholds of different waveforms can best be described by considering the fundamental and harmonics as separate channels. A sine wave and a square wave will appear identical at high spatial frequencies because the frequences of the square wave harmonics exceed the upper frequency limit of the eye and the threshold is determined by the fundamental amplitude alone. However, contrast sensitivity with the square wave is higher by a factor of $4/\pi$, corresponding to the ratio between the amplitudes of the fundamentals of the two waveforms. Similarly, at spatial frequencies too low for the fundamental to be percieved, the visibility of a square wave is determined by the harmonics alone. In this region it is impossible for the visual system to distinguish between a square wave grating and a 'missing fundamental' grating. Pathological processes producing spatial frequency selective CSF defects provided further evidence of neural channels. If the CSF were the response of a single channel mechanism, pathology would affect the curve uniformly across the spatial frequency spectrum. Specific low or medium 'notch' CSF defects have been reported in multiple sclerosis[146] and cerebral lesions.[147]

If the visual system does use Fourier principles to analyse images, these images must be transmitted in terms of their frequency, amplitude and phase to the visual cortex. Maffei and Fiorentini[148] reported on direct electrophysiological evidence for this theory from the retina from the lateral

geniculate body (LGB) and from simple and complex cortical cells of the cat. They found cells with spatial frequency tuning showing a wide range of peak response frequencies in all these areas. There was a progressive narrowing of the response curves (and hence the spatial frequency selectivity) from the retina to the LGB and then to the simple cortical cells under the same recording conditions. Hence, the simple cortical cells of the cat have the capacity to encode information about the spatial frequency, amplitude and phase of the stimulus, providing the basis for the visual system to act as a Fourier analyser.

2.B.3 CSF, Optical blur, Visual Acuity (V/A) and Pupil Size

The CSF is generally determined with sine wave gratings which show no change in harmonic composition when defocussed.[149,130] The effect of optical blur is to decrease the contrast through light scattering, so the contrast of the grating has to be increase to reach the threshold of the subject. The contrast sensitivity of a sharply focussed 20 cpd sine wave grating falls by a factor of 0.6 when 0.50 DS of blur is introduced (3mm pupil)[149] Plots of CSF show that the effect of defocus is more marked at high spatial frequencies. Low spatial frequencies are only affected by high levels of blur[130,150,151] (see Fig 2.6). It is therefore important that refractive error is fully corrected when CSF measurement is used for investigation of ocular conditions.

The anisometropic amblyopic defects of patients with uncorrected high refractive errors during early childhood can indicate the effect of high degrees of blur on the visual system. The CSF of high myopes of between -5.50D and - 14.00D is reduced at all spatial frequencies.[152,153] The movement (temporal) threshold of a -9.00D myope was found to be normal indicating that refractive error affects the X (sustained) but not the Y (transient) system.

Enoch, Ohzu and Itoi[154] measured depressions in CSF measurement with patients wearing high refractive corrections. Magnification by convex lenses of high power caused a decrease in the spatial frequency of the grating on the retina, while minification by concave lenses of high power causes an increase. If this is not accounted for, an artifactual low frequency defect in aphakia and high frequency defect in myopia might be measured. Contact lens correction would reduce these effects.

Visual acuity (V/A) measurement is the most common method for clinical determination of refractive error. Its high sensitivity to optical blur is due to the fact that V/A represents the high spatial frequency limit of the eye, and it is high spatial frequencies which are most sensitive to the reduction in contrast caused by blur. Campbell and Gregory[155] suggested that the role of the pupil was to

Fig. 2.6 Contrast Sensitivity as a function of optical blur showing that the reduction in CS increases with increasing spatial frequency and increasing optical blur. After Campbell and Green[130]

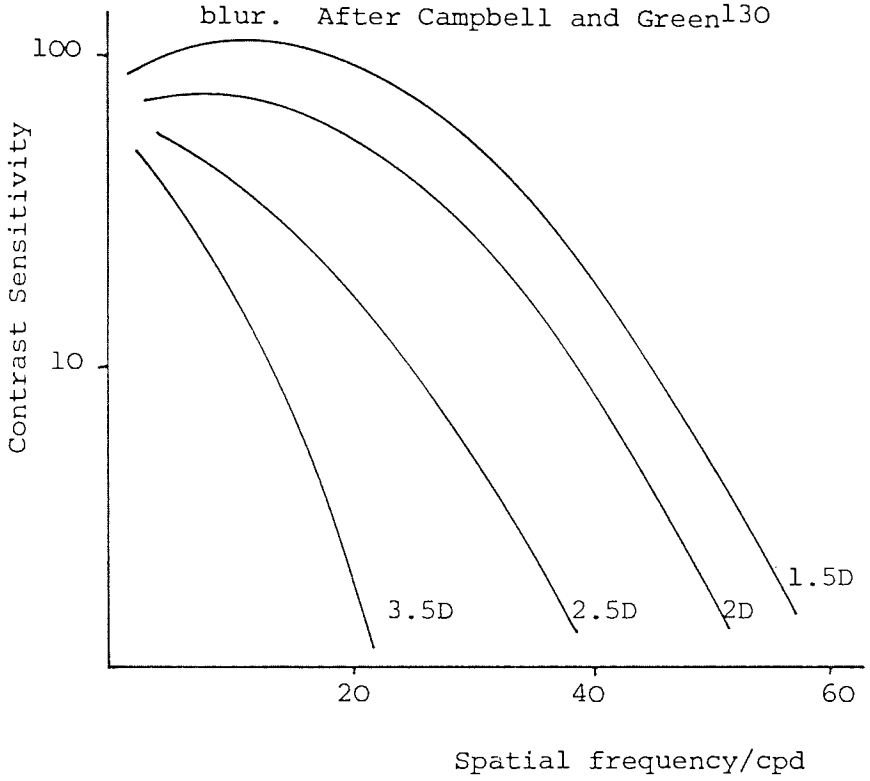

Fig. 2.7 Interference fringes pattern as it developes from 2 wave fronts focussed in the plane of the pupil. After Adler[2]

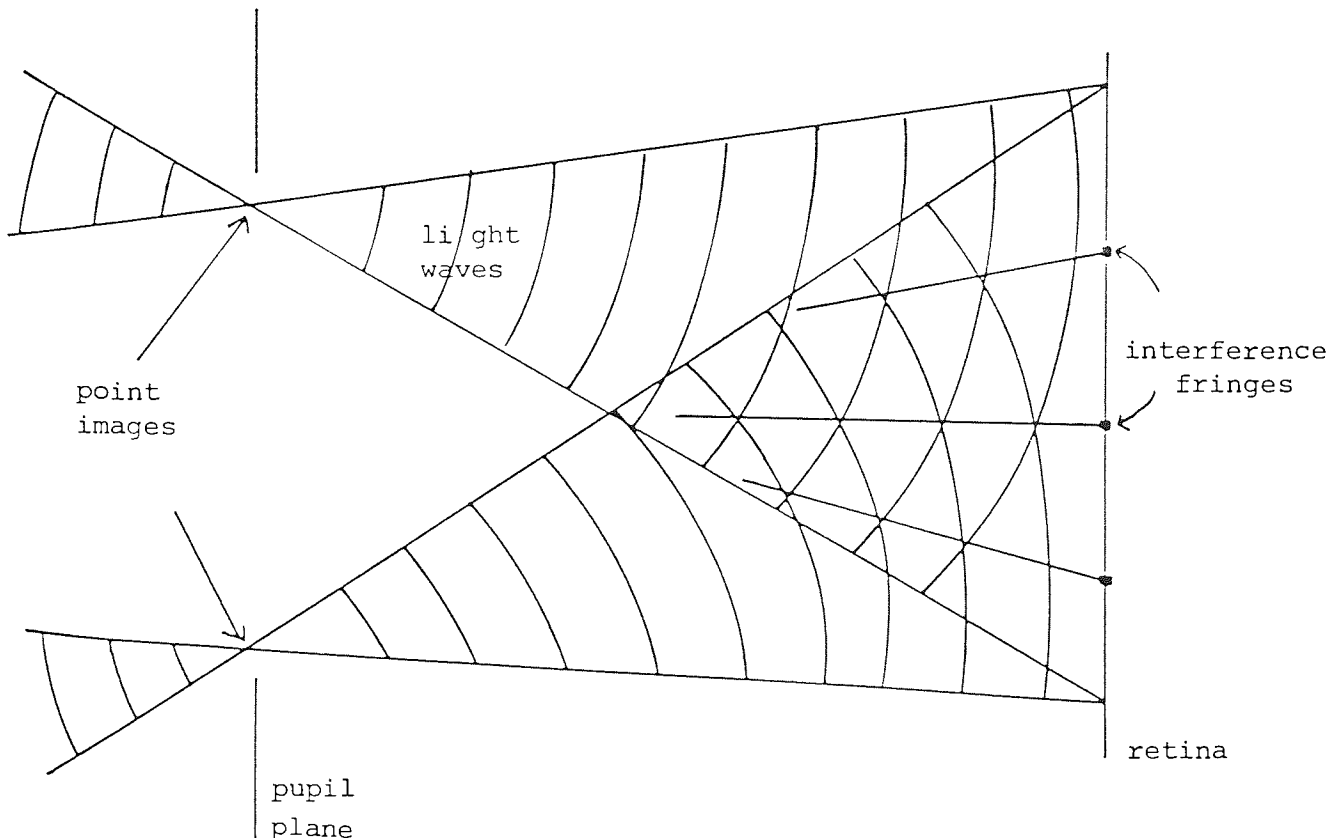

optimise V/A over a wide range of ambient luminances. They measured the visual resolution attained at a number of luminances and with a range of sizes of artificial pupil. They found that the pupil size which gave the highest resolution - the optimum - closely approximated the natural pupil at the same luminance level. Similar studies have subsequently been conducted examining the effect of pupil size on detecting low contrast levels.[130,156] Such work confirms that, over a wide range of luminances and contrast levels, the natural pupil will adopt a size close to the optimum for visual resolution.

For completeness, consider the performance of the eye with a fixed pupil of the extreme value of either 2 or 8mm diameter. With a 2mm pupil and low luminances, the loss in visual resolution is very large, up to 57% at low contrast[156] due to low levels of retinal illumination. At high light levels, where there is an abundance of photons, a 2mm pupil reduces the optical aberrations which may degrade the image and therefore, as long as the luminance is high enough, will give the best resolution. In the case of an 8mm pupil, there is no loss of resolution at low light levels, in this range the important factor is photon capture and therefore a large pupil will be the optimum. As the luminance increases the 8mm pupil performs less well, due to the optical aberrations inherent in the eye, which act in opposition to the gain in resolution from the increased retinal illumination.

2.B.4 The Laser Interferometry Principle

The importance of measuring the CSF in order to obtain a fuller understanding of the visual world of the patient has been repeatedly emphasised. One of the drawbacks of measuring the CSF by any method cited is that, as with Snellen V/A measures, it may be difficult to differentiate between attenuation of the CSF due to optical media factors and those due to neural factors.

One way to by pass the optics of the eye is to generate the sine wave fringes directly on to the retina by applying the principle of interference to laser light. This method has been developed by Campbell and Green[130] and Westheimer[157] (see Fig 2.7) Several workers have utilised this principle to determine the resolution capabilities of the retina in the presence of opacities of the ocular media (see Section 2.C.2). High contrast fringes may be formed on the retina with a low power helium - neon laser. The patient sees a circular field usually 3° to 6° in diameter that is filled with a system of parallel dark and light red stripes. The total power entering the eye is less than $0.1mW,^2$ not greater than ordinary daylight illumination. The finest interference fringes that can be seen by the patient provides a means of estimating the basic acuity of the retina. Orientation of the stripes can generally be altered to verify the end point. In the normal patient good correlation has been found with standard Snellen acuity.

2.C CSF Studies in relation to Corneal Oedema, Ageing and Cataract

Introduction

Over the past 15 years there have been at least 75 articles devoted to the measurement of contrast sensitivity as an aid to clinical diagnosis in a range of ophthalmological conditions and normal ageing processes. These have been thoroughly reviewed in the last 6 years.[119,137,158] This section reviews the CSF studies carried out on subjects with corneal oedema, ageing effects and cataract, as these 3 groups specifically demonstrate increased intraocular light scatter and depressed contrast sensitivity and are the subjects of the experimental section of this project (Chapter 3 and 4).

2.C.1 Conventional CSF Studies

Corneal Oedema

A number of studies measuring the CSF of contact lens wearers have been conducted as all contact lenses produce a certain amount of corneal oedema. Applegate and Massof[159] were the first to investigate this effect by measuring contrast sensitivity. Initially, they measured the CSF of 6 spectacle - corrected ammetropes. Subsequently, 3 of these subjects were corrected with hard (PMMA) lenses and 3 with soft (hydrophilic) lenses. The results showed that the CSF was attenuated with contact lenses compared to spectacles and that this attenuation in contrast sensitivity was higher at high spatial frequency and with soft contact lenses. Further studies have subsequently confirmed the high frequency attenuation as a result of soft lens wear.[160,161] More recently, Kirkpatrick and Roggenkamp[162] recorded the CSF on 38 eyes wearing soft contact lenses and again concluded that only the highest spatial frequency tested (ie 22.8 cpd) showed attenuation in the group. Conversely, the most recent study by Tomlinson and Mann[163] has agreed with earlier workers[164] that there was no significant loss of contrast sensitivity with soft lens wear. All these studies make the assumption that attenuation of the CSF during or after wearing contact lenses is due to corneal oedema; the

experimental section of this project (Chapter 3 and 4) investigates the effect of different types of contact lenses on the CSF and other related factors.

Two studies have measured the effect of artificially induced oedema on the CSF. Hess and Garner[89] found that induced oedema of 6% thickness change was sufficient to reduce the high spatial frequency portion of the CSF, while Hess and Carney[90] considered corneal oedema and a range of corneal pathologies and reported that high levels of oedema (11% thickness change) produced contrast attenuation for low as well as medium-high spatial frequency.

In summary, corneal oedema causes attenuation of the CSF. At high spatial frequencies, this could be due to optical defocus or/and increased light scattering. At low spatial frequencies, defocus is a very small factor and therefore contrast threshold attenuation will be due mainly to increased light scattering.

Ageing and Cataracts

Not only can the CSF measure the visual abilities of a 'normal' patient but it can also yield valuable information for a range of pathologies such as cerebral lesions,[147] macular disease[165] glaucoma[166] and amblyopia.[167] Some of these conditions are often associated with an older age group, in whom age related changes in the eye are likely to influence the results of visual function tests.

Many studies have been conducted over the last 15 years to consider the effects of age on the CSF, however, the results are contradictory. Most of the CSF tests have been conducted using oscilloscopes or TV monitors, however one test employs the use of printed grating patterns, specifically for use in clinical practice; and developed by Arden[168] (See Section 2.C.3). Some investigators have reported an age-linked loss of contrast sensitivity at all spatial frequencies,[169,170, 168] while others found attenuation at high and medium spatial frequencies only.[171-176] One group found losses only at low and medium spatial frequency.[177] It seems likely that this lack of agreement

between studies is attributable to a number of procedural differences in the type of equipment used, and to the small sample sizes in the majority of the studies. Six of the studies investigated visual performance in patients of more than 70 years.[169,170,173,175,176,177] Undoubtedly, the study of older normal subjects poses a number of difficulties for the investigator and a definition of 'normal' becomes more difficult with increasing age. The experimental section of this project will consider the effect of age on the CSF.

Several studies have been conducted on cataract patients with the use of laser interferometric principles and these will be considered in Section 2.C.2. However, a few studies have specifically measured CSF in relation to cataract patients. An early group of investigators measured the attenuation in CSF with simulated cataract[178] and found attenuation of high spatial frequencies with a "40% cataract". At a simulated "80% cataract" low spatial frequencies were also attenuated. Hess and Woo[179] were the first to record the CSF in cataract patients. They used 10 patients with uniocular senile cataract and found that 4 patients had only high spatial frequency attenuation and 6 patients had a depressed CSF over all spatial frequencies. Skalka[168] used the Arden gratings to measure the CSF in patients with early posterior subcapsular cataracts, a significant depression in contrast threshold was recorded on all the plates (spatial frequency range 0.2 to 6.4 cpd).

In summary, it appears that ageing and cataractous changes in the eye do depress the CSF and that this seems most apparent at the high spatial frequency end, however in some ageing studies and also in more advanced forms of cataract low spatial frequencies can also be attenuated.

2.C.2 Laser Interferometry Studies

Laser-generated sinusoidal grating patterns enable the direct measurement of the CSF between the retina and the brain, because interference fringes are immune to most sources of optical blurring in the eye. (Refer to Section 2.B.4) Laser fringes have been used to estimate the optical quality of the eye,[130,184] neural contrast sensitivity and neural acuity.[181,182,183] The most recent study measuring contrast sensitivity using laser generated gratings[184] employed psychophysical procedures to show that the mean contrast sensitivity for 6 observers at 60 cpd was more than a factor of 8 higher than the most sensitive previous estimates. This suggested that the neural visual system may be much more sensitive to fine detail than previously believed. Recently, Kayazowa, Yamamoto and Itoi[185]produced a study of the measurement of laser contrast sensitivity in a range of retinal diseases.

Clinically, laser interferometry is used mainly to estimate the integrity of the neural visual system in patients with optical defects such as cataract.[180,181,182,186,187] A developing cataract causes a gradual loss of vision. When the cataract has progressed to the point where the reduction in vision caused interference in normal activities even after optical correction, the only treatment is surgical removal of the lens. Good vision will be restored only if macular changes have not occurred prior to surgury. Lens opacities often make it difficult to detect such changes during ophthalmic examination, hence the clinical use of laser interferometry which projects the grating pattern directly onto the retina can give a prediction for the post operative vision which can be expected for a cataractous patient. Fig 2.8 shows a graph of results in cataract patient[186] for post operative Snellen letter acuities against preoperative laser fringe acuities (21 eyes). The extent to which the dots cluster around the line of unit slope indicates the correlation between the predicted and actually achieved acuities. 11 eyes in the operated group indicated a potential for good vision and 9 eyes either indicated poor potential or could not see the fringes. Post-operatively, all 11 eyes who could see the fine laser fringes went on to have good vision. Out of the 9 eyes where the test either indicated poor potential or was inconclusive, 2 eyes had better than poor vision. 5 of the eyes had acuities of 0.1 (6/60) or less.

Fig. 2.8 Graph of results for post-op. Snellen V/A plotted against pre-op. laser fringe V/A. Results for 21 eyes where lenses have been surgically removed. After Green[186]

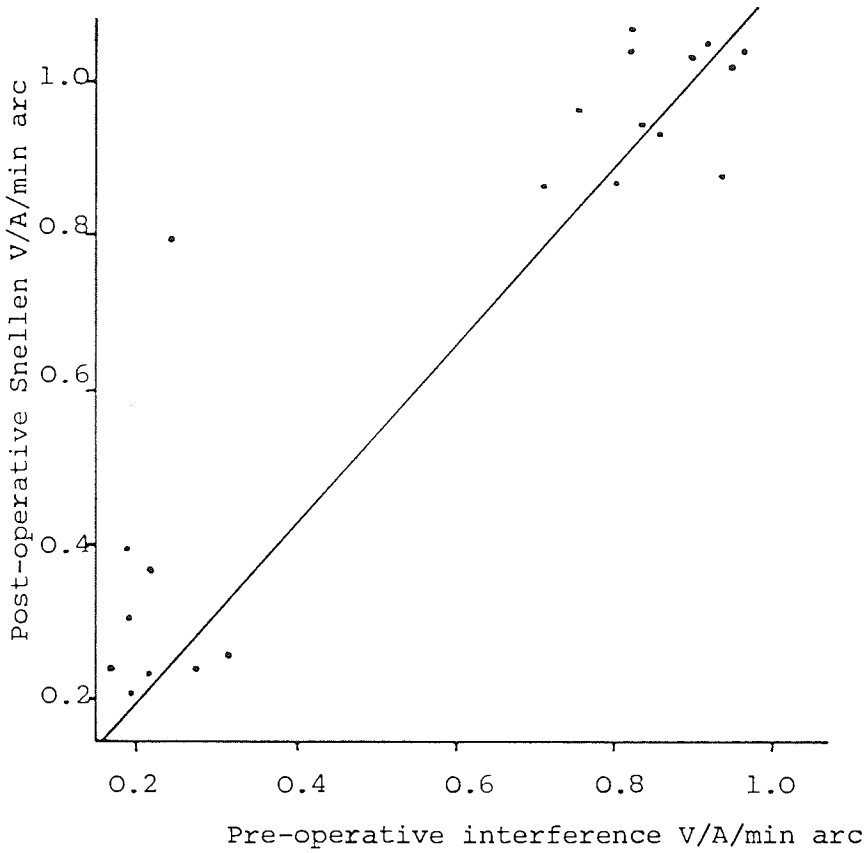

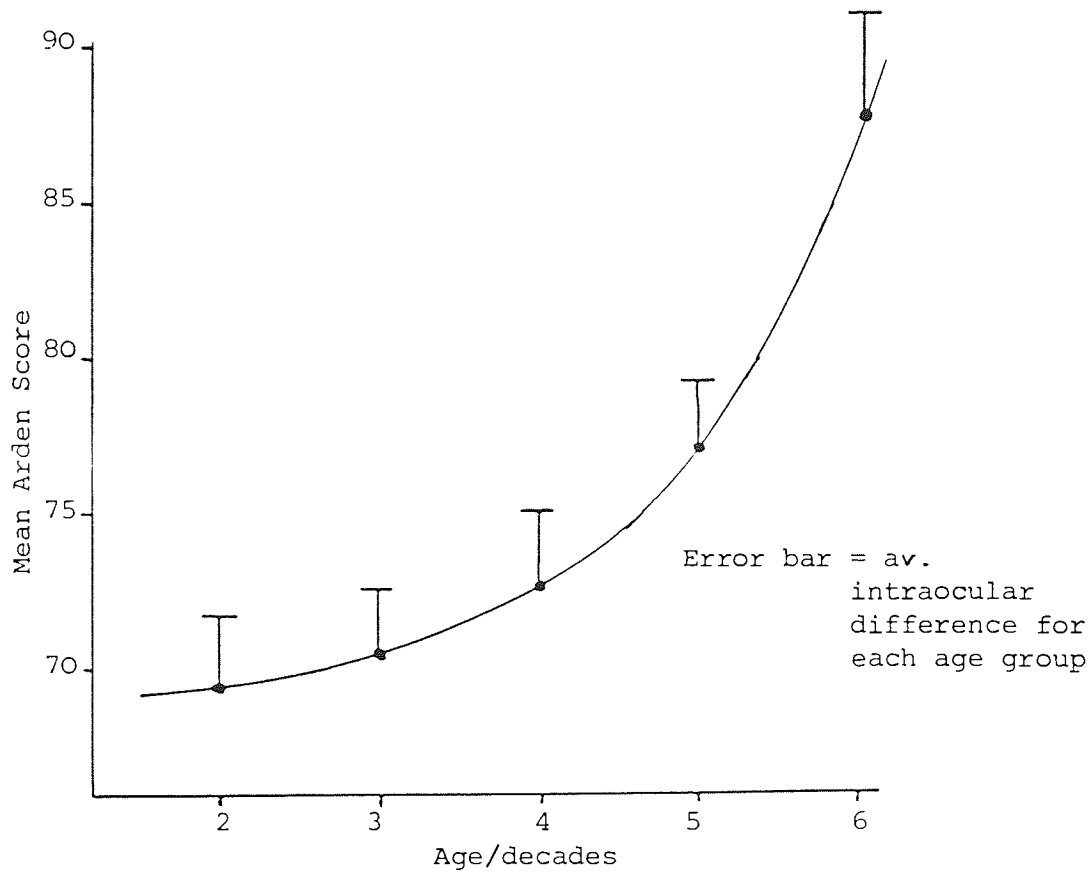

Fig. 2.9 Relationship between age and Arden Score. After Skalka[168]

Although some researchers reported poor correlation between V/A determined by interference fringes and that determined by Snellen acuity,[188,189] most work conducted on cataract patients[189,181,182,186,187] found good agreement between preoperatively determined laser fringe acuity and acuity found post-operatively. However, to produce regular fringe patterns on the retina behind an opaque lens, at least some portion of the coherent light must pass through the lens unscattered. It seems that the denser the cataract, the more difficult it becomes for patients to detect the regular fringes in the disordered pattern produced through the cataract. A clinically available interferometry technique is described in Section 2.C.3 and is applied in the experimental section of this project.

2.C.3 Clinical Applications of the CSF

The background and development of the CSF has been described in previous sections. Clearly, the CSF, as a statement of visual capabilities over a wide range of object sizes and contrasts has proved to be a valuable tool in the study of visual processing. However, results achieved in an experimental situation are not always possible or suitable in the clinical environment. Recently, the practical applications of the CSF have been reviewed.[190,191,192] This section describes 3 currently, clinically available applications of CSF measurement. Namely, the Arden Plates, the Nicolet CS 2000, and the Rodenstock Retinometer.

Arden Plates

Arden[127] has produced a booklet of printed gratings for CSF screening. The 6 gratings cover the low spatial frequency range 0.2 to 6.4 cpd which is considered sufficient to reveal neural defects while remaining unaffected by refractive error. The contrast decreases from the bottom to the top of each page, and the point at which the grating is first seen is measured on a scale at the side. The results are usually presented as the sum of the scores from the individual gratings. This "Arden score" is raised by a defect in contrast sensitivity. It has been suggested that the accuracy of this method can be improved by the presentation of the gratings in a 4 alternative 'forced choice' format.[193] Printed gratings would not be the method of choice for detailed research, due to the difficulties in standardisation of luminance and field size and the limited information provided by the method of scoring. However, they can be useful in a clinical setting for the identification of patients who would benefit from further investigation. The use of the Arden Grating Test (AGT) in optometric practice has recently been assessed by Yap, Grey, Collinge and Hurst.[194]

Despite the drawbacks of the Arden plates some research has been carried out with regard to ageing and the effects of cataracts. Skalka[168] conducted the AGT on 100 patients ranging in age from their 2nd to their 6th decade, a clear increase in test scores (decrease in contrast sensitivity) was found with

increasing age. (See Fig 2.9) and the results show that contrast thresholds rise with age despite good visual acuity. Sokol et al[174] conducted a similar study and their results reinforced those of Skalka[168] moreover, a high false positive rate was found using the AGT in subjects over age 50, emphasising the need for age-matched "normal" standards. In 1981, Skalka[195] followed up the earlier work and investigated 122 eyes of patients with early, posterior, subcapsular cataracts. A loss of contrast sensitivity was found in the patients although, again visual acuity was normal. An increasing AGT score with age was again reported.

The Nicolet CS2000

The Nicolet CS2000 Contrast Sensitivity Testing System is a clinically available, easily operated instrument for the rapid assessment and screening of visual function. The CS2000 consists of a display monitor, a keyboard control console and an observers response box. (see Fig 2.10). In the last few years, the use of the CS2000 in assessing contact lenses has been described.[162,163,196] Features are built into the CS2000 to ensure ease and flexibility of calibration, use and programming, a simple calibration procedure is available to the operator that requires no additional instruments. During testing the contrast threshold level and standard deviation (SD) are automatically calculated and printed out at any desired time. The Standard Test available consists of 8 separate trials, each of which presents a single static sinusoidal grating, the spatial frequency range is 0.5, 1,3,6, 11.4 and 22.8 cpd and the psychophysical method used is Bekesy Tracking using a logorithmic increase (and decrease) in contrast from 0 to 100% in a 30 secs ramp. A range of targets, working distances and psychophysical procedures is available.[197] These variables have been extensively investigated with reference to the clinical suitability of any such procedure.[198,199,200] The CS2000 is utilised in the experimental section of this project (Chapter 3) and currently provides an easily used method of measuring contrast sensitivity over a range of spatial frequencies.

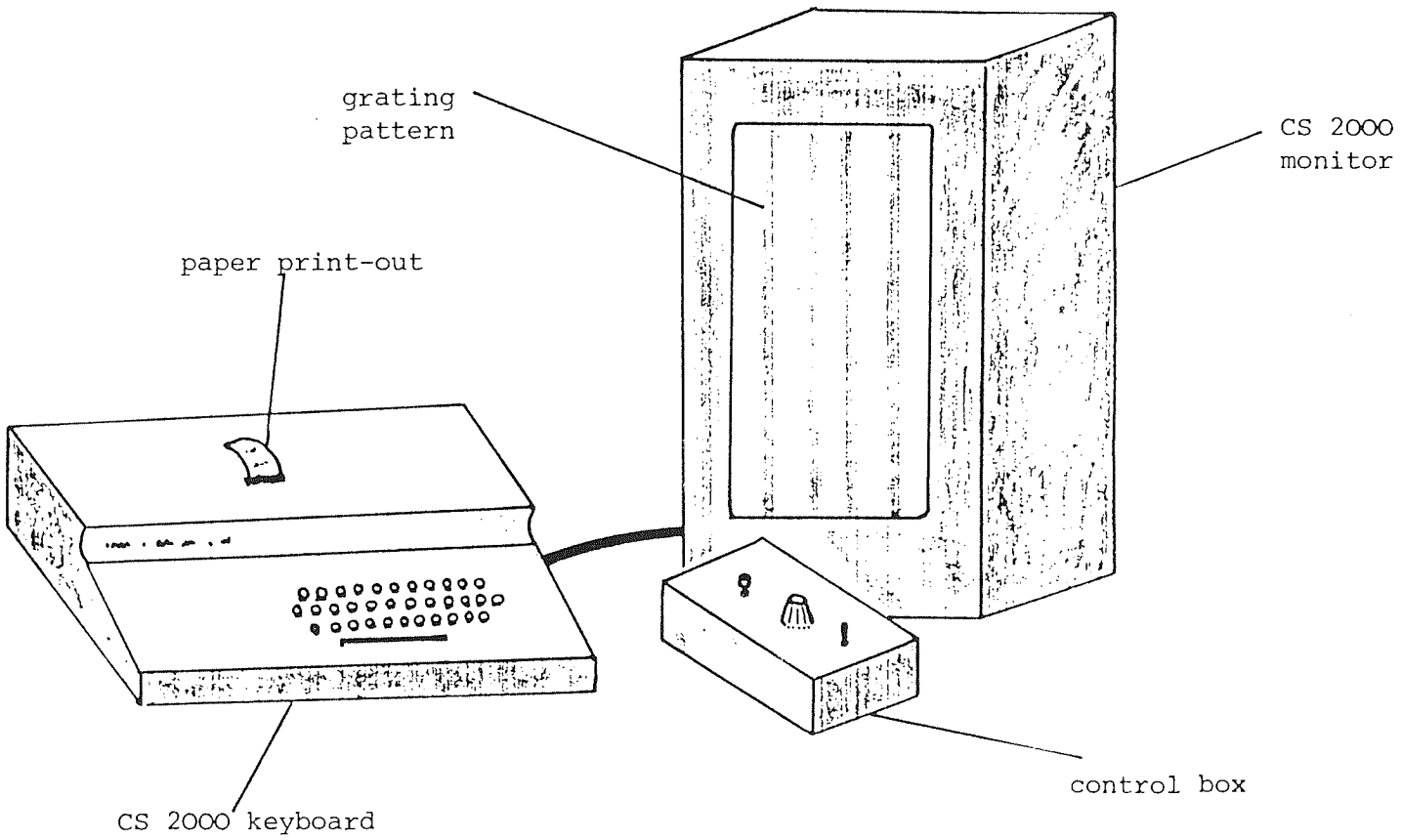

Fig. 2.10 The Nicolet CS 2000 Contrast Sensitivity Testing System

Rodenstock Retinometer

The principles of laser interferometry on which the Retinometer is based are described in previous sections (ie 2.B.4 and 2.C.2). The Retinometer provides a simple clinically available technique for the measurement of retinal visual acuity in the presence of opacities of the ocular media.[201] The equipment can be easily mounted on a slit-lamp. The examiner focuses the 2 small red dots in the pupil of the patient's eye by moving the slit-lamp joy stick (see Plate 2.1). The patient should see a series of high contrast red and black stripes. The spatial frequency range is 1 to 33 cpd, available at 2 luminance levels. The orientation of the fringes can be altered to 4 positions, ie vertical, horizontal and 2 oblique settings. The task of the patient is merely to report the presence of the red and black stripes and their orientation. In this way the retinal visual acuity may be obtained, comparison with conventional Snellen acuity will give a measure of visual loss due to the optical media. Furthermore, the Retinometer provides a simple and quick measure of visual function dependent only on patient recognition of the pattern.[201] The Retinometer is applied in the experimental section of this project.

Plate 2.1 shows the Rodenstock Retinometer in use

R = Retinometer

S = Slit-lamp mounting

P = Patient

E = Examiner

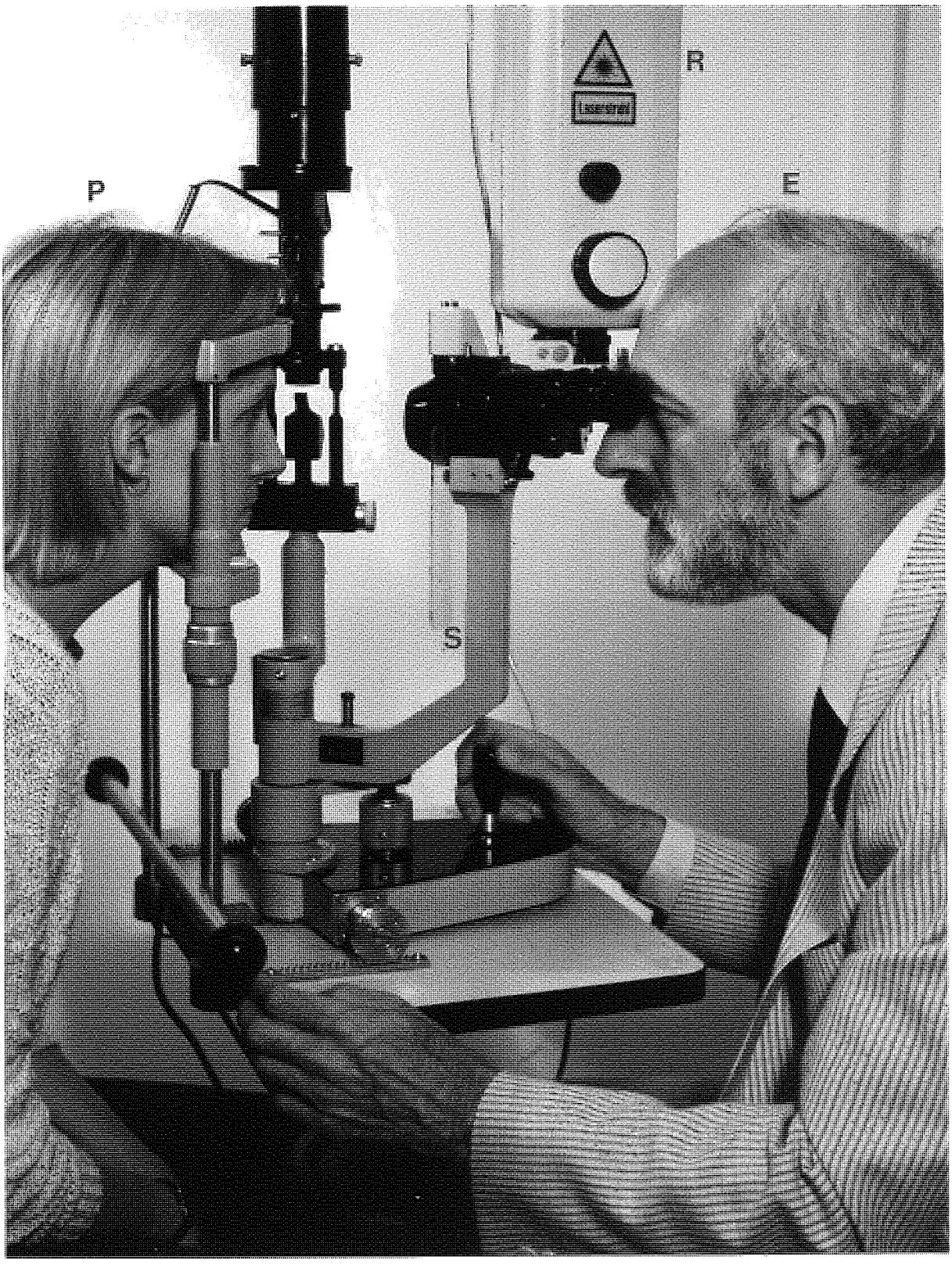

Plate 2.1

CHAPTER 3

GENERAL METHODS OF INVESTIGATION

Aims of the Project

3.1 Psychophysical Measures

3.1.A The Nicolet CS2000 - Modifications to the Standard System

3.1.A.1 Working Distance

3.1.A.2 Masking Surround

3.1.A.3 Grating Presentation

3.1.A.4 Psychophysical Techniques of Measurement

3.1.B The Addition of Glare Sources during Contrast Threshold Recordings

3.1.B.1 Measuring the Intraocular Light Scatter Effect

3.1.C The Rodenstock Retinometer - Modifications to the Standard System

3.1.C.1 Psychophysical Test Methods

3.1.C.2 Spatial Frequency Range

3.1.C.3 Projected Gratings Paradigm

3.2 Physical Measures

Pupil size

Corneal Thickness

3.3 Subject Groups

Aims of the Project

The object of the clinical experiments was to investigate, establish and quantify the relationship between contrast sensitivity, intraocular light scatter and glare. The aim was to establish the effects on vision, so that a more comprehensive understanding of the visual world of subjects prone to increased light scatter in the eye was possible. As such, the experiments are aimed particularly at the clinical environment.

The hypothesis was that intraocular light scatter was higher in certain groups of people eg. the elderly, and that the visual disability caused was not reflected in currently available vision tests or in the ophthalmic examination, as such subjects often have good V/A and seemingly clear media. In fact the ocular media will have increased turbidity and this will be demonstrated by reduced contrast sensitivity, particularly in the presence of a glare source, as a result of a decrease in retinal contrast.

Having first established the most suitable and consistent measurement method for recording contrast thresholds using clinically available equipment, the Nicolet CS2000 (Experiment 1). A pilot study quantified the connection between intraocular light scatter (as recorded by LSFs), glare angle and age (Experiment 2(i)). Subsequently, further studies measured LSFs with respect to the CSF and age in a large subject group (Experiment 2(ii)) and measured LSFs in subjects with induced corneal oedema (Experiment 3), and in subjects wearing three types of corneal contact lenses (Experiment 4).

Finally, it seemed desirable to investigate a commercially available optic bypass technique (the Rodenstock Retinometer) which is specifically designed to separate neural resolution from the effects of optical degradation.

3. General Methods of Investigation

3.1 Psychophysical Measures

3.1.A The Nicolet CS2000

The Nicolet CS2000 is a Contrast Sensitivity Testing System designed primarily for clinical use. It consists of a computer-controlled waveform generator displaying vertical sine wave gratings onto a video monitor. The Standard Test and description of this equipment has been reviewed in Section 2.C.3 and further details of standard procedures can be found in the accompanying manual.[197] The use of the CS2000 in this project involved substantial modifications to the standard system and methods in order to carry out 2 procedures:

(i) To investigate psychophysical techniques of measurement of contrast threshold and to identify the most suitable measurement method (ie Experiment 1).

(ii) To apply this measurement technique to investigate the effects on contrast threshold of glare sources which accentuate the effect of intraocular light scatter. (ie Experiments 2, 3 and 4)

Factors affecting contrast threshold and CSF measurements have been reviewed in Section 2.B while Sections 1.F and 1.G have summarised previous work conducted on the quantification of glare and light scatter. These Sections should be referred to in connection with the following explanation of experimental design using the CS2000.

Modifications to the Standard System of the CS2000 for use in this Project (Refer to Figs 3.1, 3.2 and Plates 3.1 and 3.2)

3.1.A.1 Working Distance

All contrast threshold measurements were recorded with the subject seated at 3m from the monitor. This was considered an appropriate distance for the following reasons. If the working distance were greater than 3m the target field size would be reduced to the point where low spatial frequency results

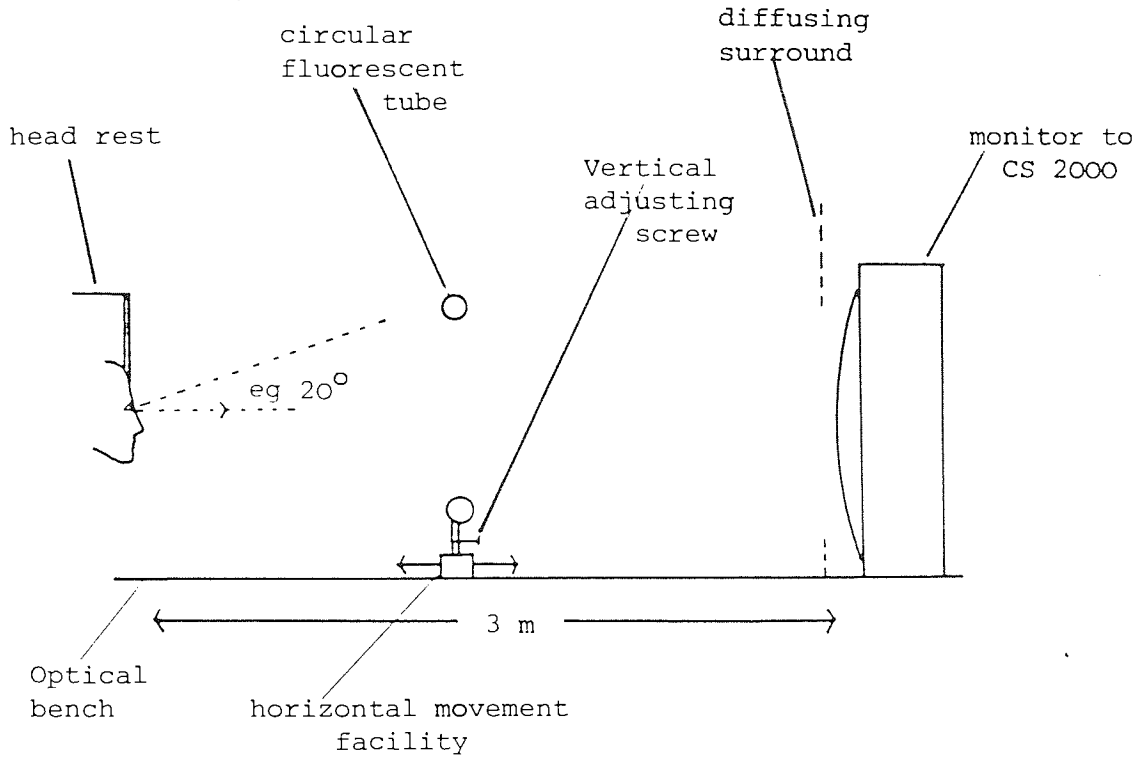

Fig. 3.1
Showing experimental arrangement for measuring the effect of circular glare sources of various radii on the contrast threshold as measured with the CS 2000.

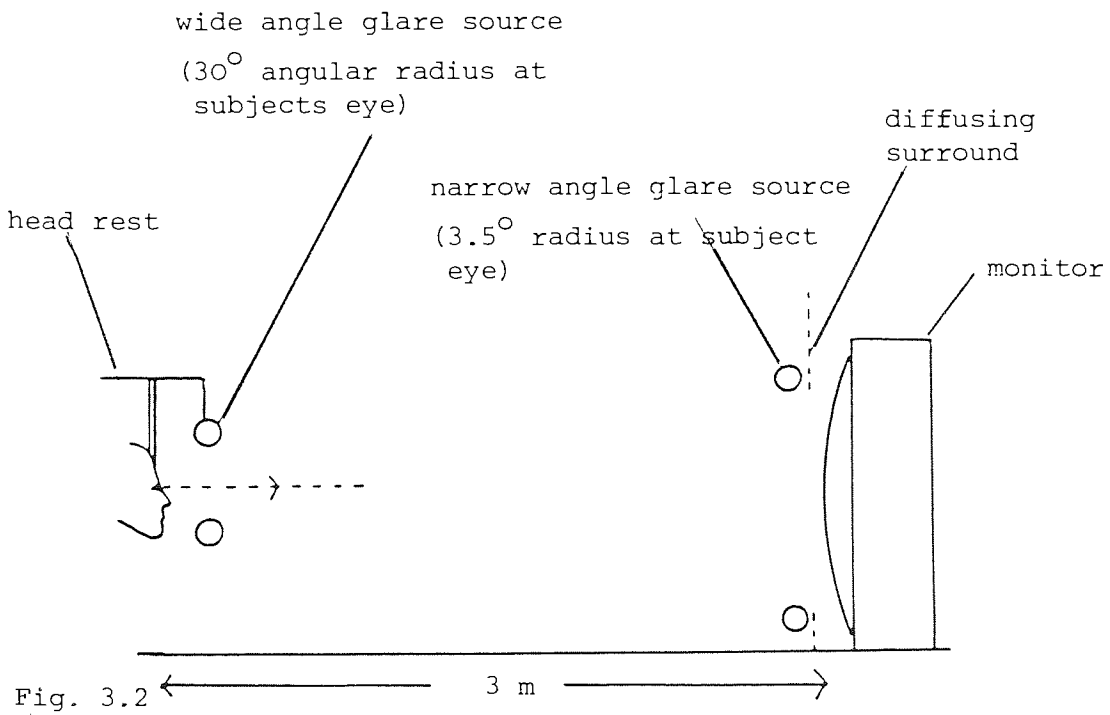

Fig. 3.2
Experimental arrangement for the measurement of contrast threshold using glare sources (circular fluorescent tubes) subtending either 30° or 3.5° angular radius.

Plate 3.1 shows the experimental arrangement for measuring the effect of a 3.5° glare source on contrast thresholds

G = 3.5° radius glare source

N = Nicolet CS2000 computer

C = Control box

M = Monitor

Plate 3.1

Plate 3.2 shows the experimental arrangement for measuring the effect of a 30° radius glare source on contrast thresholds

G = 30° radius glare source

N = Nicolet CS2000 computer

C = Control box

M = Monitor

Plate 3.2

ie 1cpd, would be attenuated.[134,141,142]

Alternatively, a working distance of less than 3m meant that the raster of the monitor was visible to the subject and would interfere with threshold measurements, particularly at high spatial frequencies. A 3m distance was also convenient because the apparatus could be easily incorporated into a conventional consulting room.

3.1.A.2 Masking Surround

The monitor screen was masked by means of adding a circular diffusing surround immediately in front of the monitor, illuminated from the rear and providing a surround approximating the mean luminance of the displayed gratings. This was designed to avoid raised contrast thresholds due to edge effects and phase differences.[134,138,139,141] Under these conditions the circular grating field of 94.5 cd/m^2 mean luminance subtended an angular radius of 2°.

3.1.A.3 Grating Presentation

Static gratings are used in the standard system however, in this project counterphase gratings of 2Hz were used with all experiments with the CS2000 (ie Experiments 1 to 4). This was a preferable presentation technique in order to reduce the subject's confusion due to after images. Moreover, a 2Hz rate provided a criteron - dependent target that approximated to the normal sampling rate of the eye.[121,122,143] A low spatial frequency value of 1 cpd was chosen as the fixed target spatial frequency for all experiments involving glare sources. This value avoids attenuation due to optical blur and hence enables intraocular light scatter due to the optic media to be studied in isolation. (Refer to Section 2.B.3). Other spatial frequency values ie 3,6 and 11.4 cpd also counterphasing at 2Hz were used in Experiments 2(ii) and 4 in order to record the CSF.

3.1.A.4 Psychophysical Techniques of Measurement

The standard manual system uses the Bekesy method with a logarithmic ramp rate of 30 secs. For this project the Method of Increasing Contrast (MIC) and a 60 sec ramp rate was chosen for the investigations utilising glare sources. (ie Experiments 2,3, and 4) The use of this psychophysical measurement technique was decided on from the results of Experiment 1 where three measurement techniques and four ramp rates ie 15, 30, 60 and 120 sec were investigated with the standard grating format (ie 1cpd and 2Hz counterphase).

The techniques were:

(i) Bekesy Method

(ii) Method of Increasing Contrast (MIC)

(iii) Method of Decreasing Contrast (MDC)

These are described as follows:

(i) Bekesy Method

In order to measure contrast threholds using this method the subject viewed the monitor screen at zero contrast. When the trial started, the target grating increased in contrast logarithmically, from 0% to 100% in the given time period alloted eg 60 secs. When the subject just saw the required target the control switch was depressed, at this moment, the contrast started to decrease logarithmically at the same rate; when the contrast had decreased to the point where the subject could no longer perceive the target, the control switch was released. This procedure was repeated 4 times giving a total of 8 threshold readings (4 ascending and 4 descending contrasts). The CS2000 computer printed out each individual reading and the mean and standard deviation (SD). For each spatial frequency tested and each Bekesy ramp rate used, this procedure was followed, hence 8 threshold readings were averaged for each individual condition.

(ii) Method of Increasing Contrast (MIC)

The MIC paradigm uses the same ascending ramp as the Bekesy method. Accordingly the subject initially viewed the monitor at zero contrast. When the trial started, the target contrast increased at the alloted logarithmic rate (eg 30 secs from 0% to 100% contrast). When the subject just saw the target the control switch was depressed, causing the contrast to return to zero and allowing the next observation to be made. For each subject and each test condition, four consecutive observations were recorded in this way. The CS2000 computer recorded the contrast threshold level of each observation with the mean and standard deviation (SD).

(iii) Method of Decreasing Contrast (MDC)

The MDC paradigm uses the same descending ramp as the Bekesy Method. The subject viewed the target at a high contrast, well above threshold, hence the target was clearly visible. The trial started when the subject depresses the control switch at which point the contrast started to decrease at the alloted rate. When the subject could just no longer see the target, the control switch was released, causing the contrast to return to a high contrast level allowing the next threshold measurement to begin. For each subject and each test condition, four consecutive observations were taken in this way. Means and SDs were recorded.

Criteria of Observation

In order to record the contrast thresholds, each subject seated at 3m held a control box with the control switch. All the experiments in this project using the CS2000 used a target that was a vertical counterphasing sine wave grating. This was in preference to static grating targets as in the Standard system where the after image problem was more acute and likely to increase the errors of measurement. However, the use of counterphase targets meant that the subject saw 2 phenomena ie the presence of the grating and the fact that it is moving. It was critical throughout the experiments to standardise the criteria of observation used for deciding both when a target was 'seen' and when it was 'not seen'. Accordingly, during the use of ascending contrast targets both the counterphase

movement and the presence of the grating had to be detected before the subject pressed the control switch to record the contrast threshold level. Similarly, on descending contrast targets both the counterphase and the presence of the grating had to disappear before the subject release the switch to record the descending threshold level. Written instructions were given to each subject to this effect (See Appendix).

3.1.B The Addition of Glare Sources during Contrast Threshold Recordings.

Contemporary literature on the CSF[119,137,158] has largely failed to consider the effect of intraocular light scatter and glare mechanisms on contrast threshold measurements, with subsequent effects on the visual world of the patient. It is rare that room lighting is quantified during CSF measurements. Even if a luminance value is stated, the effects of room lighting, in that it will increase intraocular light scatter because it is a surrounding glare source has never been investigated in this context.

Particular patient groups are especially susceptible to light scatter and glare effects with subsequent attenuation of the CSF. Much has been written about contrast threshold changes due to ageing processes[167,170], cataractogenesis[168,179] and corneal oedema[162,163] (refer to Section 2.C) but none of these studies have fully considered and quantified the role of intraocular light scatter on CSF results. The addition of glare sources during the measurement of contrast threshold would enhance the effect of intraocular light scatter (See Section 1.F and 1.G)

Accordingly, during this project, as well as the modifications to the Standard system of the CS2000 that were incorporated as described above, additional glare sources were added to the apparatus for the investigation of contrast threshold attenuation as a result of intraocular light scatter. Three separate glare arrangements were used during the project and these are described below. The first two glare conditions were provided by circular fluorescent tubes concentric with the monitor from the viewing position, providing an annulus of glare light.

Glare Conditions

(i) The first glare arrangement, shown in Fig 3.1 and used in the pilot study of Experiment 2, was a single circular fluorescent tube which could be move horizontally and vertically along an optical bench between the subject's eye and the CS2000 monitor. By this arrangement contrast thresholds (at 1 cpd and 2Hz counterphase) were recorded for each subject in the presence of the circular glare source

subtending each of a range of glare radii at the subject's eye. ie 50°, 30°, 20° and 5° and also without a glare light. The largest glare angle (50°) was used first and then the smaller glare angles in order that there was no risk of after images interfering with contrast threshold measurements. The 5 glare radii used enhanced the effects of intraocular light scatter and were also used to demonstrate the dependence of light scatter on glare angle.

(ii) The second glare arrangement, (See Fig 3.2, Plates 3.1 and 3.2) employed the use of 2 fixed circular glare sources ie a narrow angle glare source (subtending 3.5° radius at the subject's eye) and a wide angle glare source (subtending 30° radius). Contrast thresholds (at 1cpd, 2Hz counterphase) were recorded on each subject with each of the glare sources and without the glare source (See Experiments 2, 3 and 4). The 2 glare sources were chosen to enhance the effects of intraocular light scatter and to show the influence of glare angle on contrast threshold results. Also demonstrated are 2 light scattering mechanisms. The 30° glare source enhancing wide angle, Rayleigh type scattering effects and the 3.5° glare source enhancing narrow angle scattering which will be a combination of Rayleigh scattering, diffraction and in the presence of corneal epithelial oedema will cause haloes to fall within the viewing field, hence further attenuating threshold results.

Circular glare sources were used in glare conditions (i) and (ii) as they gave a uniform glare distribution[196] as opposed to previous studies where point glare sources were employed.[98,102] Most recently, Van den Berg[202] has also adopted an annulus glare design with a flickering target.

(iii) As well as visible light being scattered in the ocular media. Both cornea and especially the lens are endowed with an intrinsic fluorescence which increases with ageing. (Refer to Sections 1.C.2 and 1.D). This fluorescence causes increased light scatter and its effect will be enhanced by the use of a near U.V/blue light source. In order to investigate this phenomenon a Burton "Black light" Lamp as used in contact lens fitting (see Appendix for spectral distribution) was placed in between the subject's eye and the CS2000 monitor at the same position as the 30° glare source (See Fig 3.2). A neutral

density filter was placed in between the 2 parallel UV light tubes instead of the +5D lens, in order to reduce the monitor screen luminance to 2.7 cd/m^2. This was done in order to increase the sensitivity and to demonstrate the fluorescent effect. Contrast thresholds were recorded with and without the UV light on (See Experiment 2).

3.1.B.1 Measuring the Intraocular Light Scatter Effect

Having measured the contrast threshold for each subject with and without each particular glare source. The equation of Paulsson and Sjostrand[98] is applied (See Section 1.F.2) to calculate a Light Scatter Factor (LSF) which is a direct measure of forward intraocular light scatter. The LSF is calculated for each experiment and glare condition (See Results Section in Chapter 4).

3.1.C The Rodenstock Retinometer - Modifications to the Standard System

Section 2.C.2 reviewed the literature concerning laser generated grating patterns like those of the Retinometer. Most of the research has been aimed at estimating the integrity of the visual system in patients with media opacities eg cataract. This has usually been done using high contrast fringes. Using such an optic bypass system has made it possible to estimate post-operative visual acuity (V/A).[181,182] By comparing laser fringe V/A with conventional Snellen V/A measurement in cataract patients the optical (media) component of V/A has been assessed.

ie TOTAL V/A = OPTICAL FACTORS + NEURAL FACTORS
(eg media opacities and defocus)

↓ ↓

AS MEASURED BY SNELLEN V/A

AS MEASURED BY RETINOMETER (an optic bypass system)

Many such studies have been conducted in this way on patients with dense cataracts. However, such a system has not been used to evaluate earlier media changes eg associated with ageing (Refer to Section 1.D).

The main study in this project considered lens and corneal light scatter, using a low spatial frequency in order to avoid optical defocus. A small study has been conducted here, using a modified Retinometer procedure in order to evaluate optical and neural resolution with ageing incorporating early media change, as such this utilises high spatial frequencies.

Like the Nicolet CS2000, the Retinometer is a clinically available instrument used for recording retinal (neural) V/A, this is especially useful for acuity assessment in the presence of media opacities. Plate 2.1 shows the Retinometer in use. Section 2.B.4 desribed the principle of operation. The equipment is mounted on a slit-lamp where the subject views a series of high contrast red and black fringes, through a circular aperture subtending a 2.75° radius with a black surround. The mean luminance of the fringes can be set at 12 cd/m^2 or at 40 cd/m^2 in the case of large amounts of media opacity. The spatial frequency range is 1,2,4,6.6,10.6,13.2,16.5,20.8,26.4 and 33 cpd, the fringe

pattern orientation can be altered by the examiner to horizontal, vertical or inclined at 45° or 135°. The mean luminace and/or spatial frequency may also be changed by the examiner at any stage. The subject's task is to say whether or not the fringe pattern is visible and if so to state it's orientation. The finest grating resolved by the subject is a measure of the retinal V/A. Details of the standard procedure may be found in the accompanying manual.[201]

For use in this project, a number of modifications were made to the standard procedure of the Retinometer. These were the following; 2 separate 'forced-choice' psychophysical test methods were used and compared namely the "Shutter Method" and the "5 sec Method". These were employed in order to increase the accuracy and reliability of results that would normally be obtained from the standard viewing system. Secondly, only the highest 4 spatial frequencies were used during testing, this was due to the fact that all the gratings available were presented at high contrast, since it was the end point V/A being assessed, the 4 highest spatial frequencies would account for this. Thirdly, in order to investigate the end point of V/A both with an optic bypass (Retinometer) and a non-optic bypass system, the latter was constructed by means of a conventional projection system. Hence the appearance of the Retinometer grating patterns was copied. In this way it was possible to adapt the Retinometer in order to contrast and compare 2 psychophysical test methods and 2 methods of measuring end point V/A by means of an optic bypass ie Retinometer system (which projects the grating pattern directly onto the retina and is not effected by optic blur and minimally effected by intraocular light scatter) and by means of a non-optic bypass ie Projected System, (which will be effected by optical blur and intraocular light scatter). The details of these changes to the standard design are listed below. Both systems used a 12 cd/m^2 mean luminance value.

3.1.C.1 Psychophysical Test Methods

(i) Shutter Method

A free fall plastic shutter was placed between the Retinometer aperture and the subject. The shutter exposure duration was recorded at 30m sec by the use of a photo-cell and an averager with an X-Y recorder. Each pretrained subject viewed the grating as exposed by the shutter, the lowest spatial frequency ie 16.5 cpd was used first. The subject reported the presence and orientation of the grating. If a correct answer was given, the next highest spatial frequency was used and the procedure repeated, any of the 4 grating orientations were chosen at random by the examiner. More than 2 incorrect answers and the procedure was stopped, the last correct answer being recorded as the highest spatial frequency resolved. Hence the shutter provided the examiner with a forced choice psychophysical procedure with a 1 in 4 guess factor.

(ii) 5 Sec Method

With this psychophysical test method, the subject was allowed to view the target grating for a maximum of 5 sec, at which time the subject had to give an answer stating grating orientation. If there were more than 2 incorrect answers, the trial was stopped. The last (highest) spatial frequency to be answered correctly was taken as the end point V/A.

3.1.C.2 Spatial Frequencies

Unlike the Retinometer Manual system[201] only the 4 highest spatial frequencies were applied in this project ie 16.5, 20.8, 26.4 and 33 cpd, using both psychophysical procedures. The lowest spatial frequency was presented first (ie 16.5 cpd) at any of the 4 grating orientations. When the subject gave a correct response the next grating was presented ie 20.8 cpd and so on.

3.1.C.3 Projected Grating Paradigm

In order to compare the end point V/A with and without an optic bypass system, the appearance of the gratings in term of colour, spatial frequency, mean luminance, field size and black surround was

copied, using a conventional projection system with high contrast black and white slides mounted in any of the 4 orientations and applying a red monochromatic filter matched as closely as possible to the He-Ne laser colour (see Appendix). The procedure using the Retinometer, was repeated for the projected gratings paradigm and the 2 psychophysical test methods were applied in the same way. The results for end point V/A with both psychophysical methods and both grating presentation systems ie Retinometer and Projected systems are discussed in Chapter 4.

3.2 Physical Measures

Pupil Size

Pupil diameters were recorded for all subjects in Experiment 2 without glare and in the presence of the 3.5° and 30° glare source. The measurements were taken by eye twice, using an optical ruler to the nearest 0.5 mm.

Corneal Thickness

In Experiment 3, corneal thickness was recorded both initially and during the recovery from corneal oedema. Corneal thickness measurements were taken with a Haag-Streit pachometer and slit-lamp mounting using the modification of Mishima and Hedbys[203] to ensure perpendicular alignment of the illumination slit. Corneal thickness measurements were initially recorded prior to scleral lens insertion on each subject. Corneal oedema was induced as described in Experiment 3 and pachometry measurements were recorded continuously for 15 min following scleral lens removal. Each thickness measurement recorded was the mean of 5 consecutive settings, SDs and SEs were calculated.

3.3 Subject Groups

All subjects used in this project were tested monocularly with their preferred eye, had a V/A of 6/9 or better, wore a distance correction (spectacles) if required unless otherwise stated, and were without evidence of ocular disease. All subjects were pre-trained and familiarised with what was expected in each test. The written instructions given to each subject are described in the Appendix.

Experiment 1 and Pilot Study for Experiment 2

12 subjects took part in both of these experiments. The age range covered was 23 to 75 years. These could be split into 2 age range groups ie 6 subjects with ages 23 to 38 called the 'young' group and 6 subjects with ages 51 to 75 called the 'old' group. All the subjects were paid volunteers and trained visual observers who were either students or staff of the Vision Sciences Department or senior citizens who attended the department weekly to provide subjects for undergraduate optics clinics. The experiment lasted about 30 min.

Experiment 2

54 subjects took part in this experiment. The age range was 18 to 81 years. Subjects were chosen at random from the Ophthalmic Optics Clinic that served the staff and students at Aston University. The subjects were divided into 3 age groups with 18 in each group ie the 'young' group age 18 to 42 years, the 'intermediate' group age 43 to 61 years and the 'old' group age 62 to 81 years. All subjects were paid volunteers. The experiment lasted approximately 45 mins.

Intraocular Fluorescence A total of 18 subjects took part. 10 subjects were aged 61 to 82 years called the 'old' group, and 10 subjects were aged 19 to 27 years called the 'young' group, spectacles were not worn as this would attenuate U.V. reaching the eye. V/As were 6/12 or better. All subjects were paid volunteers, and the test lasted approximately 20 mins.

Experiment 3

7 subjects took part in this experiment. They were all emmetropic and aged 20 to 24 years. They attended on 3 occasions, firstly to be fitted with a sealed scleral contact lens on one eye, secondly, to carry out the experiment and record contrast thresholds on recovery from oedema and finally to repeat the experiment and measure corneal thickness during oedema recovery. Each occasion lasted approximately 45 mins. All subjects were student ophthalmic opticians and paid volunteers.

Experiment 4

A total of 35 subjects took part including a clinical sample of contact lens wearers. 10 subjects wearing gas permeable (GP) contact lenses. 11 subjects wearing soft contact lenses and 7 subjects wearing hard (PMMA) contact lenses, plus 7 subjects who did not wear contact lenses as a control group. All subjects were aged 18 to 26 years, and were paid volunteers. The clinical details are listed, and the experiment lasted approximately 45 mins.

Experiment 5

28 subjects took part. 14 subjects aged 60 to 80 years called the 'old' group, and 14 subjects aged 20 to 27 years called the 'young' group. All subjects were paid volunteers, the test lasted approximately 25 mins.

CHAPTER 4

THE EXPERIMENTS, RESULTS AND DISCUSSION

Using the Nicolet CS2000

4.1 Experiment 1.

Assessment of techniques for measuring contrast threshold.

4.1.1 Results
4.1.2 Discussion

4.2 Experiment 2

(i) Pilot study investigating the relationship between glare angle, intraocular light scatter and age.

4.2.1 Results
4.2.2 Discussion

4.2.3 (ii) A study of the effect of intraocular light scatter and ageing on the CSF.

4.2.4 Results
4.2.5 Discussion

4.3 Experiment 3.

The effect of epithelial and stromal oedema on the light scattering properties of the cornea.

4.3.1 Results
4.3.2 Discussion

4.4 Experiment 4.

The effect of corneal contact lens wear on the CSF and on the light scattering properties of the contact lens/corneal interface.

4.4.1 Results
4.4.2 Discussion

Using the Rodenstock Retinometer

4.5 Experiment 5.

The variation of end point V/A with age using an optic bypass (Retinometer) and non optic bypass (Projected) matched systems and 2 psychophysical procedures.

4.5.1 Results
4.5.2 Discussion

4.1 Experiment 1

Assessment of Techniques for Measuring Contrast Threshold

This first study investigated the effect of 3 psychophysical techniques of measurement on contrast threshold. The aim was to conclude the best and most consistent measurement method to use when recording thresholds with the CS2000 and to apply this technique of measurement on subsequent experiements investigating intraocular light scatter in the presence of glare sources.

The apparatus and modifications involved in the use of the CS2000 have already been examined (See Section 3.1.A). No glare sources were used in this experiment. Fig 3.1 shows the experimental arrangement, with the subject seated at 3m from the monitor and holding the control box. 3 psychophysical techniques of measurement (See Section 3.1.A.4) that is Bekesy method, MIC and MDC were used with 4 ramp rates ie 15,30,60 and 120sec along with the standard 1 cpd and 2Hz counterphase target grating.

4.1.1 Results

The results are presented in 3 tables (ie Tables 4.1, 4.2 and 4.3) and in Figs 4.1, 4.2 and 4.3. Table 4.1 shows the individual contrast threshold mean, standard deviation (SD) and standard error (SE) for each subject for the 3 techniques of measurement at a 60 sec ramp rate. Also listed is each subject's age in years at the time of testing. Table 4.2 shows the data, pooled across the 12 subjects for the threshold mean, SD and SE for each of the 3 measurement techniques at the 4 ramp rates used (note that the averaged data for the 60 sec ramp is the same as in Table 4.1).

Fig 4.1 shows each individual threshold result (at a 60 sec ramp) plotted against each subject's age. It can be seen from the spread of results that none of the 3 techniques is age dependent although for each individual the MIC always gives the smallest and MDC the largest threshold value. Recent work by

Table 4.1

Log. contrast threshold mean, SD and SE for three psychophysical techniques of measurement at a 60 sec ramp rate. Data are shown for each subject along with age.(in years)

subject	Age	BEKESY Mean	BEKESY SD	BEKESY SE	MIC Mean	MIC SD	MIC SE	MDC Mean	MDC SD	MDC SE
CT	23	2.42	0.26	0.092	2.19	0.068	0.034	2.66	0.15	0.078
JF	24	2.05	0.24	0.085	1.82	0.036	0.018	2.29	0.068	0.034
SG	25	2.23	0.31	0.11	1.95	0.064	0.032	2.50	0.19	0.095
DB	36	2.19	0.28	0.099	1.92	0.026	0.013	2.46	0.11	0.055
BG	37	2.27	0.25	0.089	2.03	0.034	0.017	2.51	0.087	0.044
LJ	38	2.14	0.21	0.074	1.94	0.091	0.046	2.33	0.077	0.039
MW	51	2.02	0.23	0.081	1.82	0.077	0.039	2.23	0.13	0.065
ND	53	2.19	0.28	0.099	1.92	0.050	0.025	2.46	0.12	0.060
PP	55	2.17	0.23	0.081	1.95	0.034	0.017	2.40	0.035	0.018
MH	72	1.87	0.20	0.071	1.71	0.12	0.060	2.03	0.13	0.065
ML	74	2.02	0.22	0.078	1.83	0.066	0.033	2.22	0.11	0.055
MSL	75	2.28	0.20	0.071	2.12	0.080	0.040	2.45	0.14	0.070
Average Intrasubject results		2.15		0.086	1.93		0.031	2.38		0.057

Fig. 4.1 Shows log. contrast threshold measurements for all 3 psychophysical techniques of measurement at a 60 sec ramp rate, plotted against each subject's age

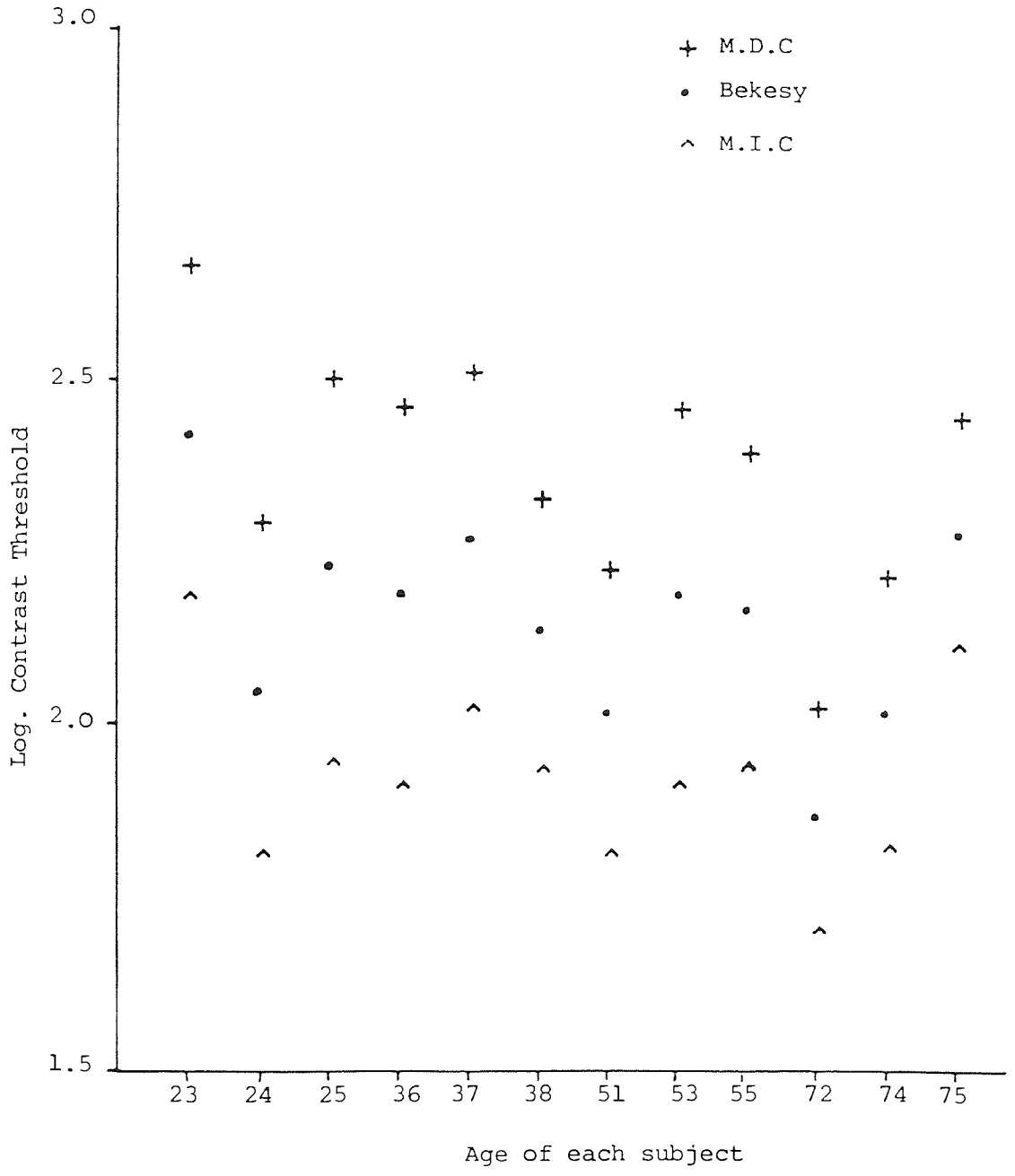

Brown and Woodhouse[204] has supported the result that measurement method is not age dependent. The SE range of results for MIC, Bekesy and MDC was 0.013 to 0.06 log units, 0.071 to 0.11 log units and 0.018 to 0.095 log units respectively. Fig 4.2(a) shows the mean threshold results for the 12 subjects for each of the 3 measurement techniques at a 60 sec ramp. Fig 4.2(b) shows the intrasubject SE only for each technique. The graphs show that MIC gives the most conservative mean threshold value and the smallest SE. The MDC gives the largest result for threshold, but the SE value is in between that for the MIC and Bekesy, the latter giving an intermediate threshold value but having the greatest SE of the 3 techniques.

Fig 4.3(a) shows the threshold for each technique plotted against ramp rate, also shown is the average subject SE. In Fig 4.3(b) SE alone is plotted against ramp rate. Table 4.3 shows the statistical significances for the 3 measurement methods at each ramp rate, clearly the 3 techniques give mean threshold results that are all significantly different from each other except for one. As the ramp rate lengthens, the SEs become less and the mean threshold results approach each other in value. This is reflected in the fact that at the 120 sec ramp the MDC and Bekesy method do not give statistically different results for contrast threshold. The most consistent measurement method with the smallest SE is the MIC with a 120 sec ramp.

Table 4.2

Log contrast threshold mean, SD and SE for three psychophysical techniques of measurement at four ramp rates. Data are pooled across the 12 subjects, hence average intrasubject results are shown.

Psychophysical techniques of measurement and ramp rate	Average log. contrast threshold intrasubject result		
	Mean	SD	SE
BEKESY			
15 sec	2.19	0.56	0.18
30 sec	2.17	0.36	0.12
60 sec	2.15	0.24	0.086
120 sec	2.09	0.14	0.053
MIC			
15 sec	1.72	0.079	0.037
30 sec	1.85	0.064	0.035
60 sec	1.93	0.062	0.031
120 sec	1.96	0.047	0.027
MDC			
15 sec	2.72	0.31	0.12
30 sec	2.50	0.19	0.079
60 sec	2.38	0.11	0.057
120 sec	2.21	0.07	0.044

Fig. 4.2 (a) shows log. contrast threshold result for each psychophysical technique of measurement (b) shows av. log S.E. only. Data are pooled across the 12 subjects to give av. intrasubject results for each method. The M.I.C gives the most conservative contrast threshold and smallest S.E.

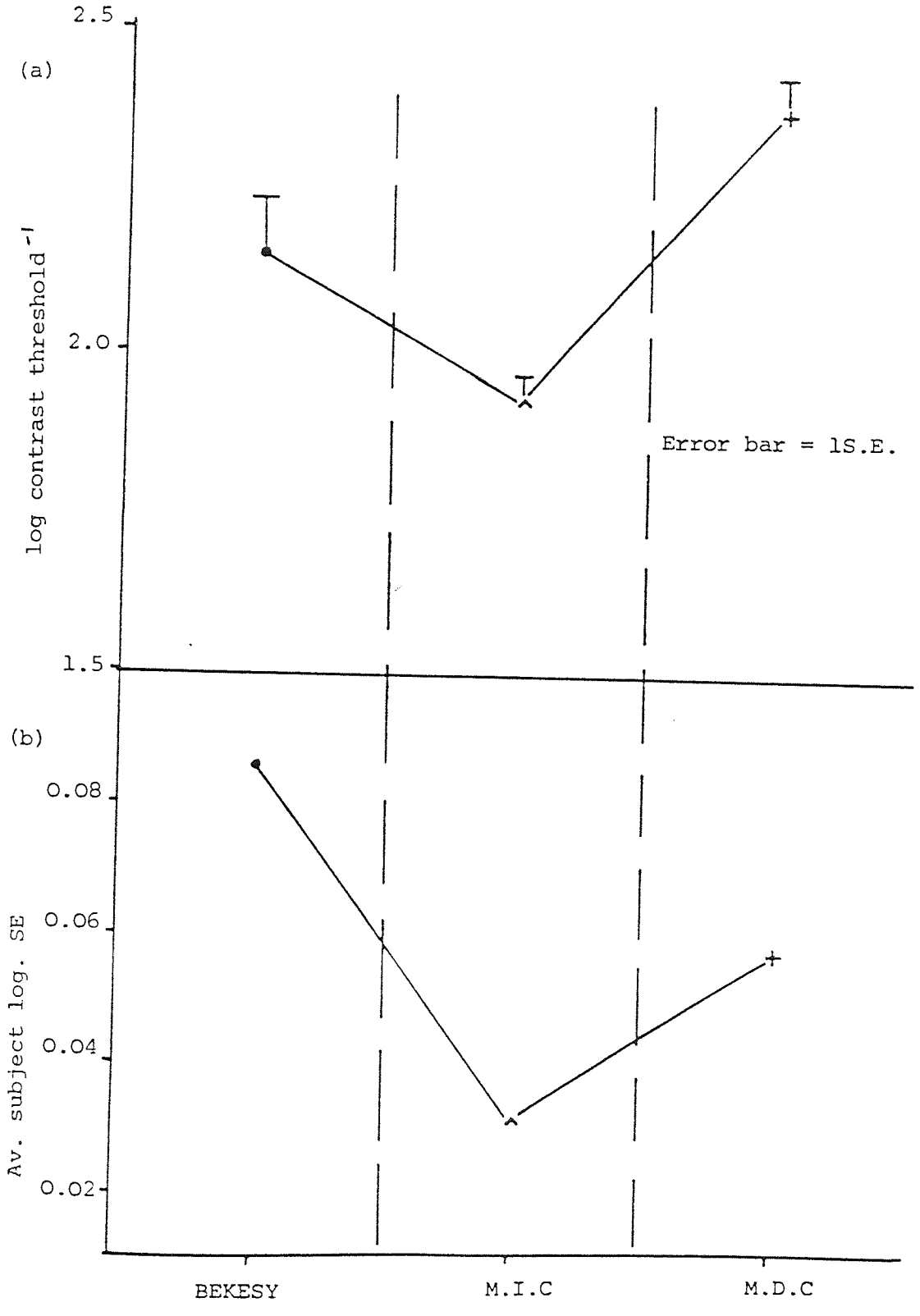

Fig. 4.3(a) Shows log. contrast threshold for each psychophysical technique of measurement at each ramp rate ie 15, 30, 60 and 120 sec. Data are pooled across the 12 subjects

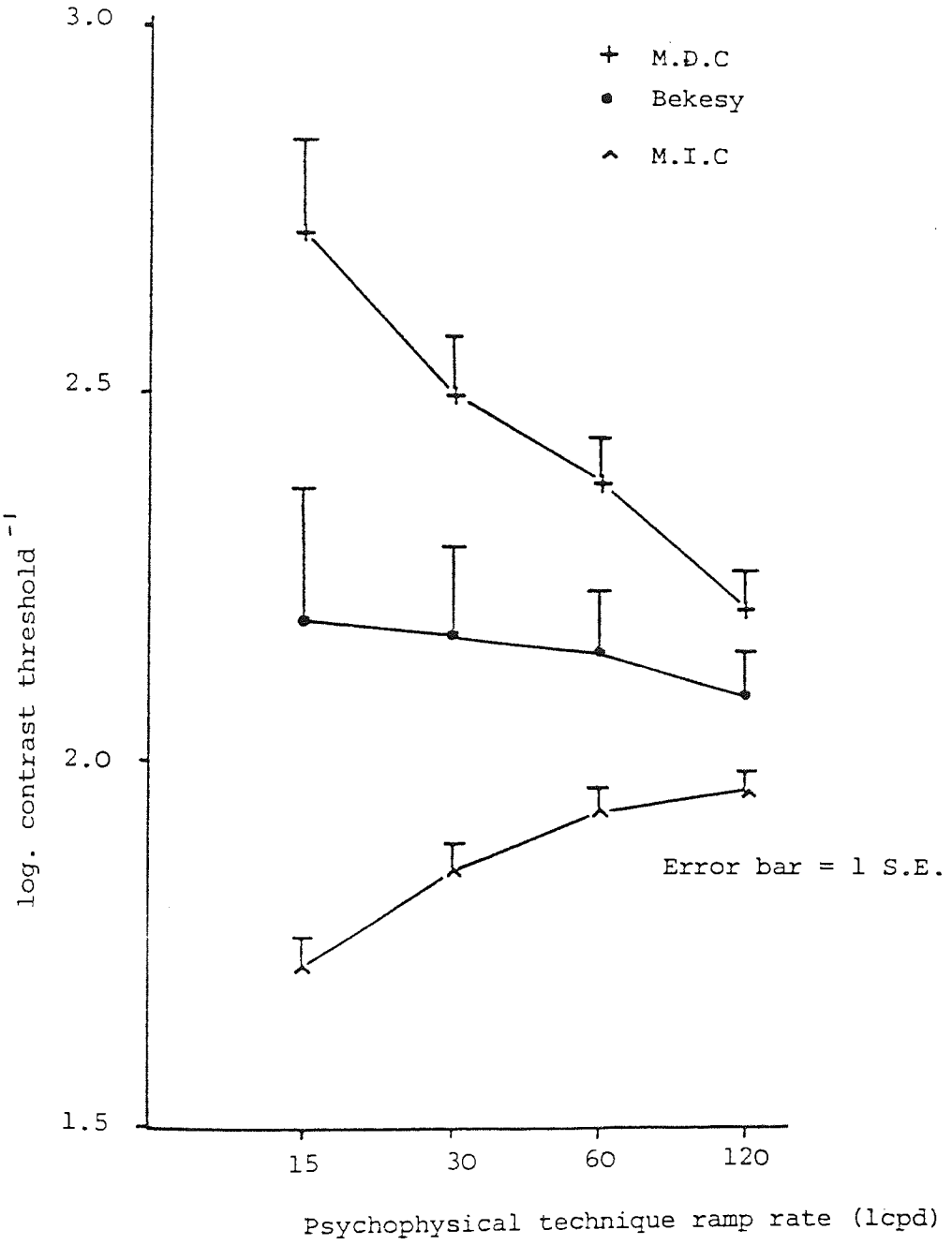

Fig. 4.3(b) Shows av. intrasubject log. S.E. for threshold results with each psychophysical technique of measurement at each ramp rate ie 15, 30, 60 and 120 sec. Data are pooled across the 12 subjects

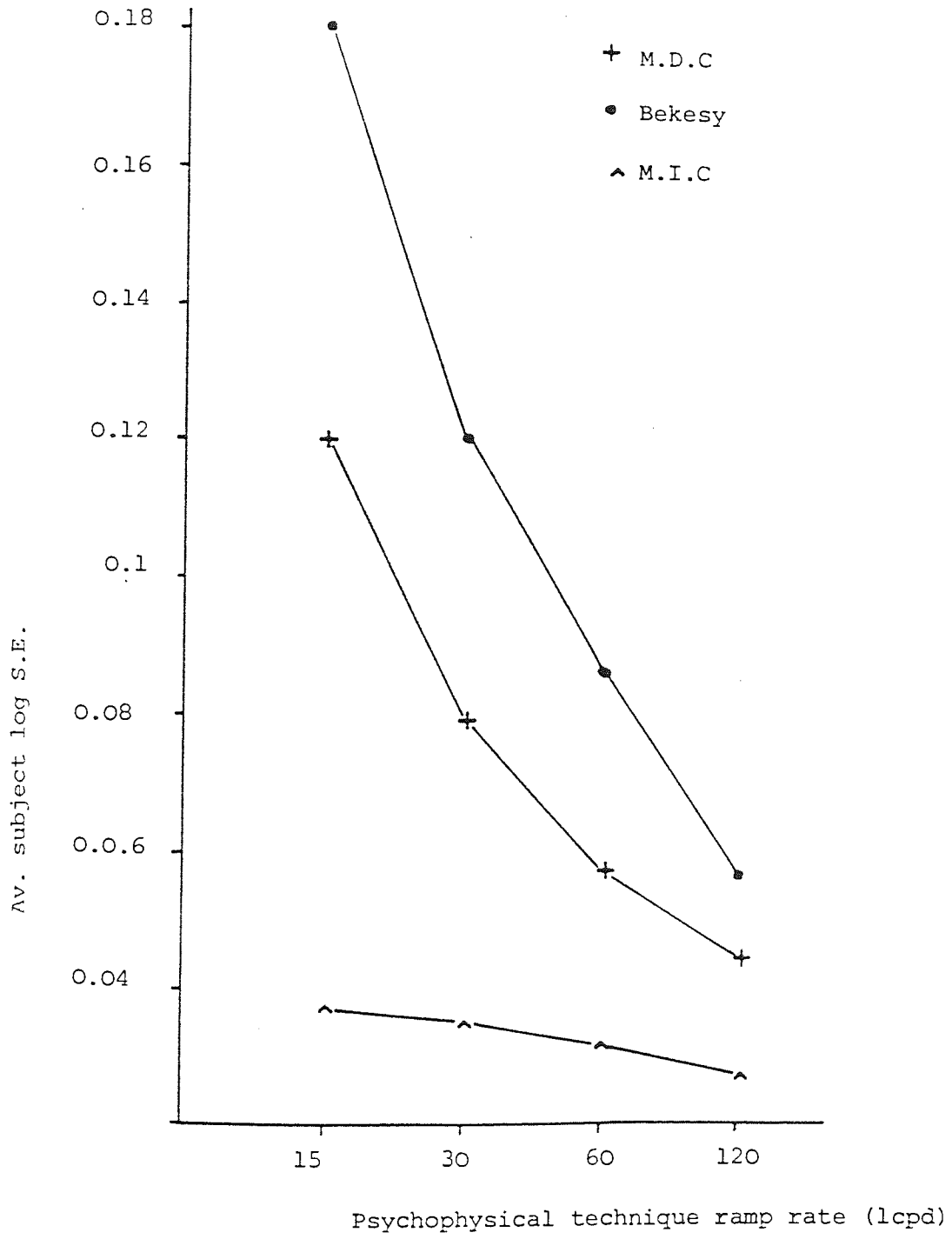

Table 4.3

Statistical significancies for the 3 psychophysical techniques of measurement at equivalent ramp rates. Comparing mean contrast thresholds (Refer to Fig 4.3 (a))

	Psychophysical technique of measurements compared		
	MDC and Bekesy	MDC and MIC	Bekesy and MIC
Ramp rate			
15 sec	$p<0.05$	$p<0.001$	$p<0.05$
30 sec	$p<0.001$	$p<0.001$	$p<0.05$
60 sec	$p<0.05$	$P<0.001$	$p<0.05$
120 sec	not sig.	$p<0.01$	$p<0.05$

4.1.2 Discussion

This study involved the investigation of 3 techniques of measurement of contrast thresholds on clinically available equipment namely the Nicolet CS2000. The aim was to select the most accurate and appropriate measurement technique over the large age range of subjects investigated ie 23 to 75 years and over 4 psychophysical ramp rates and to apply this technique to subsequent studies on intraocular light scatter using glare sources. Such a study has not previously been reported.

No variation with age was found with the 3 techniques measured (see Fig. 4.1). This is an important result as if an age effect was present in the measurement technique it would distort the subsequent results involving age dependent intraocular light scatter. The MDC always had the largest contrast threshold value and the MIC always the smallest value at equivalent ramp rates. In fact the Bekesy value was always approximately equidistant between the MIC and MDC values, although the longer the ramp rate becomes, the smaller are the mean value differences between the three methods. This is to be expected as with a longer ramp rate the subject has more time to make an accurate decision on the contrast threshold, Ginsburg and Cannon[199] have also shown this effect with respect to ramp rate. The Bekesy method is a combination of the MIC immediately followed by the MDC, hence when individual contrast thresholds are evened out it is reasonable to expect that the Bekesy value will always be approximately equidistant between MIC and MDC. In the same way, Fig 4.3(b) showing SE values only, for the 3 methods over the 4 ramp rates shows that the Bekesy method always has the largest SE value and MIC always the smallest. All the SEs drop with lengthening ramp rate, again this is to be expected (as with the mean threshold values), in that more decision time for the subject leads to smaller errors of measurement.[200] Note how the slope on the MIC graph (Fig. 4.3(b)), is much less inclined than the MDC and Bekesy slopes, the latter two having similar gradients. This indicates that most of the SE variation in Bekesy technique comes from the MDC component. However, because SEs are a method of estimating the population mean from the sample mean, Bekesy always has the largest SE as it has to include MIC and MDC values.

The results shown in Fig. 4.3 indicate that the most consistent measurement technique was the MIC at a 120 sec ramp. Subjectively, it was found that the 120 sec ramp was very slow and tedious for the subject leading to fatigue and a lack of concentration. There is little variation in SE between the 60 sec and the 120 sec MIC ramp and the former was found to be a more acceptable working ramp rate for subjects. Hence a 60 sec MIC was chosen as the psychophysical technique of measurement for subsequent experiments (Experiment 2, 3 and 4).

These findings are supported by previous work on psychophysical techniques of measuring the CSF,[198,199,200] where the MIC was found to be the most consistent measurement method. However, this is the first study of its kind on clinically available equipment and confirms studies previously conducted in more experimental conditions. Moreover, the analysis of the Bekesy method into MIC and MDC components proves that lack of consistency of results for contrast thresholds using this method are mostly due to the descending (MDC) component. Hence it is recommended that all clinical measures of contast threshold using the Nicolet CS2000 should be carried out applying the ' Method of Increasing Contrast' with a ramp rate of the order of 60 secs from zero to 100% contrast.

Experiment 2

4.2 (i) A Pilot Study Investigating the Relationship between Glare Angle, Intraocular Light Scatter and Age

The aim of this experiment was to establish the connection between circular glare sources at 5 separate angles of incidence to the observer's eye, intraocular light scatter and subject's age. In order to quantify the effects of intraocular light scatter on vision, the equation of Paulsson and Sjostrand[98] was used (See Section 3.1.B). This gives a Light Scatter Factor (LSF) based on measurements of contrast threshold with and without glare sources, pupil illuminance with each glare source and target mean luminance. The LSF gives a direct measure of forward intraocular light scatter onto the retina. Based on the results of the first experiment investigating techniques of measurement, a 60 sec MIC was the method used with the standard target grating of 1 cpd and 2Hz counterphase. Section 3.1.A.4 described the technique of measurement and Section 3.1.B Condition (i) described the glare sources ie five glare angle conditions subtending 50°, 30°, 20°, 10° and 5° at the subject's eye (See Fig. 3.1). Contrast thresholds were recorded with and without each glare condition on each subject. Light Scatter Factors[98] (LSF) were calculated for each subject at each glare angle.

4.2.1 Pilot Study Results

Direct illuminances onto the eye, E were measured with a spot photometer and applying a correction factor (See Appendix) gave the following results for pupil illuminances.

E (5°) = 212 lux

E (10°) = 848 lux

E (20°) = 2970 lux

E (30°) = 4240 lux

E (50°) = 6360 lux

The LSF was calculated for each subject at each glare angle. The results are shown in Table 4.4. The 12 subjects were divided into 2 group of 6 each by age, giving a 'young' and an 'old' age group. Fig 4.4 shows average LSFs plotted against glare angle for the 2 age groups. At each glare angle, the 'old' group shows a higher LSF value than the 'young' group. This difference in mean LSF between the 2 age groups is significant for all but the 5° glare angle (See Table 4.5). The most significant separation in mean LSF between the 'young' and 'old' age group is at the 30° glare angle ($p< 0.001$) and is in part reflected by the small SE values, while at the 50° glare angle the group mean LSF separation between 'young' and 'old' is less significant ($p< 0.05$). Note also that the range of results in both groups is greatest at the 5° radius and decreases with increasing glare angle. This is shown both in Fig. 4.4 and in Table 4.4 by the group SE values. eg group SE ('young') at 5° is 0.279 and at 50° is 0.0099 the error of measurement is very much smaller at 50° glare than 5° glare.

Table 4.4

Light Scatter Factors for each subject at each glare angle along with mean, SD and group SE for the 'young' and 'old' age groups

Subject 'Young'	Age	5°	10°	20°	30°	50° Glare angle
CT	23	0.0558	0.00133	- 0.00226	- 0.00134	0.00176
JF	24	0.215	0.0137	0.0273	0.0151	0.00247
SG	25	0.279	0.0645	0.00731	0.00856	0.00834
DB	36	0.114	0.0124	0.00464	- 0.00357	0.00305
BG	37	1.862	0.275	0.0688	0.0411	0.0638
LJ	38	0.414	0.0906	0.0222	0.0196	0.0106
mean	301/2	0.490	0.0763	0.0213	0.0132	0.0150
SD		0.684	0.103	0.0258	0.0164	0.0242
group SE		0.279	0.0420	0.0105	0.00670	0.00988
'old'						
MW	51	0.543	0.168	0.0709	0.0526	0.0411
ND	53	1.211	0.259	0.0795	0.0524	0.0299
PP	55	1.383	0.308	0.0767	0.0454	0.0247
MH	72	1.125	0.119	0.0404	0.0312	0.0147
ML	74	0.587	0.124	0.0578	0.0484	0.0366
MSL	75	0.904	0.223	0.0752	0.0683	0.0515
mean	631/3	0.959	0.200	0.0668	0.0497	0.0331
SD		0.342	0.0762	0.0150	0.0120	0.0129
group SE		0.140	0.0311	0.00612	0.00490	0.00527

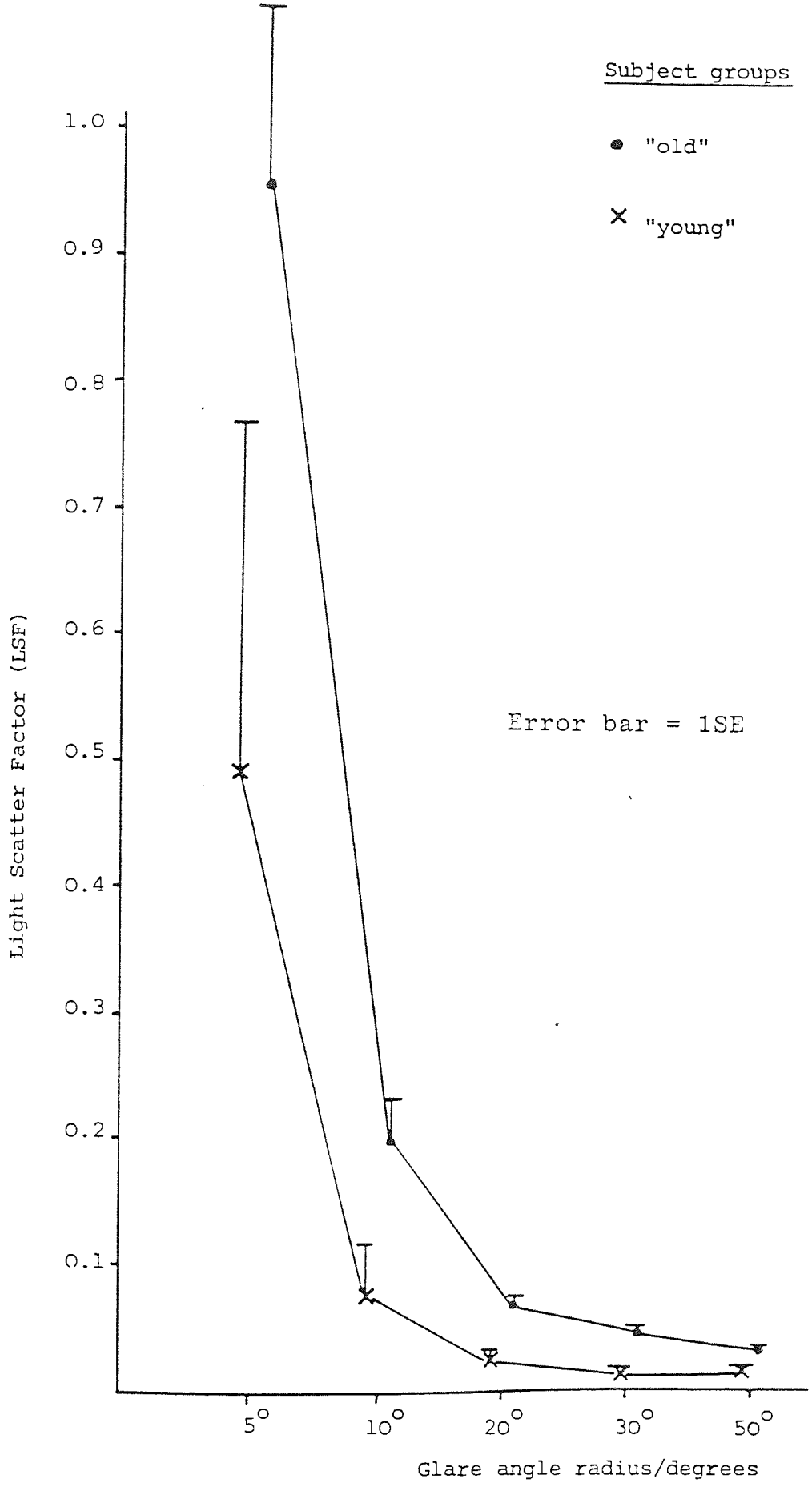

Fig. 4.4 Shows the relationship between angular glare and intraocular light scatter (with LSFs) for 2 age groups

Table 4.5

Statistical significances for group mean LSF of the 'old' subjects compared to group mean LSF of the 'young' subjects. The LSF is significantly higher for the 'old' subjects for each glare angle except the narrowest ie 5° (See Fig 4.4)

Glare radius	Comparison of mean LSF for 'old' and 'young' groups
5°	not sig.
10°	$p < 0.01$
20°	$p < 0.01$
30°	$p < 0.001$
50°	$p < 0.05$

4.2.2 Pilot Study Discussion

The direct in vivo measurement of intraocular light scatter with respect to age and glare angle using a circular glare source to provide uniform glare light distribution, and clinically available equipment namely, the Nicolet CS2000 has never been conducted before. The measurement of forward light scatter (with LSFs) in the eye by recording the contrast lowering effect of the luminous veil onto the retina has provided information about the standard of vision that may be expected in an elderly population.

Fig 4.4 shows for both age groups the expected decline in intraocular light scatter with increasing glare angle, this confirms previous experimental studies both in vitro[29,65] and in vivo.[98,104] The 'old' group showing a significantly greater LSF than the 'young' group at each glare angle demonstrates that in vivo intraocular light scatter is greater in an older population irrespective of the visibility of cataracts. Until now this increase in forward light scattering in the eye onto the retina has only been demonstrated in older groups with cataracts, or/and other pathological conditions.[98,179,202]

The LSF values are greater at smaller glare angles ie 5° and 10° than at larger values but there is greater variation in the results achieved, so much so that the difference in group mean LSF between the 'young' and 'old' subjects is not significant at 5°. This may be attributed to the difficulty of the task at this small glare angle, greater variation in lenticular light scattering properties at small angular glare values or a combination of both. The largest glare angle employed (50°) elicited a lower LSF and slightly increased measurement errors compared to 30° glare. Larger angles were found inconvenient to use because of interference from facial contours and maintainance of a consistent angle due to the small distance from the subject. Furthermore, larger glare angles produced less light scatter due to oblique angle of entry by the light. These factors could fully account for the increase in measurement error and decrease in LSF at 50°.

The most significant separation in group mean LSFs for 'young' and 'old' subjects demonstrated at 30° is the optimum glare angle for showing the age effect of forward in vivo light scatter on vision and is used in the main study for that reason. Moreover at this angle, ocular holoes (especially in the presence of corneal oedema) would not be visible in the viewing field. The pilot study has demonstrated the effect of age and glare angle on forward intraocular light scatter which increases with ageing and decreases with glare angle. The main study here conducts similar measurements at 2 specific glare angles in a large group of visually untrained observers.

4.2.3 Experiment 2

(ii) A Study of the Effect of Intraocular Light Scatter and Ageing on the CSF

The apparatus for this study is shown in Fig. 3.2 and in Plates 3.1 and 3.2. The pilot study, using 12 visually trained observers established the connection between forward intraocular light scatter (as recorded with LSFs), glare angle with respect to the observer's eye and age. The aim of the main study here was to demonstrate the results of the pilot study on a large group (N=54) of visually untrained subjects over a large age range (ie 18 to 81 years). Moreover, as a result of the pilot study findings, only 2 specific glare angles were employed. These were of 30° radius and 3.5° radius at the subject's eye; the glare sources being well separated in angular subtense. A 30° radius angle was chosen as the pilot study showed that this glare angle best demonstrated the difference in LSF between 'old' and 'young' age groups. The 3.5° glare angle was convenient to use to demonstrate the effect of narrow angle glare on intraocular light scatter, and also could produce ocular haloes in the viewing field. (Refer to Section 3.1.B Glare Condition(ii)).

Accordingly, contrast thresholds were taken on each subject (at 1 cpd 2Hz counterphase) and in the presence of each glare angle. LSFs were calculated at both glare conditions. Pupil diameters were measured for all subjects in the 'old' and 'young' groups both without glare and with each glare angle. The CSF was also recorded on each subject applying a 60 sec MIC and a 2Hz counterphasing target, spatial frequencies of 1,3,6 and 11.4 cpd were used.

Another manifestation of ocular ageing is the increase in ocular fluorescence which originates mainly from the lens. (See Sections 1.C.2 and 1.D) Accordingly Glare Condition (iii) was used (Refer to Section 3.1.B) in order to ellicite lens fluorescence. The wavelength emmission of the near UV/Burton Lamp as used in contact lens practice (See Appendix), would cause fluorogens within the

eye to become excited causing an emmission of light and depressed contrast thresholds. The LSF for both 'old' and 'young' groups was calculated. A 1 cpd 2Hz contrast threshold target was used.

4.2.4 Results

Pupil illuminance E, at the 3.5° glare angle was measured at 63.6 lux. Table 4.6 shows the averaged group data for the 54 subjects in this experiment. The contrast threshold means and group SE are plotted for each of the 3 age groups ie 'young', 'intermediate' and 'old' at each spatial frequency and are shown in Fig. 4.5. The graph shows that the'young' group have the highest CSF at all spatial frequency values compared to the 'intermediate' and 'old' groups. The latter 2 groups are not statistically different from each other at each spatial frequency. Table 4.7 summarises the statistical significance of the mean contrast thresholds for paired subject groups at each spatial frequency.

Table 4.8(i) and Fig. 4.6 show the group mean LSF for each age group plotted against the 3.5° and the 30° glare angles. For clarity, the 30° LSF results are replotted in Fig. 4.7. The same trends are shown here as in the pilot study. Namely that at both glare angles the LSF value is greater with the 'old' group than with the 'intermediate' and 'young' group; the latter 2 are not signifiicantly different in mean LSF value. Table 4.9 summarises the statistical significances of the mean LSF for paired subject groups at both glare angles.

Note that for the CSF curves (Fig. 4.5) the 'intermediate' and 'old' groups are about equally attenuated at each spatial frequency value compared to the 'young' group. Note also the slight increase in separation between the mean contrast threshold for the 'young' group compared to the other 2 groups as the spatial frequency value increases. In contrast to this Figs. 4.6 and 4.7 showing LSFs, demonstrate that only the 'old' group has a significantly higher light scatter value compared to the 'intermediate' and 'young' groups at both glare angles. The latter 2 groups show no significant increase in LSF. Table 4.10 shows the mean pupil diameters for 'young' and 'old' age groups and in

Table 4.6

Log Contrast Threshold means, SD and group SE at four spatial frequencies for each of the three age groups. A 2Hz counterphase grating and a 60 sec MIC was used.

Spatial f/cpd		1	3	6	11.4
'YOUNG' Group	mean	2.07	2.20	1.98	1.48
Age range 18-42	SD	0.10	0.12	0.19	0.43
Av. age = 31	SE	0.024	0.027	0.044	0.10
(N = 18)					
'INTERMEDIATE' Group	mean	1.84	1.84	1.45	0.79
Age range 43-61	SD	0.24	0.288	0.318	0.265
Av. age = 52	SE	0.057	0.068	0.075	0.062
(N = 18)					
'OLD' Group	mean	1.90	1.94	1.56	0.81
Age range 62-81	SD	0.18	0.20	0.21	0.30
Av. age = 74	SE	0.042	0.047	0.047	0.071
(N = 18)					

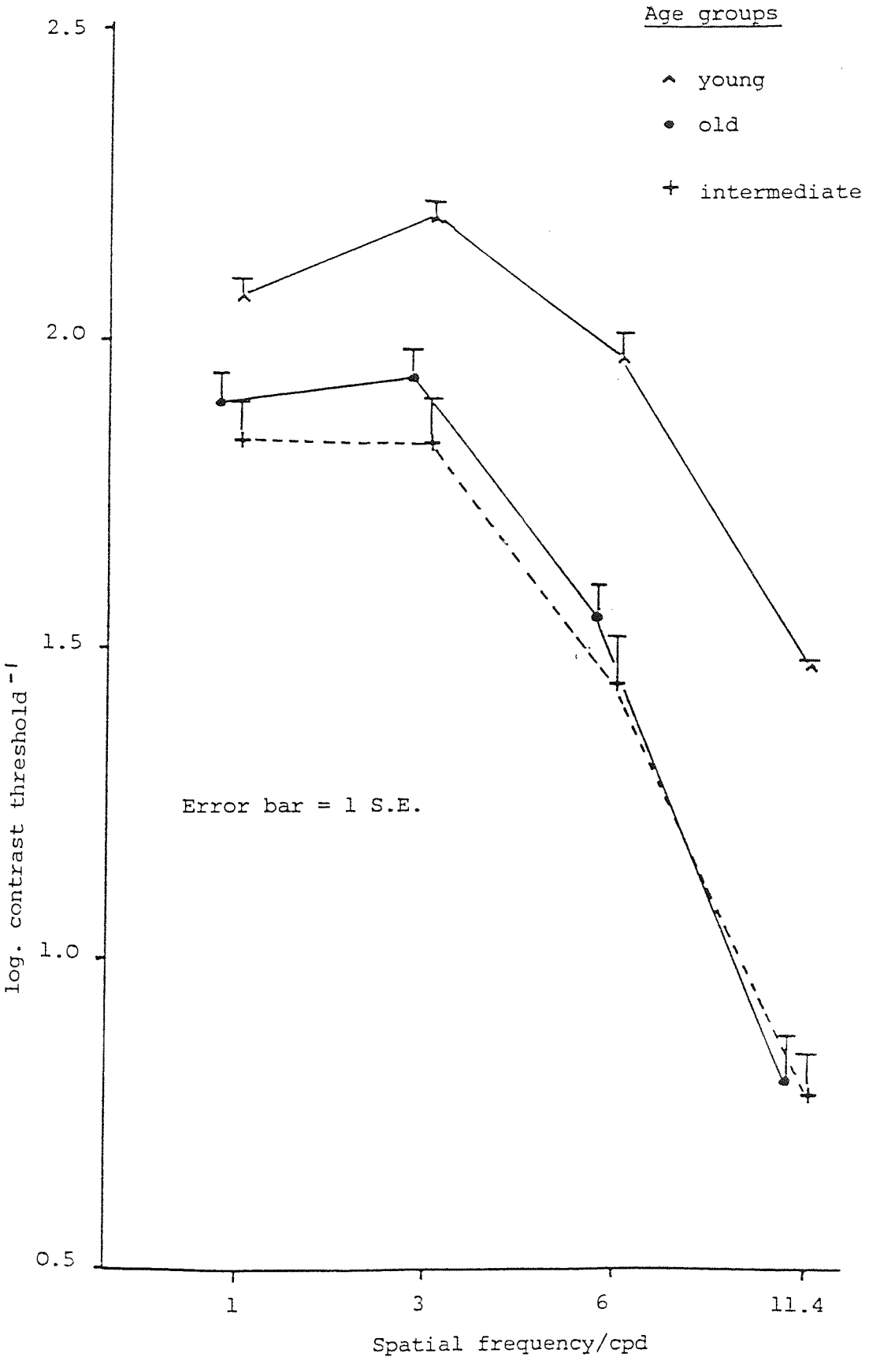

Fig. 4.5 Graph shows the contrast sensitivity function as measured at 4 spatial frequencies for each age group.

Table 4.7

Statistical Significance for mean Contrast Threshold for paired age groups at each Spatial Frequency - the 'Young' age group has a statistically higher group mean Contrast Threshold Result at each Spatial Frequency compared to 'Intermediate' and 'Old' groups which are not statistically different from each other (See Fig. 4.5)

	Statistical significance of paired age groups		
Spatial Frequency	young/intermediate	young/old	intemediate/old
1 cpd	p <0.01	p <0.01	not sig.
3 cpd	p <0.001	p <0.001	not sig.
6 cpd	p <0.0001	p< 0.0001	not sig.
11.4 cpd	p <0.0001	p <0.0001	not sig.

Table 4.8

(i) Mean LSFs along with SD and group SE at each of the 2 glare angles used and at all three age groups (ii) Mean LSF (Leq) for a 'young' and 'old' age group as a result of ocular fluorescence

			LSF (3.5°)	LSF (30°)
(i)	'YOUNG' Group	mean	1.18	0.024
	Age range 18-42	SD	0.72	0.013
	Ave age = 31	SE	0.17	0.0032
	N = 18)			
	'INTERMEDIATE'			
	Group	Mean	1.14	0.023
	Age range 43-61	SD	0.95	0.021
	Ave age = 52	SE	0.22	0.0049
	(N = 18)			
	'OLD' Group	mean	2.11	0.063
	Age range 62-81	SD	1.058	0.043
	Ave age = 74	SE	0.249	0.010
	(N = 18)			

The Effect of Ocular Fluorescence

(ii)	Subject groups		LSF (Leq)
	'YOUNG group	mean	0.64
	Age range 19-27 yrs	SD	0.66
		SE	0.21
			LSF (Leq)
	'OLD' group	mean	1.47
	Age range 61-82 yrs	SD	1.68
		SE	0.53

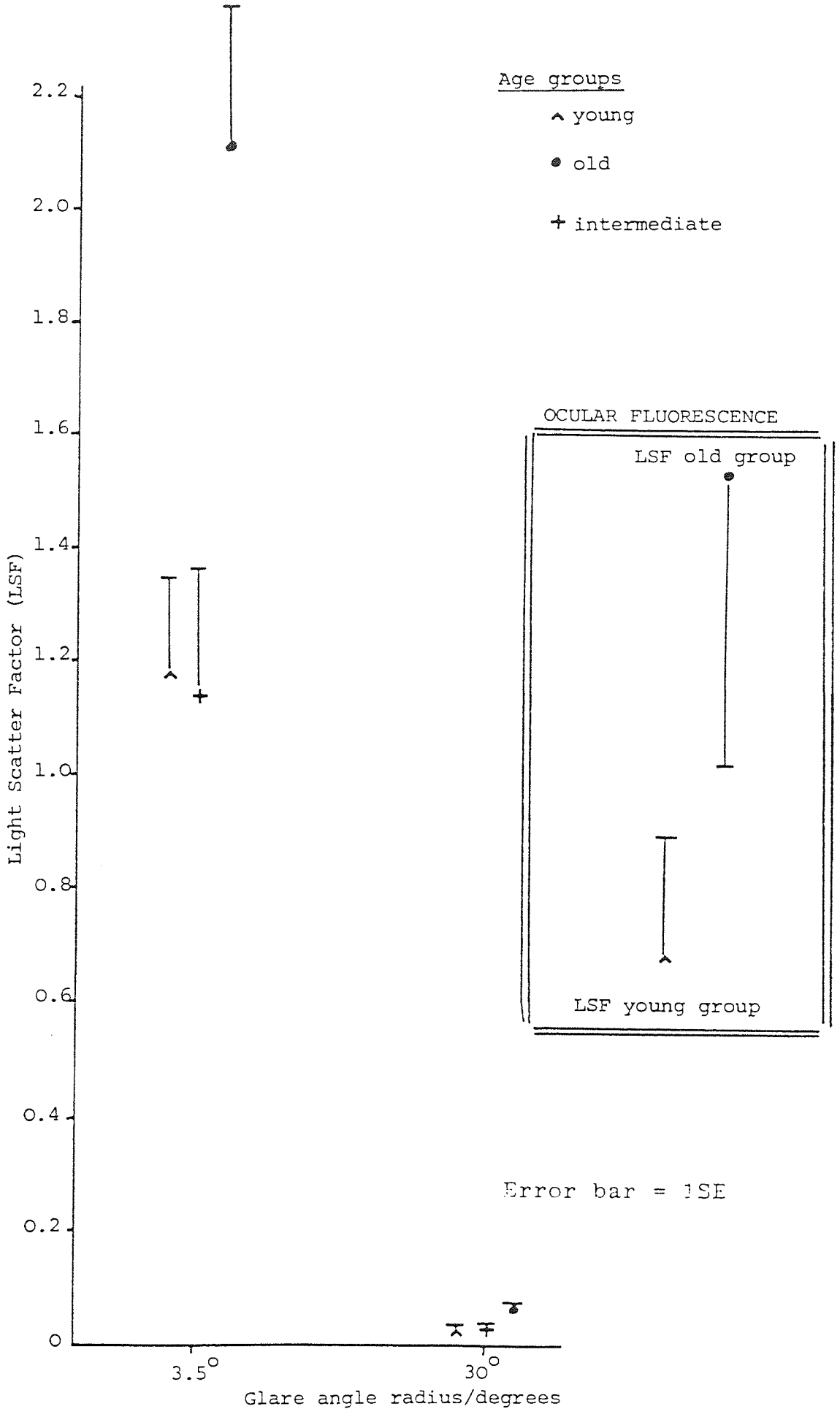

Fig. 4.6 Shows mean LSF for each age group at both glare angles ie 3.5° and 30°. Shown inset are LSFs for an old and young group of subjects due to ocular fluorescence.

Fig. 4.7 Shows LSF for each age group at the 30° glare angle (replotted from Fig. 4.6)

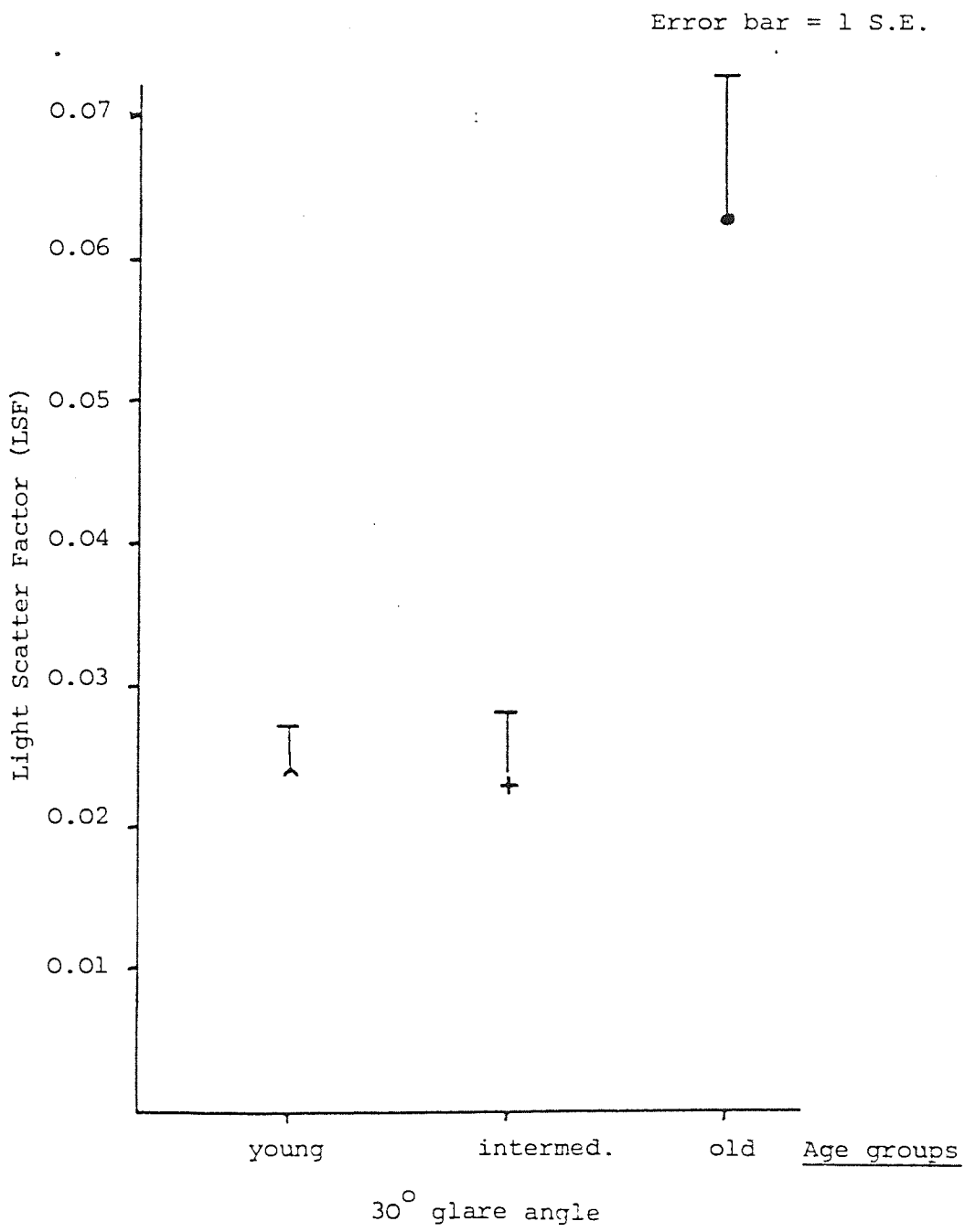

Table 4.9

Statistical significances for mean LSF for paired age groups at angular glare radii 3.5° and 30° - the 'old' age group has a statistically higher group mean LSF value at both glare angles compared to 'intermediate' and 'young' groups which are not statistically different from each other (See Figs. 4.6 and 4.7)

	Statistical significance of paired age groups		
Glare angle LSF	young/intermediate	young/old	intemediate/old
LSF (3.5°)	not sig.	p <0.01	p <0.01
LSF (30°)	not sig.	p <0.01	p <0.01

Table 4.10

Mean Pupil Diameters for 'Young' and 'Old' Groups for a No Glare, 3.5° and 30° Glare Condition

	Pupil Diameter/mm		
Age group	No Glare	3.5° Glare	30° Glare
'Young'	4.4 (SD = 0.32)	4.25 (SD = 0.79)	2.65 (SD = 0.24)
'Old'	3.2 (SD = 0.39)	3.15 (SD = 0.55)	2.7 (SD = 0.59)

both glare conditions. The data conforms to the general finding that pupil diameter decreases with age and with increasing pupil illuminance.[205]

Table 4.8(ii) shows mean LSF for 'young' and 'old' age groups as a result of ocular fluorescence. The pupil illuminance value for the UV/Burton lamp is taken at 1; this is because the fluorescent effect is not the result of visible light input against which pupil illuminance is measured, in this case then, the LSF is the equivalent veiling glare (Leq) and is a direct measure of ocular fluorescence. The mean LSF (Leq) for the 'old' group due to ocular fluorescence is significantly higher than mean LSF (Leq) of the 'young' group. ($p < 0.05$) The mean target luminance was reduced in 2.7 cd/m^2 for the purposes of this experiment (see Section 3.1.B). The inset in Fig. 4.6 shows the graphed result.

4.2.5 Discussion

The experiment confirms the results from the pilot study, this time using a visually untrained group of subjects, that intraocular light scatter as measured with LSFs with both glare conditions is higher in an 'old' age group ie 62 years and older. All LSF values for the 3.5° glare condition are higher than those for the 30° glare condition due to the inversely proportional relationship between LSF and glare angle. The 'intermediate' group ie 43 to 61 years shows no increase in LSF. This indicates that ageing effects in the media of the eye (mainly the lens) that cause increased forward intraocular light scatter must occur predominantly in the over 60 years age group. This view is widely supported by previous studies (Refer to Sections 1.C and 1.D).

By comparison, the CSF is depressed at all spatial frequency values for both 'intermediate' and 'old' age groups. If intraocular light scatter is not a predominant factor in CSF attenuation in the 'intermediate' group what then accounts for this depression? If it is not light scatter, then the majority of CSF depression with the 'intermediate' group must be due to reduce retinal illuminance and/or neural factors.

Weale[61] has estimated that the average 60 year old eye transmits approximately one third the light transmitted by the average 20 year old eye. According to Weale this is due largely to a reduction in pupil size (senile miosis) and increased optical density of the crystalline lens. Owsley, Sekuler and Siemsen[173] addressed this problem by measuring the CSF for subject groups in their 20's and in their 60's and then remeasuring for the subjects in their 20's with a neutral density filter that reduced retinal illuminance by a factor of 3 (taking into account both pupil size under these luminance conditions and estimated lenticular density for 20 year olds[61]). Hence the estimated retinal illuminace of the young subjects was reduced to the estimated level of the older subjects in their 60's. They found, in common with previous work eg Kelly,[125] Kulikowski[138] that the reduced retinal illuminance selectively depressed sensitivity for higher spatial frequencies. eg at 10 and 16 cpd. The mean pupil diameter in

this study decreases from 4.4mm in the young group to 3.2mm in the old group, representing a reduction in retinal illumination of 0.28 log units. The contrast sensitivity data of Kulikowski[138] states that at 10 cpd, a mean luminance reduction of 2 log units causes a contrast sensitivity reduction of 1 log unit. Hence with the data from this experiment a contrast sensitivity reduction of 0.14 log units will be due to decrease in pupil size alone. The total decrease in log contrast threshold at 11.4 cpd in the data was 0.67 log units. Therefore approximately one fifth of the reduction in contrast threshold is due to decrease in pupil size.

The decrease in pupil size with age would not be expected to produce a deterioration in the optical quality of the image, in fact the pupil diameter of the older group is the closest to the 2.4 mm pupil diameter shown by Campbell and Gubisch[206] to represent the best optical image quality due to the minimum combined effects of peripheral aberration and diffraction (including the Stiles-Crawford effect).

Since reduced retinal illuminance has very little effect at low spatial frequencies, this does not account for the 0.17 log unit reduction in contrast threshold recorded at 1 cpd. At the other end of the spatial frequency range 0.53 log units of attenuation in contrast threshold is unaccounted for at 11.4 cpd. These reductions are due to media absorption, intraocular light scatter and/or neural changes. If intraocular light scatter is responsible for threshold differences between 'young' and 'old' subjects, it is reasonable to expect that the forward scattering light onto the retina that increases the mean luminance and decreases contrast would do so equally for any pattern imaged on the retina. If it is assumed for a moment that the whole of the 0.17 log units attenuation at 1 cpd is due to light scatter, this still leaves 0.36 log units of contrast threshold depression unaccounted for at the 11.4 cpd level. Hence it can be concluded if only at high spatial frequencies, that at least 0.36 log units is due to media absorption and/or neural changes.

A few cautionary notes must be added at this point. Firstly, the calculations for reduction in retinal

illuminance with age calculated from Weale's data[61] can only be considered as an estimate. Secondly, the small log unit values being considered here are within the measurement errors for the experiment eg. 0.17 log units and therefore must be treated with caution, although this may account for the fact that the 'intermediate' group shows no increased LSF. On the other hand added glare sources are usually sufficient to elicit an effect. It seems unlikely that all the attenuation in contrast threshold at 1 cpd level is due to intraocular light scatter alone. It seems more likely that it is a mixture of absorption, intraocular light scatter and neural factors. While at the 11.4 cpd level it is a mixture of reduced retinal illuminance, absorption, light scatter and neural factors. Recent studies on the variation of CSF with age have also supported this view.[173,125,175,176]

The inset on Fig. 4.6 shows the significantly higher LSF (Leq) result for the 'old' group from the 'young' group as the result of ocular (mainly lenticular) fluorescence. In 1985, Weale[207] published a paper on human lenticular fluorescence and transmissivity and their effects on vision. Using freshly excised lenses of a wide age range, the data showed that light of wavelength 381 to 428 nm would interact with at least 2 fluorogens and that a wavelength of about 397 nm would be maximally effective at eliciting human lens fluorescence - this is very close to the peak wavelength of the near UV/Burton lamp used in this study (ie 405 nm, See Appendix). Moreover, Weale[207] states that light sources in the spectral range of 405 to 500nm would cause a mixture of transmission and fluorescence in the lens. Hence the near UV/Burton lamp was an ideal and safe light source, causing a mixture of lens transmission and fluorescence. In this study, it is not possible to know in what proportions the light scatter from the lens was due to which mechanisms. However, it would seem from previous work[52,56,207] that the majority of lens light scatter using a near uv/Blue glare source, may be due to the fluorescent effect. Obviously, a more effecient UV light source that did not emit any visible light could theoretically have been used although because of the in vivo nature of the study this was eliminated on safety grounds.[52] Weale [207] also hypothesised on the potential role of lenticular fluorescence on vision and using the data of Campbell and Robson[129] concluded that at the age of 60 and above the results of lenticular fluorescence would be to form a light scattering haze on vision

which would be 'generally noticeable'.

This study into the fluorescent properties of the eye by measuring the reduction in contrast thresholds and subsequent increase in LSF (Leq) is a unique attempt to quantify this effect on subjects using clinically available equipment and the in vivo situation, allowing a direct measure of ocular fluorescence. The results indicate an increase in LSF (Leq) with age when the Burton Lamp is applied, just as was found with the 'white light' glare sources, however, when using the Burton Lamp as a short wavelength/near UV source, it is postulated that the increase in light scatter may be due mainly to lens fluorescence.

4.3 Experiment 3

The Effect of Epithelial and Stromal Oedema on the Light Scattering Properties of the Cornea

The glare apparatus used for this experiment is shown in Fig. 3.2 and Plates 3.1 and 3.2 (Refer to Section 3.1.A and 3.1.B with Glare Condition (ii)). The aim of this experiment was to quantify loss of corneal transparency by means of LSFs and to identify sources of light scatter in the cornea with the presence of corneal oedema. To this end, contrast thresholds at 1 cpd and a 60 sec MIC were recorded under 3 conditions; a no glare condition, a 3.5° glare radius condition and a 30° glare radius condition. The 2 circular glare sources enhanced corneal light scatter effects. The 3.5° glare source was designed to enhance epithelial halo effects within the viewing field and also increased stromal and lenticular light scatter. The 30° glare source did not produce observable haloes in the field of view but was designed to enhance stromal and lenticular light scatter. Young subjects were selected so that lenticular light scatter was at a minimum and this would not be affected by the course of the experiment, hence the glare sources used were designed to separate light scatter effects from epithelial (with 3.5° glare) and stromal (with 30° glare) tissues.

On each subject, in order to induce corneal oedema, a previously fitted sealed scleral contact lens was inserted with sterile distilled water (ie a hypotonic solution) and left on one eye for 25 mins. Contrast thresholds were monitored for 15 mins after lens removal during the recovery from osmotic stress using the 2 glare sources in turn. Contrast thresholds and corneal thickness measurements (Refer to Section 3.2) were performed on separate occasions for each subject due to the after-image effects from the pachometer slit-lamp source.[82] LSFs were calculated from contrast threshold results using each glare source along with corneal thickness data and are presented in the results.

4.3.1 Results

Figs. 4.8 and 4.9 show interpolated results for LSF (3.5°) and LSF (30°) respectively against recovery time; also shown for comparison is the initial LSF for each glare condition prior to scleral contact lens insertion. (Refer to Tables 4.11, 4.12 and 4.13) LSF in both glare conditions is highest at 3 min after scleral contact lens (CL) removal and steadily diminishes with time to 12 min as oedema recovers, although comparison with pre-oedema in both cases shows that recovery is still underway at 12 min after CL removal. The LSF (3.5°) is higher at all values for the averaged group data.

Fig. 4.10 shows the individual subject percentage corneal thickness changes at 3, 6 and 12 mins after CL removal; and demonstrates the wide range of values and differing rates of decrease in corneal thickness during the recovery time (see Table 4.14). The maximum percentage increase in corneal thickness recorded following CL removal was 10.7%. SDs on pachometry readings ranged from 0.004mm to 0.029mm, the largest SDs always being associated with readings when corneal oedema was greatest, at this time it was most difficult to line up the pachometer split-image accurately. Fig. 4.11 shows the averaged corneal thickness values at 3, 6 and 12 mins after CL removal and also the pre-CL insertion mean corneal thickness value. Note that the pre-CL insertion value of corneal thickness is not significantly different from mean corneal thickness at 3, 6 or 12 mins during recovery. In contrast to this both LSF (3.5°) and LSF (30°) have values prior to CL insertion that are all highly significantly different ($p < 0.001$) from the LSFs at 3,6 and 12 mins during recovery. In Fig 4.12 the interpolated and normalised results for LSF (3.5°), LSF (30°) and change in corneal thickness for the subject group are plotted against recovery time at 3,6 and 12 mins after CL removal (refer to Tables 4.11, 4.12 and 4.14). The graph shows that the fastest rate of reduction in LSF with recovery from oedema is demonstrated with the 3.5° glare angle, the LSF (30°) shows a slower rate of reduction (less inclined gradient) while the change in corneal thickness demonstrates the slowest reduction rate with recovery time.

Fig. 4.8 Av group LSFs for glare radius 3.5° at 3,6 and 12 min after scleral lens removal also shown is the LSF prior to lens insertion.

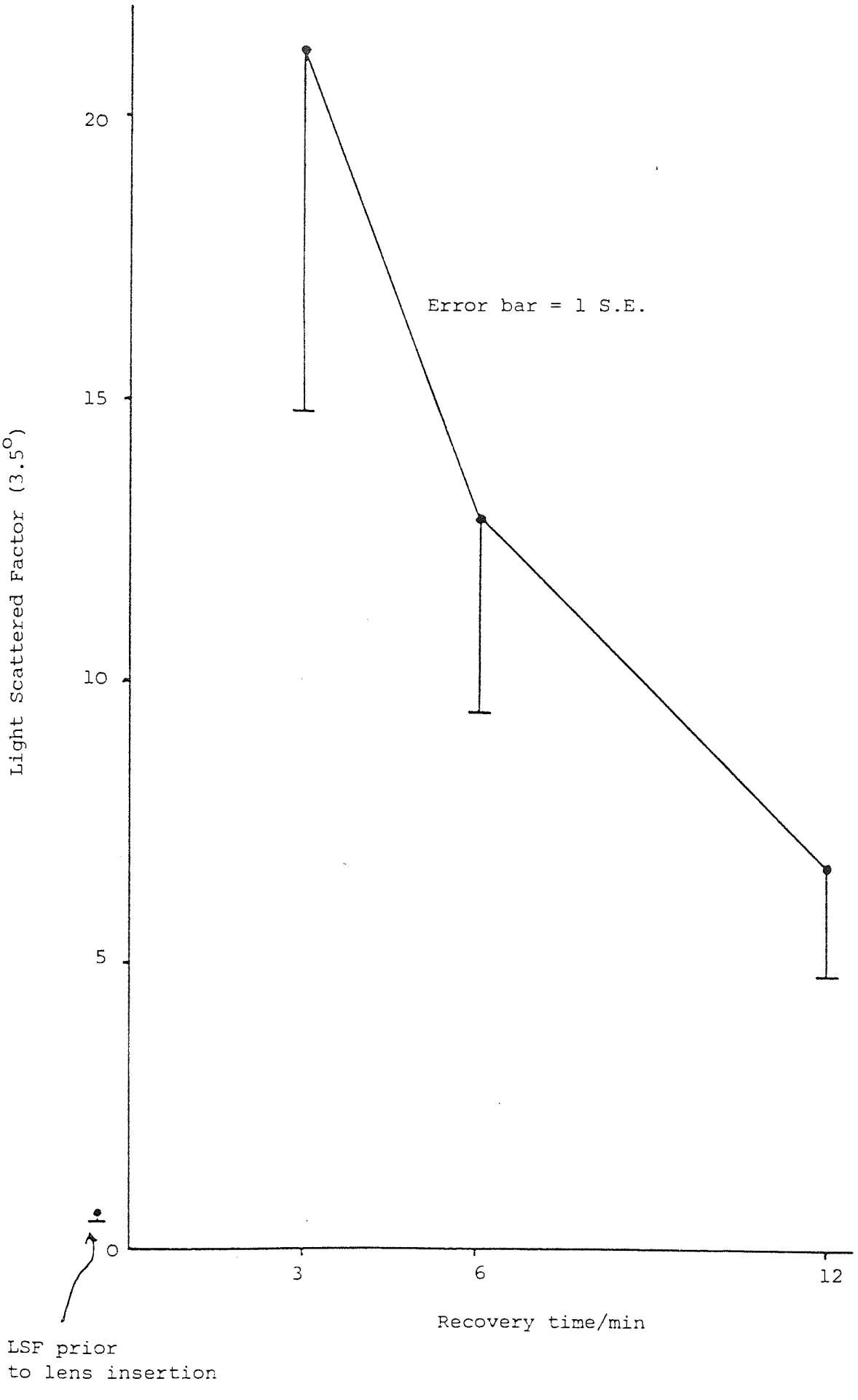

Table 4.11

Interpolated and Normalised Light Scattering Factors (LSF) for Glare Radius = 3.5° at 3,6 and 12 mins after Scleral Contact Lens Removal

Subject	3 min		6 min		12 mins	
	Interpolated	Normalised	Interpolated	Normalised	Interpolated	Normalised
JR	3.71	1.0	2.48	0.67	1.24	0.33
DUF	6.44	1.0	3.71	0.58	1.24	0.19
RH	22.28	1.0	14.60	0.66	8.66	0.29
MD	49.50	1.0	25.99	0.53	8.66	0.18
CT	32.05	1.0	22.52	0.70	16.09	0.50
DB	27.23	1.0	14.85	0.55	6.44	0.24
GV	7.43	1.0	6.44	0.87	4.95	0.67
N = 7						
mean	21.23	1.0	12.94	0.65	6.75	0.34
SD	16.68		9.18	0.11	5.14	0.17
SE	6.30		3.47	0.041	1.94	0.063

Fig. 4.9 Av group LSFs for glare angle 30^{o} at 3,6 and 12 min after scleral lens removal; also shown is the LSF prior to lens insertion.

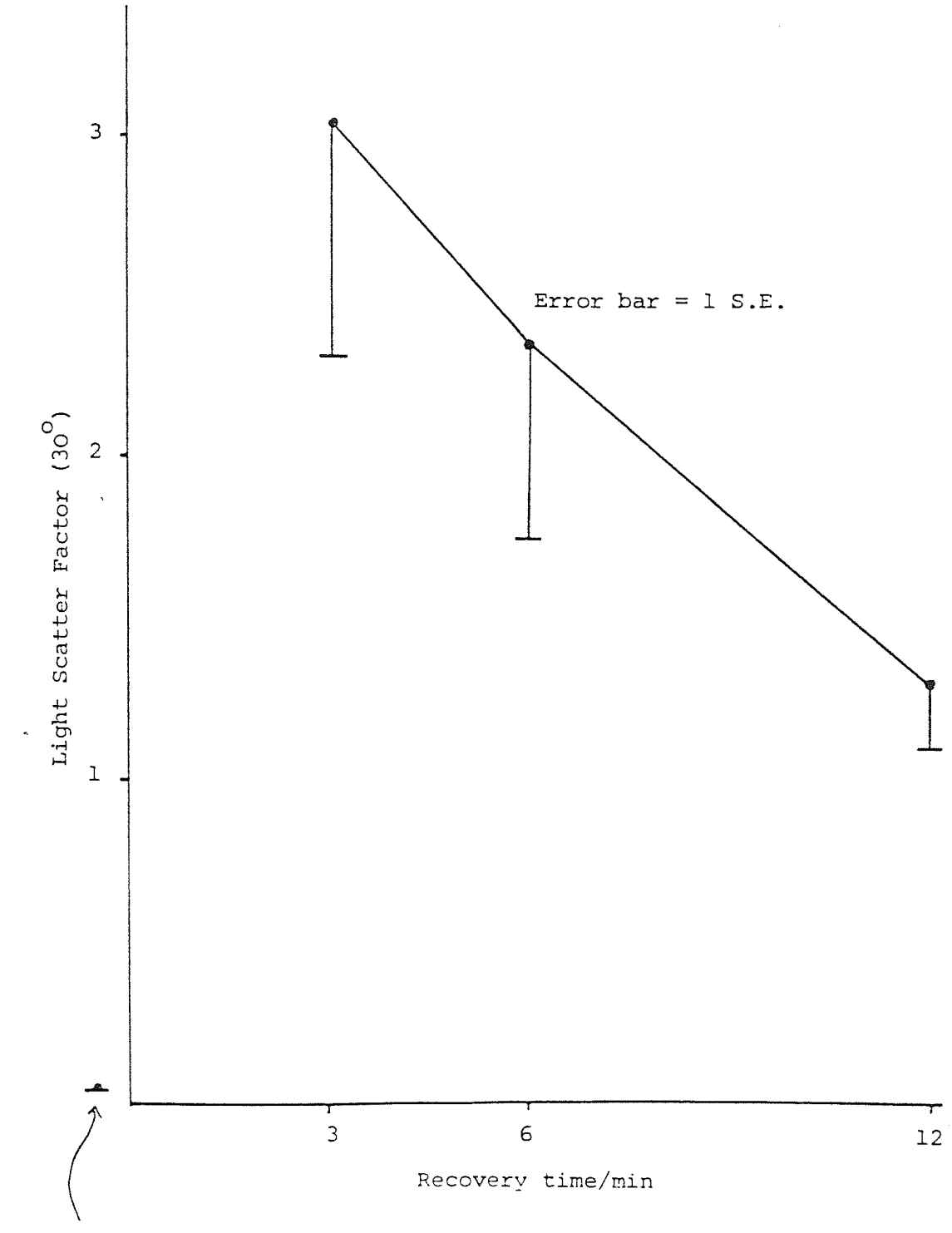

Table 4.12

Interpolated and Normalised Light Scattering Factors (LSF) for Glare Radius = 30° at 3,6 and 12 mins after Scleral Contact Lens Removal

Subject	3 min		6 min		12 mins	
	Interpolated	Normalised	Interpolated	Normalised	Interpolated	Normalised
JR	0.95	1.0	0.67	0.71	0.56	0.59
DUF	3.12	1.0	1.78	0.57	0.89	0.29
RH	3.45	1.0	2.34	0.68	1.84	0.53
MD	1.34	1.0	1.17	0.88	1.06	0.79
CT	3.85	1.0	3.07	0.80	2.06	0.54
DB	6.58	1.0	2.68	0.41	1.56	0.24
GV	2.00	1.0	1.7	0.88	1.14	0.57
N = 7						
mean	3.04	1.0	2.36	0.70	1.30	0.51
SD	1.90		1.55	0.15	0.54	0.18
SE	0.72		0.59	0.058	0.20	0.066

Table 4.13

Initial LSFs Calculated Prior to Contact Lens Insertion, also LSFs Calculated from the Equations of Vos et al[102]

Subject	LSF(3.5°)	LSF(30°)
JR	1.03	0.043
DUF	1.11	0.018
RH	0.36	0.016
MD	0.24	0.026
CT	0.19	0.0072
DB	0.37	0.013
GV	0.82	0.033
Mean	0.60	0.022
SD	0.37	0.012
SE	0.14	0.0045
Vos et al[102]	LSF = 0.78	LSF = 0.011

Fig. 4.10 Percentage change in individual subject corneal thickness interpolated at 3,6 and 12 min after scleral lens removal

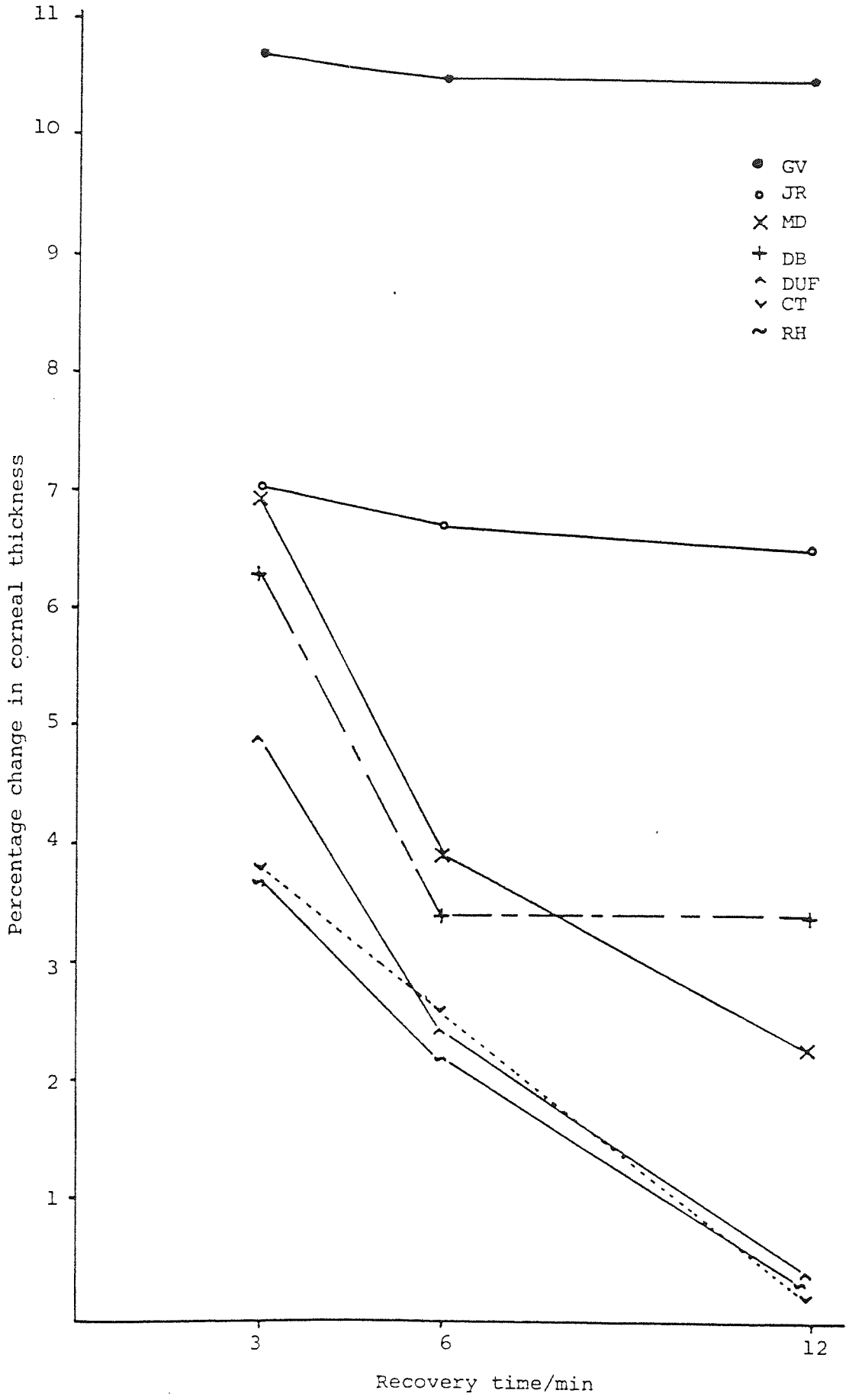

Table 4.14

(i) Initial Corneal Thickness Values for each subject Prior to Scleral Contact Lens Insertion

Subject	Corneal Thickness value/mm
JR	0.460
DUF	0.464
RH	0.454
MD	0.516
CT	0.500
DB	0.414
GV	0.534
Mean	0.477
SD	0.0413
SE	0.0156

(ii) Interpolated, Percentage Change and Normalised Corneal Thickness Values at 3,6 and 12 min after Scleral Lens Removal

Subject	3 min			6 min			12 min		
	Interp.	%Change	Normal.	Interp.	%Change	Normal.	Interp.	%Change	Normal.
JR	0.492	7%	1.0	0.491	6.7%	1.00	0.490	6.5%	1.00
DUF	0.488	4.9%	1.0	0.478	2.4%	0.98%	0.466	0.4%	0.95
RH	0.471	3.7%	1.0	0.464	2.2%	0.99	0.456	0.4%	0.97
MD	0.552	7%	1.0	0.536	3.9%	0.97	0.528	2.3%	0.96
CT	0.519	3.8%	1.0	0.513	2.6%	0.99	0.501	0.2%	0.97
DB	0.440	6.3%	1.0	0.428	3.4%	0.97	0.428	3.4%	0.97
GV	0.591	10.7%	1.0	0.590	10.5%	1.00	0.590	10.5%	1.00
Mean	0.508		1.0	0.50		0.986	0.494		0.974
SD	0.0510			0.0526		0.0127	0.53		0.019
SE	0.019			0.0199		0.0048	0.020		0.0072

Fig. 4.11 Interpolated mean corneal thickness values at 3,6 and 12 min after scleral lens removal, also shown is mean corneal thickness prior to lens insertion.

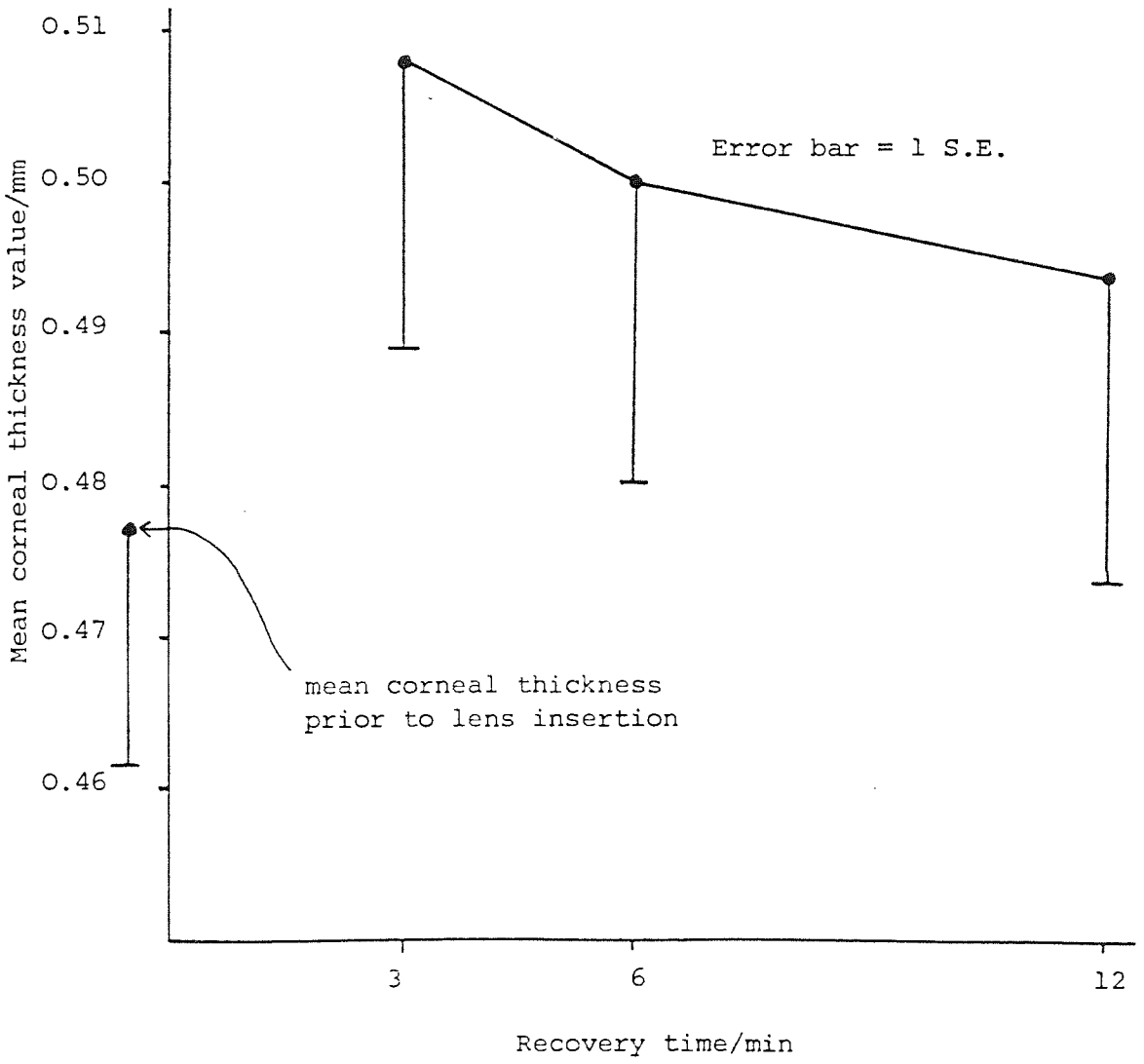

Fig. 4.12 Rate of change of LSF for glare angles 30° (×) and 3.5° (o) and rate of change of corneal thickness (•)

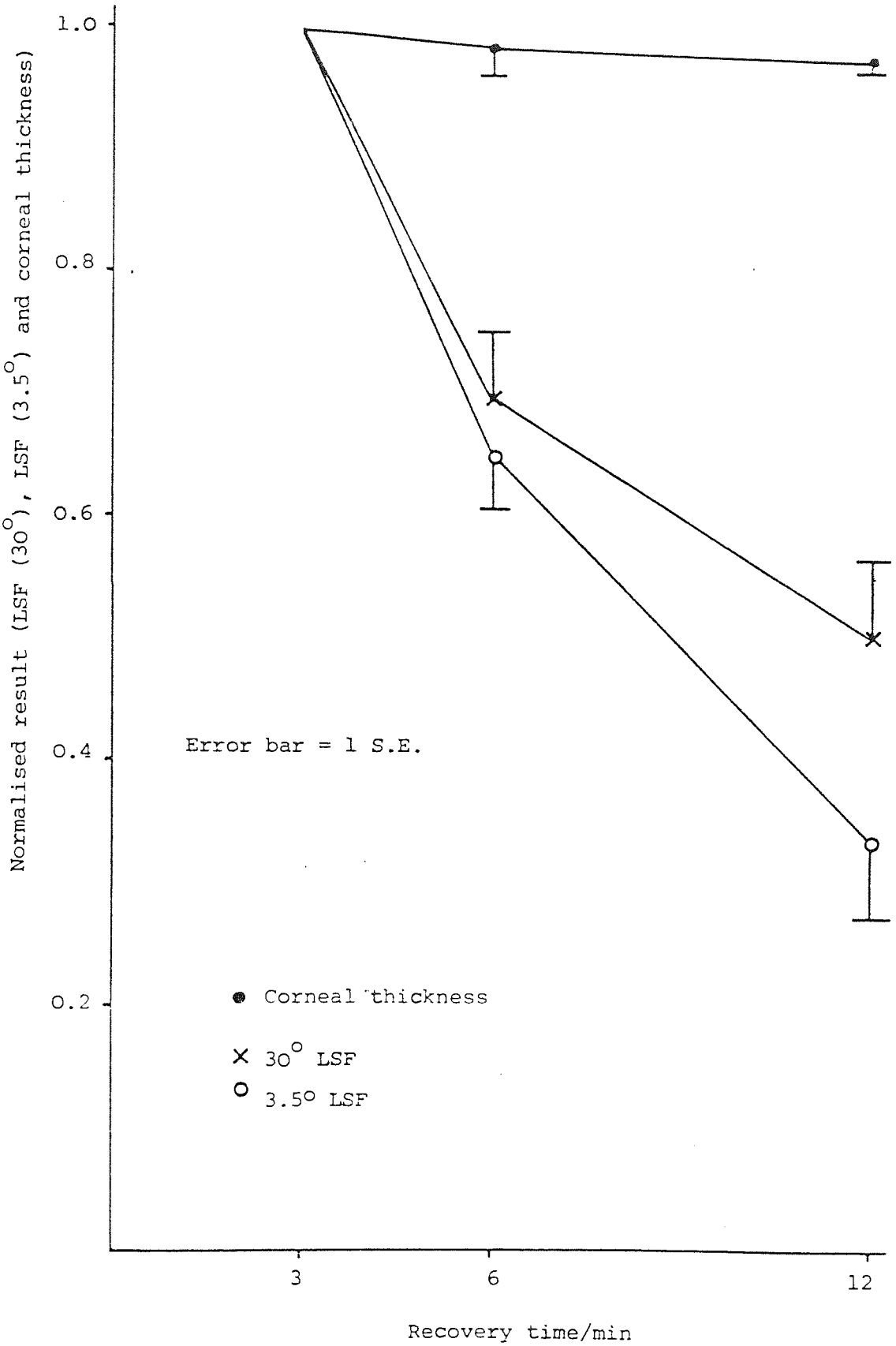

4.3.2 Discussion

This study shows that the quality of a patient's vision is diminished in the presence of corneal oedema (ie contrast thresholds are reduced) and that this is due to the combined light scattering properties of the corneal epithelium and stroma; these effects are increased by the addition of glare lights.

The LSFs calculated using the 3.5° glare source are larger at all points relative to comparable LSFs with the 30° glare source. This is expected due to the inversely proportional relationship between light scatter and glare angle[66,83] (See Section 1.C) When the results obtained for LSFs are normalised it is possible to compare the rate of reduction of light scatter as demonstrated by the 3.5° and 30° glare sources during oedema recovery time (Fig. 4.12). The 30° glare source avoids production of epithelial haloes in the viewing field. The decline in LSF (30°) with oedema indicates the variation in the scattering effect of the corneal stroma as the scattering effect of the lens is constant. The 3.5° glare source, inducing high levels of epithelial haloes and some stromal scattering shows a faster recovery of contrast sensitivity (reduction in LSF) with time than does the 30° glare ring. If this effect were due solely to stromal scattering, the gradient of the 2 graphs would be similar. Therefore the difference in gradients shows the contribution to light scatter of haloes caused by epithelial oedema. The steeper gradient with LSF (3.5°) indicates the more rapid recovery of epithelial oedema relative to stromal oedema. Hess and Garner,[89] Lambert and Klyce[91] and Stevenson et al[82] have all commented on the rapid recovery of epithelial oedema relative to stromal oedema both with measurement of corneal thickness and the presence (or absence) of epithelial haloes, this study confirms this, using an available clinical technique with added glare sources.

Also shown in Fig. 4.12 is the rate of change of corneal thickness over the group. The rate of change (or slope) is much less inclined than either the slope for LSF (30°) or LSF (3.5°), the latter having the steepest gradient. Corneal thickness, as measured by pachometry, records stromal thickness

changes normal to the corneal surface only. It neither records any lateral thickness changes or epithelial thickness changes. Clearly, measuring corneal thickness does not differentiate between stromal and epithelial factors in the way LSFs can. Moverover it does not give a measure of the reduction in the patient's visual ability in the presence of oedema (ie reduced contrast thresholds).

Vos et al[102] gave an empirical relation for LSF against glare source radii for the 'normal' eye.

Equation (1) $LSF = \frac{29}{(\theta + 0.13)^{2.8}}$ $0.15° < \theta > 8°$

Equation (2) $LSF = \frac{10}{\theta^2}$ $4° < \theta > 100°$

These equations summarise previous work on retinal light profiles from point sources where data were obtained from fundus reflectometry for small values; and from stray light measurements from glare studies for larger values. The LSF results for the 'normal' eye in this study (Table 4.13) can be compared to the values found from Vos' equations. Paulsson and Sjostrand[98] found on average LSF = 4.9 for θ = 1.7°; equation (1) gives LSF = 5.4. Vos comments that equation (1) may give an under estimation for LSF, particularly for small angular distances. Both the results in this study and those of Paulsson and Sjostrand[98] indicate the opposite trend for LSF with small θ values. Conversely, Table 4.13 shows that for θ = 30° this study gives a larger LSF value than equation (1) indicates. Vos also comments that values obtained for LSF are 'not exact description of ocular imagery for a standard observer'. It may be that the differences highlighted here for comparative LSF values can be explained by the radically different procedures employed for obtaining light scatter data.

The technique described here separates attenuation of the retinal image contrast caused by epithelial oedema of the cornea and stromal oedema of the cornea and puts quantifiable values to normal light scatter and that due to epithelial and stromal elements; this has not been reported previously.

The results could have important clinical implications, particularly in contact lens practice where present techniques for observing and monitoring corneal oedema are limited. With this technique it is possible to quantify the smallest changes in corneal transparency, this is obviously of great advantage to the clinican and may help evaluate contact lens designs.

4.4 Experiment 4

The Effect of Corneal Contact Lens wear on the CSF and on the Light Scattering Properties from the Contact Lens/Corneal Interface

The effect of very large amounts of induced oedema on light scattering in the cornea has been demonstrated in the previous study (Experiment 3). This study measured intraocular light scatter and the CSF in groups of adapted corneal contact lens wearers. The amounts of corneal oedema involved in such groups will be small. Hence the aim was the assessment of intraocular light scatter in 3 contact lens groups ie Hard (PMMA), Gas permeable and soft (Hema) and in a control (Non contact lens) group, such as would be encountered in optometric practice.

The apparatus is shown in Fig. 3.2 and Plates 3.1 and 3.2, Glare condition (ii) was applied (Section 3.1.B). In order to measure corneal light scatter each subject had their contrast threshold at 1 cpd and 2Hz counterphase recorded with and without the 3.5° and 30° glare sources, in the afternoon after 7.5 hours of continuous contact lens wear. The CSF was also measured at 1,3, 6 and 11.4 cpd with a 2Hz counterphasing grating and applying the 60 sec MIC. The main stipulation for the contact lens wearers to take part in this study was that they should be happy with their lenses, wear them most of the time and attend for testing after 7.5 hours wear that day (Refer to Clinical details). LSFs were calculated from thresholds taken with and without both glare sources and are presented here along with data on the CSF.

4.4.1 Results

The results are represented in Figs. 4.13 and 4.14, the data is shown in Tables 4.15, 4.16 and 4.17. The CSFs shown in Fig. 4.13 indicate that the non CL (control) group has the highest contrast sensitivity at all spatial frequencies and the Gas Permeable (GP) CL wearer have the lowest contrast sensitivity at all spatial frequencies. The range in contrast threshold depression between these 2

Fig. 4.13 Contrast Sensitivity Functions for each subject group, also contrast thresholds for both glare conditions for each group.

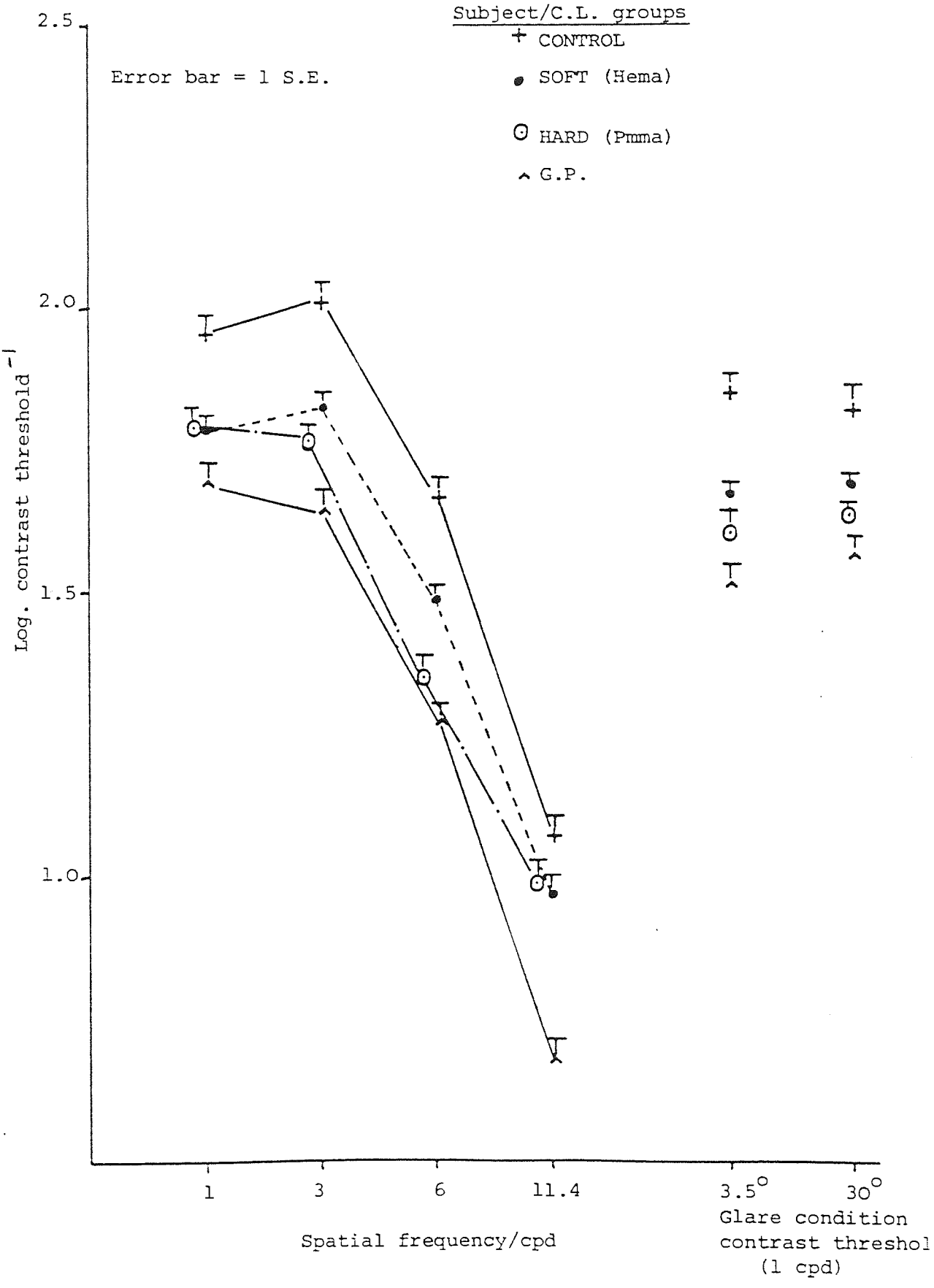

Table 4.15

Log Contrast Thresholds at 1 cpd for both Angular Glare (ie 30° and 3.5°) and also Contrast Thresholds at Spatial Frequencies 1.3, 6 and 11.4 cpd for each Subject Group

SUBJECT Group		30° glare threaholds	3.5° glare thresholds	1 cpd	3 cpd	6 cpd	11.4 cpd
GAS PERM	m	1.57	1.52	1.7	1.65	1.28	0.68
	SD	0.11	0.11	0.10	0.11	0.095	0.098
	SE	0.036	0.034	0.032	0.035	0.03	0.031
SOFT	m	1.70	1.68	1.79	1.83	1.49	0.97
	SD	0.066	0.090	0.1	0.083	0.093	0.11
	SE	0.02	0.027	0.03	0.025	0.028	0.034
PMMA	m	1.65	1.62	1.80	1.78	1.36	1.00
	SD	0.053	0.085	0.066	0.053	0.093	0.079
	SE	0.02	0.032	0.025	0.02	0.035	0.03
CONTROL	m	1.83	1.86	1.96	2.02	1.67	1.07
	SD	0.13	0.093	0.079	0.093	0.077	0.066
	SE	0.05	0.035	0.03	0.035	0.029	0.025

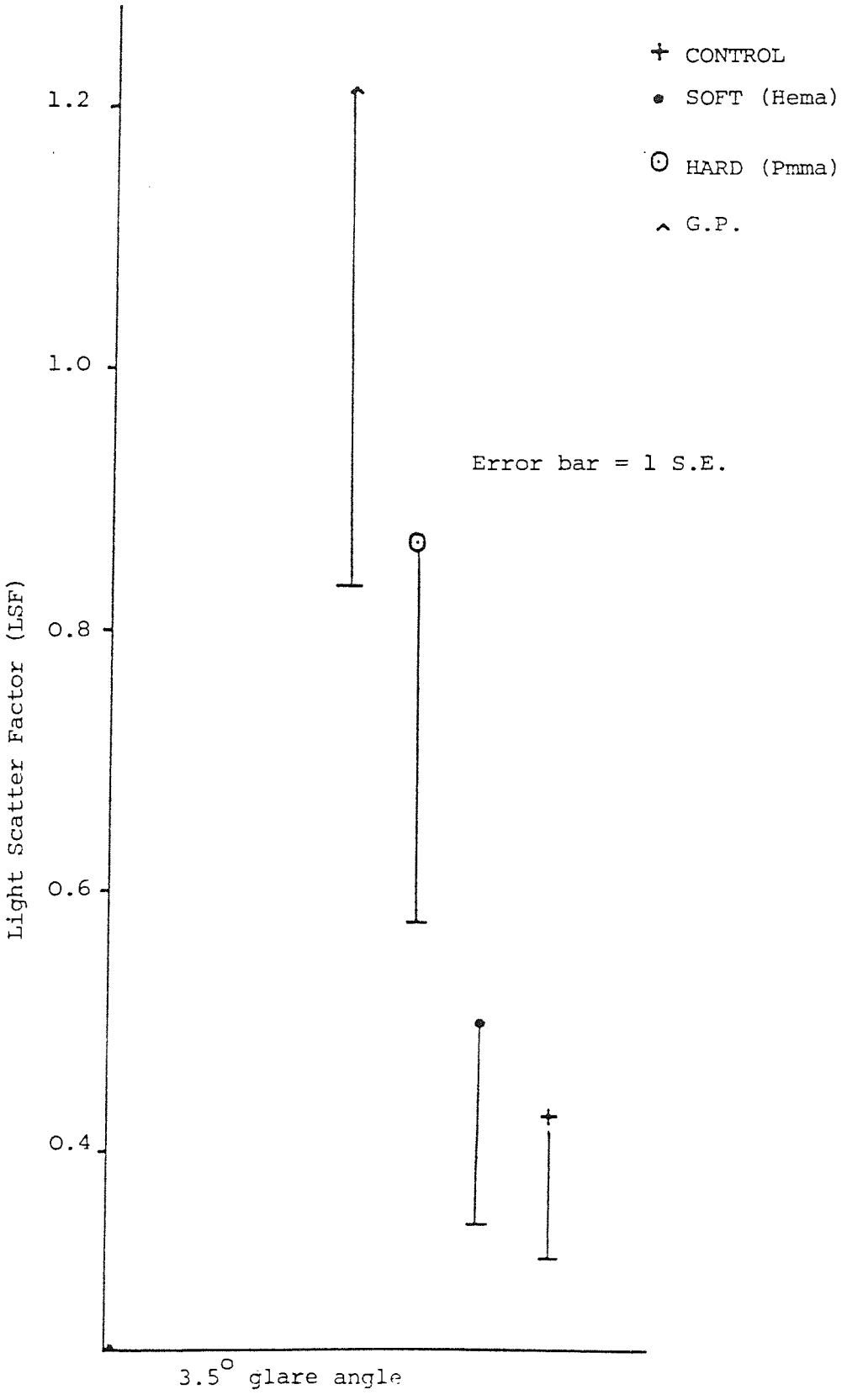

Fig. 4.14 Group mean LSF at 3.5° glare angle for each subject group.

Table 4.16

Average LSFs for both Glare Angles and each Subject Group

		Small (3.5°) LSF	Large (30°) LSF
GAS PERM.	m	1.22	0.0097
(N=10) group	SE	0.38	0.0038
SOFT	m	0.50	0.0062
(N=11) group	SE	0.15	0.0018
PMMA	m	0.87	0.012
(N=7) group	SE	0.29	0.0064
CONTROL	m	0.43	0.0098
(N=7) group	SE	0.11	0.0040

Table 4.17

Statistical Significances for paired Subject Groups at Mean Values: (A) for Contrast Thresholds at 4 Spatial Frequencies, (B) Contrast Thresholds with each Glare Source, (C) for LSFs with each Glare Source (Refer to Figs. 4.13 and 4.14)

Statistical Significance of paired Subject Groups

Subject Group	GP/ Control	GP/ PMMA	GP/Soft	Soft/ PMMA	Soft/ Control	PMMA/ Control
(A)						
1 cpd	$p<0.001$	$p<0.05$	$p<0.05$	not sig.	$p<0.001$	$p<0.001$
3 cpd	$p<0.001$	$p<0.05$	$p<0.001$	not sig.	$p<0.001$	$p<0.001$
6 cpd	$p<0.001$	not sig.	$p<0.001$	$p<0.05$	$p<0.001$	$p<0.001$
11.4 cpd	$p<0.001$	$p<0.001$	$p<0.001$	not sig.	not sig.	not sig.
(B)						
30°glare contrast threshold	$p<0.001$	$p<0.05$	$p<0.05$	not sig.	$p<0.01$	$p<0.001$
3.5° glare contrast threshold	$p<0.001$	$p<0.01$	$p<0.05$	not sig.	$p<0.001$	$p<0.001$
(C)						
LSF (30°)	not sig.	not sig.	not sig.	not sig.	not sig.	not sig.
LSF (3.5°)	$p<0.01$	not sig.	$p<0.05$	not sig.	not sig.	not sig.

groups is 0.26 log units at 1 cpd to 0.39 log units at 11.4 cpd. The other 2 CL groups fall in between the control and GP group. ie at 1 cpd and 3 cpd the soft and PMMA CL wearers have similar mean contrast threshold values to each other, at 6 cpd the PMMA wearer have a significantly higher threshold value than the soft lens wearers ($p < 0.05$), while at 11.4 cpd the threshold values are not significantly different. Similar trends are found with the contrast threshold values recorded at both glare angles (Fig. 4.13) this is also reflected in the LSF (3.5°) results (See Fig. 4.14) where the GP lens wearers have the highest LSF result, the control group the lowest LSF result with soft and PMMA wearers falling in between. LSF values at the 30° glare source were not significantly different from each other for any paired subject groups (See Table 4.17). This shows that light scatter differences being calculated were very small and that changes in wide angle (30°) scatter between subject groups was negligible.

Clinical Details of Contact Lens Wearing Subjects

Soft CL Group N= 11. (M=3, F=8)

M = Male
F = Female

Subject	Spec Rx	Type of CL	History
1. SC (F)	R-6.00/+0.75 x 80 6/6 L-6.25DS 6/5	Soft (Hema)	1st pr. CLs MaxW.T/day =14hr Had CLs for 11/2 yrs. No probs
2. HD (F)	R-5.00/+0.50 x 105 6/5 L-4.25/+0.75 x 85 6/5	Soft	1st pr CLs MaxW.T/day = 16hr Had CLs for 10 mnth. no probs
3. MS (F)	R-6.50/+0.25 x 95 6/5 L-5.50/+0.75 x 80 6/6	Soft	2nd pr CLs MaxW.T/day = 8hr Had CLs 2yrs- 1st pr GP CLs Never comfortable hence refit
4. CW (M)	R-3.00/+0.25 x 145 6/5 L-3.75/+0.50 x 90 6/5	Soft	2nd pr CLs Last pr also soft, but probs after 2 yrs, hence refit. Max W.T/day = 15hr No probs since new pr.
5. MS (F)	R-5.00 DS 6/6+ L-5.50/+0.25 x 180 6/5	Soft	4th pr CLs previous prs also soft-lost several lenses. Max W.T/day = 12 hr No probs
6. MW (F)	R-9.00/+1.00 x 135 6/6 L-9.25/+1.25 x 45 6/6-1	Soft	2nd pr CLs. Last pr PMMA was uncomfortable plus wanted to play sport - hence refit with soft CLs - No probs now. Max W.T/day = 10 hr.
7. AG (F)	R-3.50 DS 6/5 L-2.25/+0.50 x 90 6/5	Soft	1st pr Cls. MaxW.T/day = 16 hr Had CLs 6/12. No probs
8. YT (M)	R-3.50/+1.00 x 100 6/5 L-4.00/+3.00 x 80 6/12	Soft	1st pr CLs Max W.T/day = 11 hr No probs
9. HG (F)	R+4.00 DS 6/6 L+4.75 DS 6/6	Soft	2nd pr CLs. 1st G.Ps found uncomfortable and reduced W.T, hence refit with soft - No probs now. MaxW.T/day = 8 hrs Wear spec R_x during day occasionally.

Subject	Spec	Rx	Type of CL	History
10. AR(F)	R-4.50/+0.25 x 70 6/5 L-3.00/+0.25 x 100 6/5		Soft	2nd pr CLs. Last pr also soft and probs after 3 yrs hence refit. Max W.T/day = 141/2 hrs No probs now.
11.ALG(F)	R-5.35 DS 6/6 L-5.00DS 6/6		Soft	2nd pr CLs. Last pr PMMA - never comfortable, hence refit to soft. MaxW.T/day = 12 hrs No probs now

GP CL Group. N= 10 (M=2, F=8)

Subject	Spec Rx	Type of CL	History
1 JC (F)	R-4.25 DS 6/5 L-4.50 DS 6/5	GP	2nd pr CLs. Last pr also GPs- after 3 yrs v. scratched. Hence refit. Max WT/day = 16 hrs No probs now
2 SG (F)	R-5.00 DS 6/5 L-5.50 DS 6/5	GP	About 3rd pr GP CLs - other lenses lost, had present CLs 11/2 yr - had CLs polished once. No probs now. Max W.T/day = 13 hrs
3. CH (M)	R-2.75 DS 6/5 L-2.00DS 6/5	GP	2nd pr CLs, 1st pr PMMA could not wear more than 5hr/day - hence refit - Max W.T/day = 13 hrs. No probs now.
4. JM (M)	R-3.25/+0.25 x180 6/5 L-3.00/+0.25 x 180 6/5	GP	3rd pr CLs. 1st pr PMMA - lots of probs, bad fit and corneal oedema. Refitted with soft for 3yrs until advised to stop wearing CLs due to corneal neovascularisation. After 6/12 break refitted with current pair of GP CLs - no probs now. Max W.T/day = 14 hrs
5. MT (F)	R-4.25 DS 6/5 L-3.50 DS 6/5	GP	3rd pr CLs. 1st pr GPs - refitted due to scratched surfaces after 2 yrs. - refitted 1 yr later with stronger Rx. MaxW.T/day = 15 hrs. No probs now.
6. DT (F)	R-3.50/+2.00 x 12 6/9 L-3.25/+1.75 x 160 6/6	GP	2nd pr CLs. 1st pr soft no probs with fit but changed to GP for improved V/A. MaxW.T/day = 15 hrs. No probs now
7. MG (F)	R-4.25 DS 6/5 L-4.24 DS 6/5	GP	1st pr CLs. Max.W.T/day = 16 hrs. No probs. Had CLs 1 yr.

Subject	Spec Rx	Type of CL	History
8. ME (F)	R-8.00DS 6/6 L-7.00/+5.00 x 80 6/36	GP	5th pr CLs over 10 yrs. Only wears on R.E. 1st 3 yrs wore PMMA - advised to change to GP for extra comfort. No probs now. Max W.T/day = 14 hrs
9. SL (F)	R-3.50/+0.50 x 180 6/5 L-4.00 DS 6/5	GP	2nd pr CLs. 1st pr also GPs but became stratched with reduced V/A after 2 yrs. - hence refitted MaxW.T/day = 12 hrs. No probs now
10.GS (F)	R+4.00/-2.00 x 70 6/24 L+3.00/-1.50 x 120 6/6	GP	2nd pr CLs. 1st pr soft but changed to GP for improved V/A Max W.T/day = 15 hrs No probs now

Hard (PMMA) CL Group N = 7 (M=1 F=6)

Subject	Spec Rx	Type of CL	History
1. KE (F)	R-3.25/+1.25 x 175 6/6 L-3.25/+1.25 x 10 6/6	PMMA(hard)	1st pr. CLs. Never had any probs Max W.T/day = 15 hrs
2. KP (M)	R-1.50 DS 6/5 L-1.50 DS 6/5	PMMA	1st CLs. No probs MaxW.T/day = 13 hrs
3. SU (F)	R-5.25/+0.50 x 180 6/5 L-5.00/+0.25 x 170 6/5	PMMA	3rd pr CLs. 1st pr PMMA, after 2 yrs, advised to change to GP - does not know why never happy with GP CLs - greasing up continually, hence 6/12 mths ago refitted with PMMA - no probs now. Max W.T/day 12 hrs
4. EP (F)	R-4.00/+2.00 x 90 6/6 L-3.00/+2.50 x 80 6/9	PMMA	2nd pr of PMMA lenses. Originally wanted soft but advises against this due to reduced V/A. Never wears Spec Rx. MaxW.T/day = 16 hrs. No probs
5. MT (F)	R-3.00 DS 6/5 L-2.50 DS 6/5	PMMA	2nd pr CLs. 1st soft but lenses kept getting damaged and solutions expensive. Changed to PMMA 2 yrs ago, since then no probs
6. JE (F)	R-6.50 DS 6/5 L-8.00 DS 6/6	PMMA	3rd pr CLs. Always had PMMA hates specs. No probs. Max W.T/day = 15 hrs
7. JN (F)	R-3.00 DS 6/5 L-3.25/+0.75 x 90 6/5	PMMA	2nd pr CLs. Originally had GPs but always greasy. Hence refitted - had these CLs polished 6/12 mnths ago - no probs now. MaxW.T/day = 10 hrs

4.4.2 Discussion

The previous study (Experiment 3) involved inducing high levels of corneal oedema and used the 3.5° and 30° glare sources in order to differentiate between light scatter from epithelial and stromal tissues. The aim of this study was to examine the light scattering properties of the CL/corneal interface causing reduced CSFs and increased LSFs in groups of adapted corneal contact lens wearers, such a study has not been conducted previously.

The results show that surprisingly, the CSF is most attenuated in the GP lens wearers compared to the control (non CL) group and also that this attenuation in contrast threshold is of the same order at all spatial frequencies ie about 0.35 log units. The other 2 CL groups show similar trends with approximately equal threshold depressions at all 4 spatial frequencies ie about 0.16 log units for the PMMA lens wearers and about 0.19 log units for the soft CL wearers (Refer to Fig. 4.13) Previous studies on CL wearers and the CSF (See Section 2.C.1) have generally concluded that contrast threshold attenuation, assumed to be due to corneal oedema, occured (if at all) at the high spatial frequencies and that low spatial frequencies were largely unaffected. This study contradicts that result and shows that in these particular subjects, contrast thresholds are significantly depressed at low as well as high spatial frequency values in the CL groups. Similar trends are shown for the contrast threshold (at 1 cpd) for each subject group with each glare source (Fig. 4.13) emphasising this point. The slightly greater threshold attenuations shown at the high frequency end of the CSFs may indicate the defocus effect in the results.

Fig. 4.14 shows the range of LSF values obtained for each CL group with the 3.5° glare source. The results indicate that the GP lens wearers have the greatest LSF compared to the control with the other 2 CL groups having LSF values in between. This is consistent with the contrast threshold results and it may be concluded that contrary to the expected result, the GP CL wearers have the most depressed CSF with the highest light scattering properties from the lens/corneal interface. GP lens materials

allow more oxygen to the cornea than PMMA. It would be expected that various contact lenses could attenuate the CSF and increase light scattering and this is shown clearly in Figs.4.13 and 4.14, but what factors account for the surprising result that the most marked effect is with the GP CL wearers? These are discussed as follows;

One possibility that could account for these results is that the subjects in the GP group were more oedema prone. Examination of the Clinical Details listed, show that GP subject numbers 3 (CH), 4 (JM) and possibly 8 (ME) may have had this problem and they account for 30% of the group. However similar proportions of subjects in the other 2 CL groups also had problems in the past that may have been oedema related. Another factor effecting the amount of oedema in female subjects is the taking of oral contraceptives[208] although improvements in these drugs now means that these effects are reduced. Moreover, the proportions of female subjects is similar in each subject group.

The main criteria for a CL subject to take part in this study was a V/A of 6/9 or better in the preferred eye, and the fact that they were contented with their lenses and wore them most of the time, therefore the subjects constituted a clinical selection of CL wearers such as might be encountered in optometric practice. Hence a number of factors not quantified here could have influenced results. GP lenses can be fitted up to 0.2mm larger in overall size than PMMA, hence any improvement in oxygen permeability due to GP material may be lost in the larger corneal surface area that is covered. Moreover central fit of the CLs eg BCOR, would also effect oedema levels, especially since GP lenses have a tendancy to become distorted. GP lenses are also known to collect surface deposits (mainly protein) more readily than PMMA. This could potentially have quite a marked effect on the CSF, deposits on the lens surface may reduce oxygen transmission, however high light scatter values with GPs could be due not to corneal oedema but to the properties of the lens surface. Moreover frequency of use of CL cleaners and protein tablets would also effect this.

Comparison of LSF (3.5°) results for this study (See Fig. 4.14), and for Experiment 3 the induced oedema study (See Fig. 4.8), shows that the amounts of light scatter and therefore oedema involved were as expected much smaller. Maximum LSF (3.5°) in this study found with the GP CL group was measured at 1.22. In contrast to this, LSF (3.5°) recorded in the induced oedema study, at 12 mins after scleral lens removal was 6.75. This confirms the fact that in Experiment 3 recovery from oedema was still underway even at 12 mins after removal of the scleral CL.

In conclusion this experiment measured the visual abilities of 3 groups of adapted corneal contact lens wearers after 7.5 hours of continuous wear. The results show significant reductions in the CSF at all spatial frequencies in all CL groups, but particularly in the GP wearers. Also manifest is an increase in light scatter (as measured by LSFs) at the 3.5° glare angle in all CLs but most significantly with the GP wearers. Numerous factors could have accounted for these results and these have been discussed ie clinical history of subjects, fit and overall size of the lenses, surface deposits, cleaning regimes etc. The control group who did not wear CLs had the best overall vision (highest CSF and lowest LSF). However, in the CL wearers examined here, all of whom were contented with their lenses and had a good V/A, subjects with GP lenses had the worst overall standard of vision, (most attenuated CSF) and demonstrated the greatest amount of light scatter (highest LSF with 3.5° glare angle). Soft and PMMA CL wearers fall in between the control and GPs. The fact that the trends in LSF were not significant at the 30° glare angle may indicate that the oedema present was mainly epithelial in origin.

Hence this study shows that depression in the CSF and increase in light scatter was greatest in the gas permeable contact lens wearing group of subjects. This is due to the properties of the contact lens/corneal interface in this particular group. It is proposed that the majority of this result is due to the surface properties of the lenses themselves but may in part be caused by epithelial oedema. This technique has allowed quantification of forward light scatter onto the retina from subjects wearing 3 types of corneal contact lenses, this has not been conducted previously. The results give additional

information to the clinician particularly applicable to the practice situation where the variables that effect the visual capabilities of contact lens wearers cannot be strictly controlled. Moreover, the results could aid in future evaluations of contact lenses.

4.5 Experiment 5

The variation of end point visual acuity with age using an optic bypass (Retinometer) and non optic bypass (Projected) matched systems and 2 psychophysical procedures

The aim of this study was to show the variation in end point V/A due to both ageing and psychophysical techniques in subjects with good V/A and without advanced cataracts, using clinically available equipment ie the Rodenstock Retinometer. The procedure and methods have been described in Section 3.1.C. The Retinometer provides a system for assessing V/A that bypasses most optical components (which cause light scatter) and therefore gives an estimate of the neural V/A.

4.5.1 Results

Figs. 4.15 and 4.16 shows the results where number of eyes seeing the target grating are plotted against spatial frequency, the 2 graphs demonstrate the 2 psychophysical methods used ie 'Shutter' method and '5 sec' method (Refer to Section 3.1.C) for the same subject groups. In Fig. 4.15 all of the 'young' group (ie N =10) saw all spatial frequencies for the Retinometer presentation, where as with the projected presentation one subject failed to see the 26.4 and 33 cpd targets. To compare, with the 'old' group, only 3 out of 10 eyes saw the Retinometer 33 cpd target and only 1 subject the projected 33 cpd target. In comparison Fig. 4.16 employing the 'Shutter' method, shows that the reduction in viewing time from 5 secs to 30msecs greatly reduces the end point V/A results for both groups, this is most striking with the 'old' group and the projected presentation where no subjects saw a target spatial frequency higher than 20.8 cpd. All other end point results also dropped; ie with the 'young' group the Retinometer 33 cpd result fell from 10 to 8 eyes seen, the Projected 33 cpd result went from 9 to 7 subject's eyes seen while the Retinometer end point result for the 'old' group went from 3 to 2 eyes seen.

Fig. 4.15 Shows the end point of V/A at 4 high spatial frequencies for a "young" and an "old" age group using Retinometer and projected gratings. No. of eyes seeing the target grating is plotted against spatial frequency.

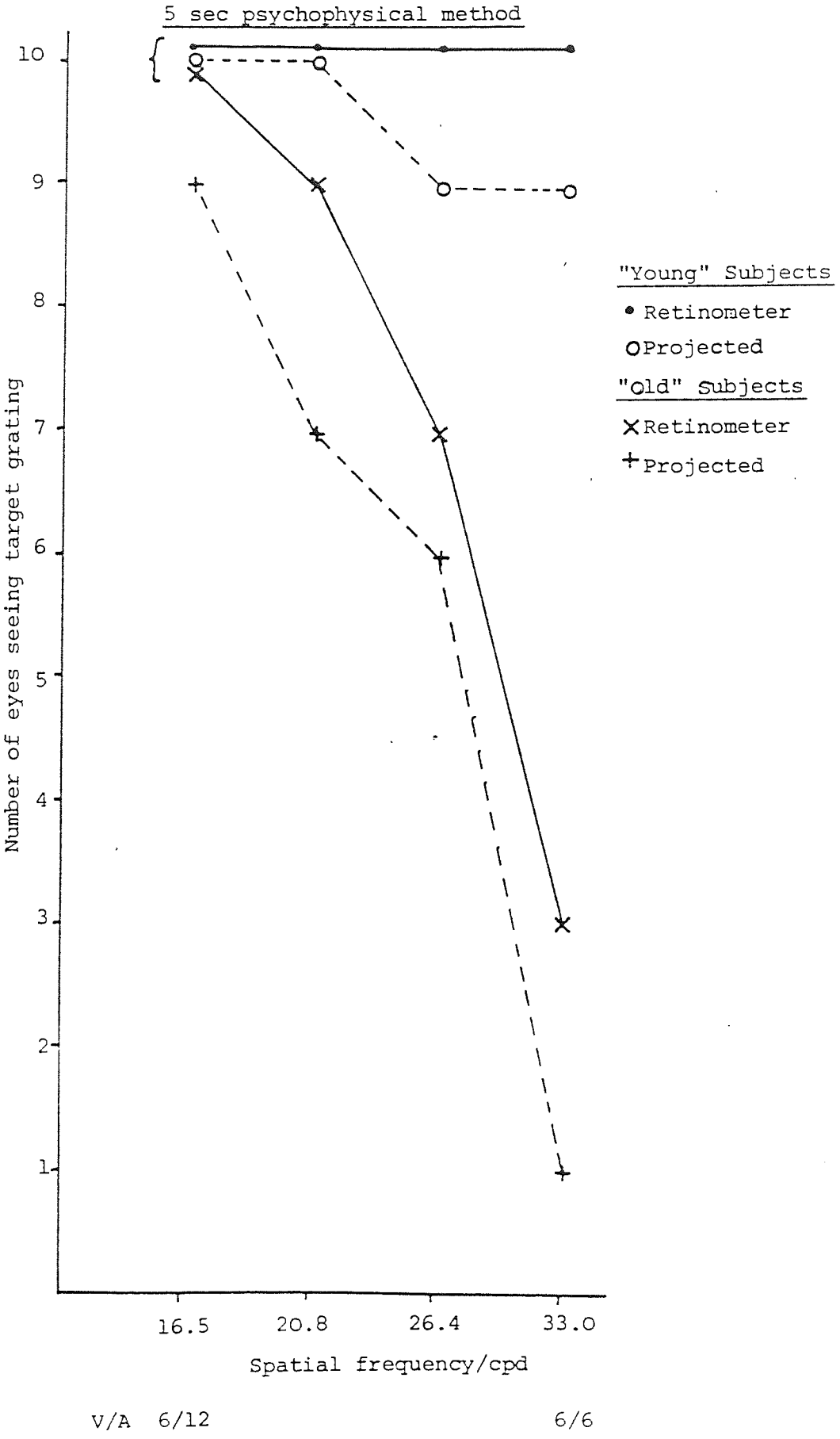

Fig. 4.16 Shows the end point of V/A at 4 high spatial frequencies for a "young" and an "old" group using Retinometer and projected gratings.
No. of eyes seeing the target grating is plotted against spatial frequency.

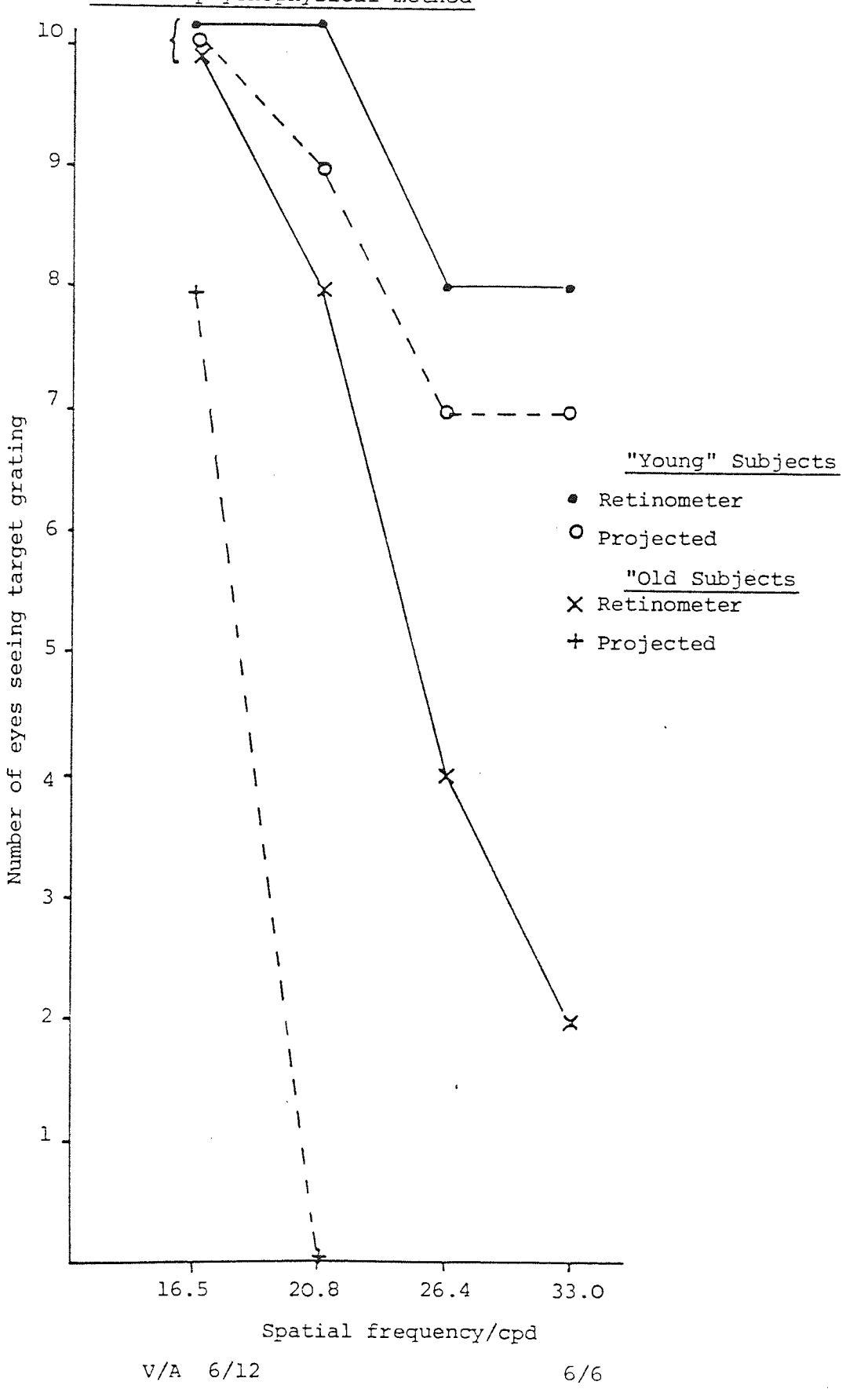

4.5.2 Discussion

The results demonstrate that end point V/A was lower at any age with a projected presentation compared to a Retinometer (optic bypass) presentation, but this reduction in V/A was much more pronounced in the 'old' age group. This implies that there may be slight media opacities/irregularities even in the 'young' group, however in the 'old' group, the drop in V/A is expected due to media opacities/light scattering associated with ageing. Hence in Fig. 4.15 the drop at 33 cpd for the 'old' group from 3 eyes (Retinometer) to 1 eye (Projected) is wholly due to optic media input. Conversely the difference in Retinometer result for 'young and 'old' groups ie 10 eyes to 3 eyes represents the effect of the neural input in the 'old' group.

Fig. 4.16 demonstrates the marked effect that a change in psychophysical technique can have on measuring end point V/A. Although Fig. 4.16 shows the same trends ie Retinometer V/A is always greater than Projected V/A for equivalent groups, the reduction of viewing time to 30msec so attenuates the results as to give the Projected result for the 'old' group an end point spatial frequency no higher than 20.8 cpd. The reactions of elderly people are bound to be slower and at least part of this drastic change in result will be due to this. However, Fig. 4.16 in comparison to Fig.4.15 shows clearly that a change in psychophysical method can alter results, and it may be that a 30msec exposure time is too short for a clinical environment. This emphasises the need to standardise procedures for clinical and experimental use of the Retinometer.

In conclusion this study gives quantified data on the effect of ageing on optical and neural resolution with high contrast fringe patterns of high spatial frequency using subjects with good V/A and without advanced cataracts using clinically available equipment, namely the Rodenstock Retinometer, this has not been done previously. (Refer to Sections 2.C.2 and 1.D) The results taken from Fig. 4.15 demonstrate that in the elderly group, at 33 cpd about 66% of the attenuation in resolution is due to neural input. Hence about 33% is due to optical media/light scattering factors. This agrees well with

the data of Campbell and Green[130] and Weale.[61] Conversely, Williams[184] found that resolution to interference fringes at high spatial frequencies was very much higher than the results of previous studies[130,157,209] due to the presence of Moire fringes. The difference that psychophysical technique can make to results has been clearly demonstrated in this study, and it may be that differences in procedures, interferometer design and subjects would account for lack of agreement between studies.

CHAPTER 5

CONCLUSIONS

Chapter 5

Conclusions

The experiments described in Chapter 4 involving clinical psychophysical measurement of the CSF in the presence of glare sources have led to the following conclusions about the role of intraocular light scatter in vision.

(1) Psychophysical Techniques of Measurement of Contrast Sensitivity

The techniques of measurement for any experiment will affect the results. This has been amply demonstrated in Experiments 4.1 and 4.5. For clinical testing of contrast sensitivity the need is for a quick, easy to understand and consistent measurement method. The Nicolet CS2000 was designed to provide this. Experiment 4.1 investigated 4 logarithmic ramp rates and 3 measurement techniques ie MIC, MDC and Bekesy. Such a study has not been conducted previously on this clinically available equipment. The results, in common with previous laboratory studies showed that the MIC was the most consistent measurement method, this was especially so at the slowest ramp rate examined ie 120 sec. Subjectively a 120 sec ramp was found to take too long causing fatigue and lack of concentration among the subjects. In view of the fact that the difference in measurement errors for the 60 sec ramp was only slightly greater than the 120 sec ramp, and the 60 sec ramp was more acceptable to the subjects, the study recommended a 60 sec MIC technique for measuring contrast thresholds. Further analysis of the three measurement techniques showed that the lack of consistency of results using the Bekesy method was mainly due to the descending (MDC) component. The MIC contrast thresholds varied little with change in logarithmic ramp rate compared to the Bekesy and MDC techniques where measurement errors increased steadily with shorter ramp rates.

No correlation between subject's age and measurement method could be demonstrated with the CS2000, although examination of Fig.4.1 indicated that there may be a small (if insignificant) trend

towards reduced contrast thresholds with all three methods with increasing age of the subjects.

Experiment 4.5 also considered the effect of psychophysical technique of measurement on the clinical recording of end point V/A using the Rodenstock Retinometer and a Projected Gratings Paradigm, employing high contrast, high spatial frequency targets. Such a study has not been conducted previously. The results showed that by reducing the target viewing time for the subjects from 5 sec to 30msec, the end point V/A fell markedly from a maximum of 33cpd to a low of 20.8cpd in the 'old' age group, although the 'young' group result fell to a lesser extent. This emphasised the need for consistent measurement methods in order to be able to compare clinically obtained data on the same equipment. The greater depression in end point V/A with the 'old' group showed the need to age match results.

(2) Recording the CSF

Following the results of 4.1, the 60 sec MIC measurement technique was applied on all subsequent measures of contrast threshold using the CS2000.

(i) The Effect of Age and Intraocular Light Scatter

The CSF was measured on a large group of subjects (N=54) divided into a 'young', 'intermediate' and an 'old' age group (Fig 4.5). The results showed that the CSF was attenuated at all spatial frequencies measured, for both 'intermediate' and 'old' age groups (compared to the 'young' group). In contrast to this, measurements of intraocular light scatter by recording Light Scatter Factors (LSFs) for the same subject groups showed that only the 'old' group (over 60 years), had higher Light Scatter Factor values than the other two groups, at both narrow (3.5°) and wide (30°) glare angles. Analysis of the results concluded that the attenuation of the CSF shown with the 'intermediate' group was due mainly to media absorption and/or neural factors while about one fifth of the result may be due to a fall in retinal illuminance caused by reduced pupil size. In the 'old' group intraocular light scatter (demonstrated with increased Light Scatter Factors) was likely to be the major reason for CSF depression.

Such a study permitting the quantification of forward intraocular light scatter causing reduced contrast thresholds and increased Light Scatter Factors with respect to age has not been conducted before on clinically available equipment and in subjects without visible media opacities. These studies have provided new information and given quantified values to the effects of light scatter in the eye.

The fact that circular glare sources concentric with the eye enhanced the effect of forward intraocular light scatter which increased with age has been amply demonstrated. (Fig. 4.4, 4.6 and 4.7). This is due to the increasing number of light scattering particles in the optic media of the eye ie increasing turbidity (mainly in the lens) which is a normal part of the ageing process.

(ii) The Effect of Contact Lens Wear, Corneal Oedema and Intraocular Light Scatter

Fig 4.13 shows the CSFs recorded in a clinical sample of soft, PMMA and GP corneal contact lens wearers and a control (non CL) group. The results show that the CSF was attenuated at all spatial frequencies in all the contact lens wearing groups and was most attenuated with the GP wearers. The CSF was highest with the control group. In addition, Light Scatter Factors with the 3.5° glare angle were high in the contact lens wearers (highest in the GP group) and lowest in the control group. Analysis of the results concluded that this was due to the properties of the corneal/contact lens interface in this particular clinical sample, and that the result with the GP wearers was mainly due to lens surface properties themselves, although epithelial oedema may have been a factor. It can be stated that the quality of vision in this clinical sample of GP contact lens wearers was lower than both soft and PMMA contact lens wearers. The control group had the best vision. Such a study quantifying the effects of light scatter and contrast thresholds on three different groups of contact lens wearers using clinically available equipment has not been previously conducted. The results have important implications for optometric practice and prescribing of contact lenses, and could aid in contact lens designs.

The clinical measurement of contrast thresholds in the presence of corneal oedema and with the addition of glare sources to enhance corneal light scatter provided new information not previously reported. Experiment 4.3 monitored the recovery from gross corneal oedema by measuring the contrast thresholds and Light Scatter Factors with a 3.5° and 30° glare angle in seven subjects. Corneal thickness changes were also monitored. The results enabled the quantification of 'normal' light scatter values and those due to epithelial and stromal elements. The study concluded that epithelial oedema recovery was faster than stromal oedema recovery, and that measuring Light Scatter Factors gave additional information about the physiological condition of the cornea, ie the highest values were at maximum oedema and fell as oedema diminished. Moreover, Light Scatter Factors gave a measure of the quality of vision that might be expected in an individual.

The quantification of intraocular light scatter and contrast sensitivity and its effects on vision are of major importance in optometry and ophthalmology. The assessment of visual fields, of contact lenses and of ageing processes are all greatly effected by these factors, plus a range of pathological conditions eg corneal dystrophies, uveitis and advanced cataracts. It is hoped that future research will more fully consider the effects of light scatter in the eye on contrast sensitivity and incorporate the results in order to achieve a more complete assessment of vision in the clinical environment, both on simple refractive patients and those with pathological conditions.

APPENDICES

Appendix 1

Calibration of the "Mini-Spot" Hand held Photometer

In order to verify the accuracy of photometric measurements conducted throughout this project with the "Mini Spot" Photometer, a series of 7 luminance values were recorded (range 3.39 to 1,610 cd/m^2) comparing the "Mini-Spot" result (plotted on the x axis) with the UDT 80X optometer with photometric head result (on the y axis) the latter being calibrated against the Bentham M300BA Monochromator -based Computerised telespectroradiometer and photometer system (Bentham Instruments Ltd) which was calibrated with a Hoffman Radiance standard. Fig. A.1 shows the values recorded. By means of linear regression analysis it was calculated that the correct luminances and illuminances were 1.35 times larger than the "Mini-Spot" reading. All such values stated in this project had this calibration correction applied.

Fig. A.1. Calibration of the "Mini-Spot" hand held photometer against the U.D.T. photometer

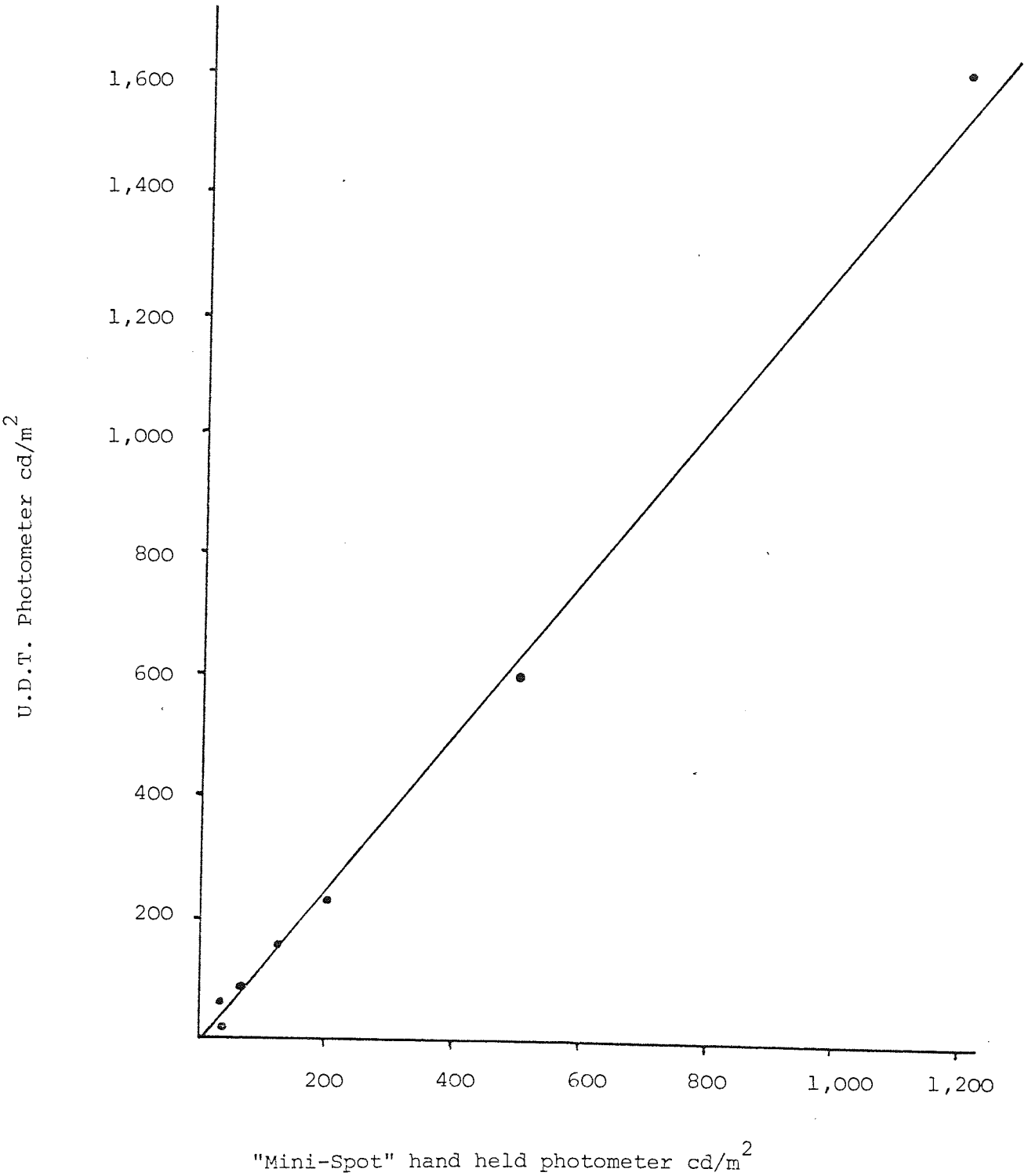

Appendix 2

The Spectral Distributions of the Burton Lamp (Experiment 2) and of the Projected Filter (Experiment 5)

Fig. A.2 shows the spectral distribution for the near UV/blue Burton Lamp output as used to excite ocular fluorogens (Experiment 2). The peak wavelength is at 405nm and confirms the suitability of the Lamp in this study.

Fig. A.3 shows the spectral distribution for the red filter used in the projected gratings system (Experiment 5). The peak wavelength is at 645 nm; this compares to the Retinometer (He -Ne Laser) wavelength of 633 nm.

Both distributions were plotted with the Bentham M300BA Monochromator - based computerised telespectroradiometer and photometer (Bentham Instruments Ltd).

Peak power (rel. mW/nm) 11.5179995490479
Peak wavelength (nm) 405
Peak index 6
Total power (mw rel) 46.6332944370806

CHROMATICITY CIE:9603197E 003

Y% [illegible] candela rel

[illegible]
.0544 .0560 .1468

CCT out of range

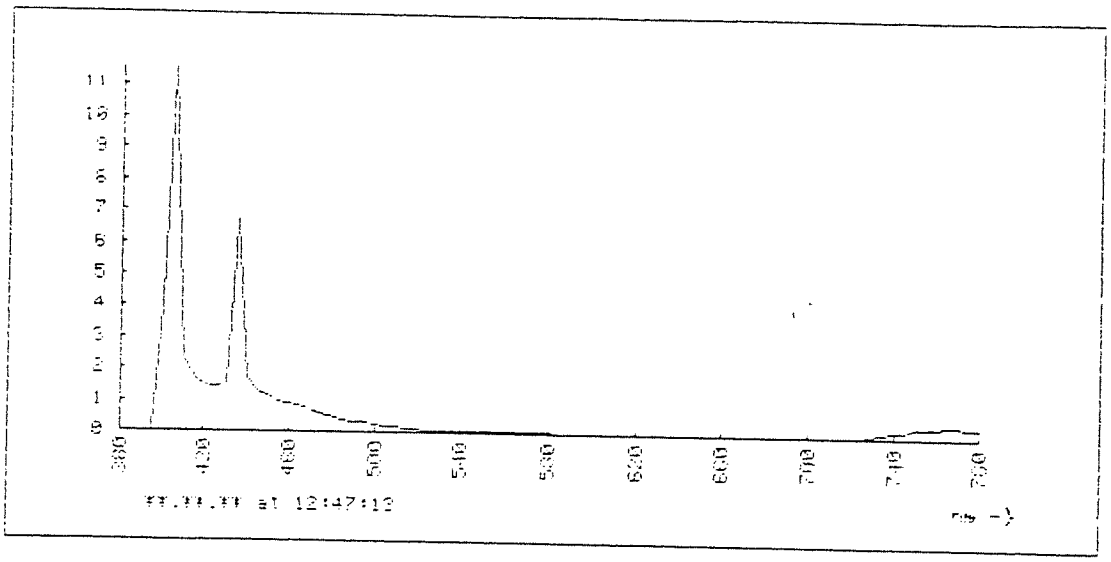

Fig. A.2 Spectral Distribution of the UV/blue Burton Lamp

BENTHAM (C) 1984 CH/3 Rev.(7-85) Software

..**
Peak power (rel. mW/nm) 869.599975585938
Peak wavelength (nm) 645
Peak index 54
Total power (mW rel) 1979.88128727347

CHROMATICITY CIE1960&1976 UCS

Y% 1758 (lux/candela rel)

x .7208 u .5886 u' .5886
y .2783 v .3409 v' .5114

CCT out of range

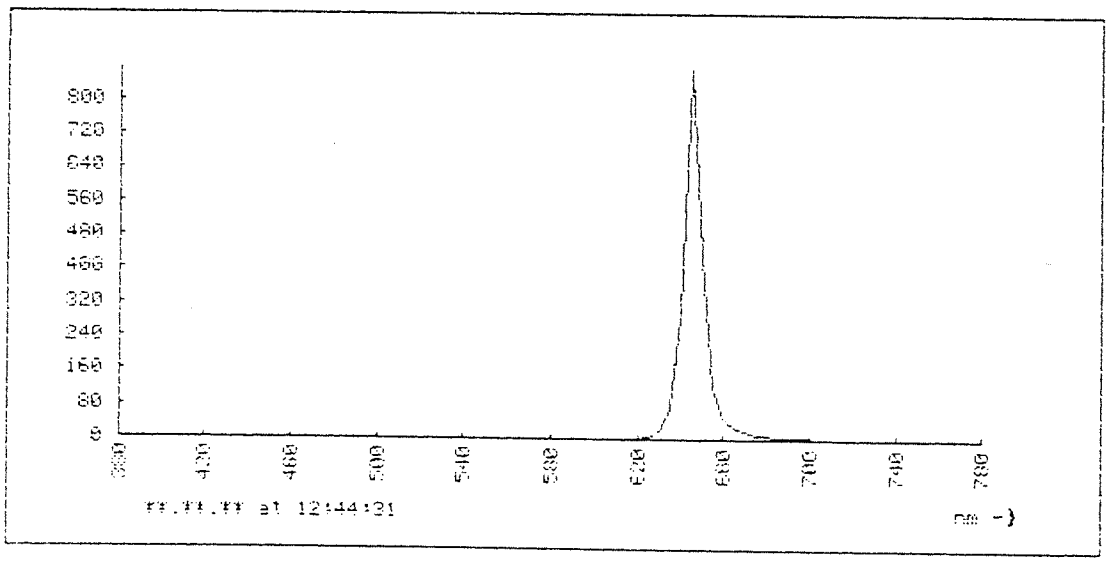

Fig. A.3 Spectral Disbribution of the Red Filter (Experiment 5)

Appendix 3

Instructions and Letters to Subjects

Written instructions 1) 2) and 3) were given to each subject for psychophysical testing when using the Method of Increasing Contrast (MIC) the Bekesy Method and the Method of Decreasing Contrast (MDC) respectively (Experiment 1). Instructions for the MIC were also used in subsequent experiments.

Letter 1 was given to each volunteer member of the public who participated in Experiment 2(ii).

Letter 2 was sent to each contact lens subject who participated in Experiment 4, the replies are summarised in the Listed "Clinical Details."

1) Subject Instructions For MIC

Thank you for participating in this study.

The circular TV screen that you are facing looks blank at the moment, but when you hear a "bleep" a pattern will slowly start to appear. The pattern consists of vertical fuzzy lines that are jumping side-to-side. What you have to do is press the button on the control box when you can just see both the side-to-side movement and the vertical lines. When you do this the pattern will disappear. There will be a short pause and then the next pattern will start to appear. This will happen 4 times.

If you cannot see both the side-to-side movement and the lines do not press the button - wait until you just can.

You will be given trial runs for practice!

Thank you.

2) Subject Instructions for Bekesy

Thank you for participating in this study.

The circular TV screen that you are facing looks blank at the moment, but when you hear a "bleep" a pattern will slowly start to appear. The pattern consists of vertical fuzzy lines that are jumping side-to-side. What you have to do is press the button on the control box when you can just see both the side-to-side movement and the vertical lines and keep your finger down on the button as the pattern now starts fading away. When both the vertical lines and the side-to-side movement have just disappeared take your finger off the button.

There will be a short pause and then the next pattern will start to appear, and you will repeat the exercise. This will happen 4 times.

You will be given trial runs for practice!

Thank you.

3) Subject Instructions for MDC

Thank you for participating in this study.

The circular TV screen that you are looking at has a pattern consisting of vertical fuzzy lines that are jumping side-to-side. When you press the button on the control box the pattern will start to fade away. When both the fuzzy lines and the side-to-side movement have just disappeared release the button. This will cause the pattern to re-appear. When you press the button for the 2nd time the pattern will start to fade again and you will repeat the process a total of 4 times.

You will be given trial runs for practice!

Thank you

ASTON UNIVERSITY

Letter 1

Research into Vision

The aim of this work is to measure normal vision using people over a wide age range and also to consider the effect of bright lights (e.g strip lighting) on eye sight.

The test takes about 1/2 hours, and involves looking at a T.V screen, and pressing a button when a certain pattern is seen. A range of different patterns and lights are used, and you will be shown examples of the patterns before recording begins.

£1.00 will be paid to each person who participates.

Thank You.

STELLA GRIFFITHS

Letter 2

Dear

Recently you took part in a study involving measuring Contrast Sensitivity using glare sources. You were asked to participate because you wore contact lenses.

I would be grateful if you would answer the questions below and return you replies to the Postgraduate pigeon hole in Vision Sciences.

Thank you

Stella Griffiths

Q1 At the time of the study, were the contact lenses that you wore your first and only pair?

- if not, please briefy state your contact lens wearing history including the type of lenses you have worn (ie PMMA, GP or SOFT) and why you changed.

Q2 Please state your current spectacle Rx

R:

L:

Appendix 4

Publications

1. Griffiths S.N., Barnes D.A. and Drasdo N. (1983) Psychophysical aspects of contrast sensitivity attenuation induced by glare. Ophthal. Physiol. Opt. 4:233

2. Griffiths S.N., Barnes D.A., Drasdo N. and Sabell A.G. (1984) The relationship between corneal thickness (with induced oedema) and retinal contrast attenuation using glare sources. Ophthal: Physiol. Opt. 5:236

3. Griffiths S.N. (1984) Passing round the plate - the use of the AO Contrast Sensitivity Test. Optician June 29, Vol. 187: 18-21

4. Griffiths S.N., Drasdo N. and Barnes D.A (1984) A method of measuring the light scattering properties of the cornea and crystalline lens using the contrast sensitivity function. B.C.O.O. The Frontiers of Optometry. 11-14 April Transactions 2: 173-180

5. Griffiths S.N. (1985) The use of induced glare to assess retinal contrast attenuation in contact lens wearers. AVA' 85 - Visual Performance: 11

6. Griffiths S.N., Drasdo N., Barnes D.A. and Sabell A.G. (1986) Effect of epithelial and stromal edema on the light scattering properties of the cornea. Am. J.Optom. (In Press)

Pgs 216 - 236

References

1. Wolff E. (1976) Anatomy of the eye and orbit Lewis, London, UK

2. Adler's Physiology of the eye (1975) 6th Edition Ed. Moses, R.A.Mosby, Saint Louis, USA

3. Physiology of the eye (1980) 4th Edition. Ed. Davson, H. Churchill Livingstone, UK

4. La Tessa A. Teng C. and Katzin H. (1954) The histochemistry of the basement membrane of the cornea. Am. J. Ophthal. 58: 171-180

5. Levenson J. E. (1973) The effect of short term drying on the surface ultrastructure of the rabbit cornea: a scanning electron microscopic study. Ann. Ophthal. 5: 865-878

6. Jakus M. A. (1964) Ocular fine structure. Selected electron micrographs. In Retina Foundation, Inst. Biol. Med. Sci. Monographs and Conferences. Vol. 1 Churchill, London, UK

7. Ruskell G.L. (1980) Anatomy and physiology of the cornea and related structures in Contact Lenses Vol. 1 Ed. Stone J. and Phillips A. J. Butterworths, London, UK

8. Iwamoto T. and Smelser G.K. (1965) Electron microscopy of the human corneal endothelium with reference to transport mechanisms. Invest. Ophthal. 4: 270-284.

9. Kaye G.I. and Pappas G.D. (1962) Studies on the cornea. 1. The fine structure of the rabbit cornea and the uptake and transport of colloidal particles by the cornea in vivo. J. Cell Biol. 12: 457-479.

10. Dikstein S. and Maurice D.M. (1972) The metabolic basis to the fluid pump in the cornea. J. Physiol. 221: 29-41

11. Maurice D. and Giardini A. (1951) Swelling of the cornea in vivo after the destruction of its limiting layers. Br. J. Ophthal. 35: 791-802

12. Harris J. (1960) Transport of fluid from the cornea p.73 in Transparency of the cornea Ed. Duke Elder S. Thomas, Ill, USA

13. Ruben M. (1967) Corneal changes in contact lens wear. Trans. Ophthal. Soc. UK 87: 27-43

14. Farris R.L. Kubota Z. and Mishima S. (1971) Epithelial decompensation with corneal contact lens wear Arch. Ophthal. 85: 651-660

15. Millodot M. (1975) Effect of hard contact lenses on corneal sensitivity and thickness. Acta Ophthal. 53: 576-584

16. Gerstman D.R. (1972) The biomicroscope and Vickers image - splitting eyepiece applied to the diurnal variation in human central corneal thickness. J. Microsc. 96: 385-388

17. Vos J.J. and Bouman M.A. (1964) Contribution of the retina to entopic scatter. J. Opt. Soc Am. 54: 95-100

18. Wolf E. and Gardiner J.S. (1965) Studies on the scatter of light in the dioptric media of the eye as a basis of visual glare. Arch. Ophthal. 74, 338-345.

19. Allen M.J. and Vos J.J. (1967) Ocular scattered light and visual performance as a function of age. Am. J. Optom. 44: 717-727

20. Tanford C. (1961) Physical Chemistry of macromolecules. Wiley, New York, USA

21. Kerker M. (1969) The scattering of light and other electromagnetic radiation. Academic Press, New York, USA

22. Einstein A. (1910) Theory of the opalescence of homogenous liquids and liquid mixtures in the neighbourhood of the critical state. Ann. Phys. 33, 1275-1298.

23. Debye P. (1944) Light scattering in solutions. J. Appl. Phys. 15: 338-342

24. Goldman J. and Benedek G.B. (1967) The relationship between morphology and transparency in the nonswelling corneal stroma of the shark. Invest. Ophthal. 6 574-581

25. Jakus M.A. (1961) The fine structure of the human cornea. In The Structure of the Eye Academic Press, N.Y and London.

26. Maurice D.M. (1957) The structure and transparency of the cornea. J. Physiol. 136: 263-286

27. Hart R.W. and Farrell R.A. (1969) Light scattering in the cornea. J. Opt. Soc. Am. 59: 766-774

28. Benedek G.B. (1971) Theory of transparency of the eye. Appl. Optics 10: 459-473

29. Feuk T. and McQueen D. (1971) The angular dependence of light scattered from rabbit corneas. Invest. ophthal.10: 294-229

30. Kikkawa Y. (1960) Light scattering studies of the rabbit cornea. Jap. J. Physiol. 10:292-301

31. McCally R.L. and Farrell R.A. (1976) The depth dependence of light scattering from the normal rabbit cornea. Exp. Eye. Res. 23: 69-81

32. Lindstrom J.I., Feuk T. and Tengroth B. (1973) The distribution of light scattered from the rabbit cornea Acta Ophthal. 51: 656-69

33. Simpson G.C. (1953) Ocular haloes and coronas Br. J. Ophthal. 37: 450-486

34. Bettelheim F.A. and Vinciguerra M.J. (1971) Laser diffraction patterns of highly ordered superstructures in the lenses of bovine eyes. Ann. N.Y. Acad. Sci. 172: 429 439

35. Philipson B. (1973) Changes in the lens related to the reduction of transparency. Exp. Eye Res. 16: 29-39

36. Benedek G.B., Clark J.I., Serralach E.N., Young C.Y., Mengel L., Sanke T., Bagg A. and Benedek K. (1979) Light scattering and reversible cataracts in the calf and human lens. Philos. Trans R. Soc. London Ser. A. 293-329

37. Clark J.I. Mengel L. and Benedek G.B. (1980) Scanning electron microscopy of opaque and transparent states in reversible calf lens cataracts. Ophthal. Res. 12: 16-33

38. Trokel S.L. (1962) The physical basis for transparency of the crystalline lens. Invest. Ophthal. 1; 493-301

39. Philipson B. (1969) Distribution of protein within the normal cat lens. Invest. Ophthal. 8: 258-270

40. Bettelheim F. A. and Siew E.L. (1982) in Cell Biology of the Eye Ch 6. Biological - Physical basis of lens Transparency. Academic Press, N.Y., USA

41. Mie G. (1908) Optics of turbid media. Ann. Phys. 25 377-445

42. Bettelheim F.A. and Siew E.L (1980) Light scattering and lens morphology in red blood cell and lens metabolism. Dev. Biochem. 9: 443-446

43. Debye P. and Bueche A.M. (1949) Scattering by an inhomogenous solid. J. Appl. Phys. 20: 518-526

44. Bettelheim F.A. (1979) Syneresis and its possible role in cataractogenesis. Exp. Eye Res. 28: 189-197

45. Bettelheim F.A. and Paunovic M. (1979) Light scattering of normal human lenses. I Application of random density and orientation fluctuation theory. Biophys. J. 26: 85-100

46. Bettelheim F.A. (1975) On the optical anisotropy of lens fibre cells. Exp. Eye Res. 21: 231-234

47. Hemenger R.P. (1982) Optical density of the crystalline lens. Am. J. Optom. 59: 34-42

48. Said F.S. and Weale R.A. (1959) The variation with age of the spectral transmissivity of the living human crystalline lens. Gerontologia 3: 213-231

49. Zigman S., Groff J., Yulo T. and Griess G. (1976) Light extinction and protein in the lens. Exp. Eye Res. 23: 555-567

50. Ludvigh E. and McCarthy E.F. (1938) Absorption of visible light by the refractive media of the human eye. Arch. Ophthal. 20: 37-51

51. Bettelheim F.A. and Siew E.L. (1983) Effect of change in concentration upon lens turbidity as predicted by the random fluctuation theory. Biophys. J. 41: 29-33

52. Lerman S. (1980) Radiant energy and the eye MacMillan N.Y, USA

53. Walls G.L. and Judd H.D. (1933) Intra-ocular colour filters of vertebrates. Br. J. Ophthal. 17: 641-703

54. Wald G. (1952) Alleged effects of the near ultraviolet on human vision. J. Opt. Soc. Am. 42: 171-177

55. Borkman R.F. and Lerman S. (1978) Fluorescence spectra of tryptophan residues in human and bovine lens protein. Exp. Eye. Res. 26: 705-713

56. Lerman S. (1976) Lens fluorescence in ageing and cataract formation. Doc. Ophthal. Proc. Series 8: 241-260

57. Stocker F.W. and Moore L.W. (1975) Detecting changes in the cornea that come with age. Geriatrics 30: 57-69

58. Boettner E.A. and Woltner J. R. (1962) Transmission of the ocular media. Invest. ophthal. 1:776-782

59. Pau H. (1955) Die Doppelbrechung van Sklera und Cornea. Klin. Monatsbl. Augenheilkd. 131: 610-615

60. Laing R. A., Sandstrom M.M. and Leibowitz H.M. (1979) Clinical specular microscopy. II Qualitative evaluation of corneal endothelial photomicrographs. Arch. Ophthal. 97: 1720-1725

61. Weale R.A. (1982) A Biography of the Eye Lewis H.K. and Co. Ltd, London, UK

62. Maurice D.M. (1962) Distribution and movement of plasma protein in the cornea. J. Physiol. 162: 2P

63. Klang G. (1948) Measurements and studies of the fluorescence of the human lens in vivo. Acta Ophthal. Suppl. 31

64. Broekhuyse R.M. (1975) The lipid composition of ageing sclera and cornea. Ophthalmologica 171: 82-85

65. McAndrew G.M. and Ogston D. (1965) Arcus senilis in middle aged men. Br. Med. J. 1: 425-427

66. Olsen T. (1982) Light scattering from the human cornea. Invest. Ophthal. 23: 81-86

67. Cinotti A.A. and Patti J.C. (1968) Lens abnormalities in an ageing population of nonglaucomatous patients. Am. J. Ophthal. 66: 25-32

68. Wolf E. (1960) Glare and age. Arch. Ophthal. 64: 502-514

69. Hess R.F. and Woo G. (1978) Vision through cataracts. Invest Ophthal. 17: 428-435

70. Goldmann H. (1964) Senile changes of the lens and vitreous. Am. J. Ophthal. 57: 1-13

71. Hoenders H.J. and Van Kamp G.J. (1972) Eye lens development and ageing processes of crystallins. Acta Morphol. Neerl. Scand. 10: 215-221

72. Spector A., Li L.K. and Sigelman J. (1974) Age - dependent changes in the molecular size of human lens protein and their relationship to light-scatter. Invest. Ophthal. 13: 795-798

73. Jedziniak J., Kinoshita J.H., Yates E.M. and Benedek G.B. (1975) The concentration and localisation of heavy molecular weight aggregates in ageing normal and cataractous human lenses. Exp. Eye. Res 20: 367-369

74. Harding J.J. and Dilley V.J. (1976) Structural proteins of the mammalian lens. A review with emphasis on changes in development, ageing and cataract. Exp. Eye. Res 22: 1-73

75. Kramps H.A., Stols A.L.H., Hoenders H.J. and deGroot K. (1975) On the quaternary structure of high molecular weight proteins from the bovine eye lens. Eur. J. Biochem. 50: 503-509

76. Tanaka T., Ishimoto C. and Chylack L.T. (1977) Phase seperation of a protein and water mixture in cold cataract in the young rat lens. Science 197: 1010-1012

77. Lowenstein M.A., and Bettelheim F.A. (1979) Cold cataract formation in fish lenses. Exp. Eye. Res. 28: 651-663

78. Kinoshita J.H. (1965) Cataracts in glactosemia. Invest. Ophthal. 4: 786-799

79. Philipson B. (1969) Light scattering in lenses with experimental cataract. Acta Ophthal. 47: 1089-1101

80. Miller D. and Benedek G. (1978) Intraocular light scattering. Thomas C.C., Springfield, USA

81. Finkelstein I.S. (1952) Part II. The biophysics of corneal scatter and diffraction of light induced by contact lenses. Am. J. Optom. Arch. Am. Acad. Optom. 29: 231-259

82. Stevenson R., Vaja N. and Jackson J. (1982) Corneal transparency changes resulting from osmotic stress. Ophthal. Physiol. Opt. 3: 33-39

83. Remole A. (1981) Effect of saline solution emmersion on corneal scattering characteristics. Am. J. Optom. Phys. Opt. 58: 435-444

84. Twersky V. (1975) Transparency of pair correlated, random distributions of small scatterers, with applications to the cornea. J. Opt. Soc. Am. 65: 524-530

85. Farrell R.A. and McCally R.L. (1975) On corneal transparency and its loss with swelling. J. Opt. Soc. Am 66: 342-354

86. Duncan G. (1981) Mechanisms of cataract formation in the human lens. Academic Press, London, UK

87. Pirie A. (1968) Colour and solubility of the proteins of human cataracts. Invest. Ophthal. 7: 634-340

88. Marcantonio J.M., Duncan G., Bushell A.R. and Davies P.D. (1980) Classification of human senile cataracts by nuclear colour and sodium content. Exp. Eye. Res. 31: 227-237

89. Hess R.F. and Garner L.F. (1977) The effect of corneal edema on visual function. Invest. Ophthal. 16: 5-13

90. Hess R.F. and Carney L.G. (1979) Vision through an abnormal cornea; a pilot study of the relationship between visual loss from corneal distortion, corneal edema, keratocous and some allied corneal pathologies. Invest. Ophthal. 18: 476-483

91. Lambert S.R. and Klyce S.D. (1981) The origins of Satler's veil. Am. J. Ophthal. 91: 51-56

92. Lovaskik J.V. and Remole A. (1983) An instrument for mapping corneal light-scattering characteristics. Ophthal. Physiol. Opt. 3: 247-254

93. Siegelman J., Trokel S.L. and Spector A. (1974) Quantitative biomicroscopy of lens light back scatter. Arch. Ophthal. 92: 437-442

94. Ben-Sira I., Weinberger D., Bodenheiner J. and Yassur Y. (1980) Clinical method for measurement of light backscattering from the in vivo human lens. Invest. Ophthal. 19: 435-437

95. Chylack L.T. (1978) Classification of human cataracts. Arch. Ophthal. 96: 888-892

96. Lerman S., Hockwin O. and Dragomirescu V. (1981) UV-visible slit lamp desitography of the human eye. Exp. Eye Res. 33: 587-596

97. Vos J.J. (1962) On mechanisms of glare. Institute for perception RVO-TNO, Soesterberg. Netherlands

98. Paulsson L.E. and Sjostrand J. (1980) Contrast sensitivity in the presence of a glare light. Invest. Ophthal. 19: 401-406

99. Hopkinson R.G. and Collins J.B. (1970) The ergonomics of lighting. p.80-104. Macdonald, London, UK

100. Holladay L.L. (1926) The fundamentals of glare and visibility. J. Opt. Soc. Am. 12: 492-531

101. Vos J.J. and Boogard J. (1963) Contribution of the cornea to entoptic scatter. J. Opt. Soc. Am. 54: 110-115

102. Vos J.J, Walraven J. and Van Meeteren A. (1976) Light profiles of the foveal image of a point source. Vis. Res. 16: 215-219

103. Demott D.W. and Boynton R.M. (1958) Retinal distribution of entoptic stray light. J. Opt. Soc. Am. 48: 13-30

104. Boynton R.M. and Clark F.J.J. (1964) Sources of entoptic scatter in the human eye. J. Opt. Soc. Am. 54: 110-117

105. Sturgis S.P. and Osgood D.J. (1982) Effects of glare and background luminance on visual acuity and contrast sensitivity: Implications for driver night vision testing. Human factors 24: 347-360

106. Miller D. and Miller R. (I981) Glare sensitivity in simulated radial keratotomy. Ophthal. 99: 1961-1962

107. Nadler D.J., Jaffe N.S., Clayman H.M., Jaffe M.S. and Luscombe S.M. (1984) Glare disability in eyes with intraocular lenses. Am. J. Ophthal. 97: 43-47

108. Van der Heijde G.L., Weber J. and Boukes R. (1985) Effects of stray light on visual acuity in pseudophakia. Doc. Ophthal. 59: 81-84

109. Hirsch R.P., Nadler M.P. and Miller D. (1984) Glare measurement as a predictor of outdoor vision among cataract patients. Annals Ophthal. 16: 965-968

110. Le Claire J., Nadler M.P., Weiss S. and Miller D. (1982) A new glare tester for clinical testing. Arch. Ophthal. 100: 153-158

111. Hubel D.H. (1963) The visual cortex of the brain. Sci. Am. 209 54-62

112. Barlow H.B., Fitzhugh R. and Kuffler S.W.J. (1957) Dark adaptation, absolute threshold and Purkinje shift in single units of the cat's retina. J. Physiol. 137: 327-337

113. Sekuler R. (1974) Spatial vision. Ann. Rev. Psychol. 25: 195:232

114.. Hubel D.H. (1982) Exploration of the primary visual cortex, 1955-78. Nature 299: 515-524

115. Wiesel T.N. (1982) Postnatal development of the visual cortex and the influence of environment. Nature 299: 583-591

116. Ikeda H. and Wright M.J. (1974) Is amblyopia due to inappropriate stimulation of the "sustained" pathway during development? Br. J. Ophthal. 58: 165-175

117. Derrington A.M. and Fuchs A.F. (1979) Spatial and temporal properties of X and Y cells in the cat lateral geniculate nucleus. J. Physiol. 293: 347-364

118. Movshon J.A., Thompson I.D. and Tolhurst D.J. (1978) Spatial and temporal contrast sensitivity of neurones in areas 17 and 18 of the cat's visual cortex . J. Physiol. 283: 101-120

119 Bodis-Wollner I.and Camisa J.M. (1980) Contrast sensitivity measurement in clinical diagnosis. In Neuro-ophthalmology Vol. 1. P.373-401, Harper and Row, N.Y, USA

120. Green M. (1981) Psychophysical relationships among mechanisms sensitive to pattern, motion and flicker. Vis. Res. 21: 971-983

121. Kulikowski J.J. and Tolhurst D.J. (1973) Psychophysical evidence for sustained and transient detectors in human vision. J. Physiol. 232: 149-162

122. Robson J.G. (1966) Spatial and temporal contrast sensitivity functions of the visual system. J. Opt. Soc. Am. 56: 1141-1142

123. Sperling G. (1964) Linear theory and the psychophysics of flicker. Proc. Symp. Physiology of flicker Docum. ophthal. 18: 3-15

124. Schade O.H. (1956) Optical and photoelectric analog of the eye. J. Opt. Soc. Am. 46.721-739

125. Kelly D.H. (1977) Visual contrast sensitivity. Optica Acta 24: 107-129

126. Campbell F.W. and Maffei L. (1974) Contrast and spatial frequency. Sci. Amer. 231: 106-111

127. Arden G.B. (1978) The importance of measuring contrast sensitivity in cases of visual disturbance. Br. J. Ophthal. 62:198-209

128. Abadi R.V. (1974) Visual analysis with gratings. Brit J. Physiol. Opt: 47-56

129. Campbell F.W. and Robson J.G. (1968) Application of Fourier analysis to the visibility of gratings. J. Physiol. 197: 551-566

130. Campbell F.W. and Green D.G. (1965) Optical and retinal factors affecting visual resolution. J. Physiol. 181: 576-593

131. Levi D.M. and Harworth R.S. (1977) Spatio-temporal interactions in anisometropic and strasbismic ambyopia. Invest.Ophthal. 16: 90-95

132. Thomas J. (1978) Normal and amblyopic contrast sensitivity functions in central and peripheral retinas. Invest.Oophthal. 17: 746-753

133. Sjostrand J. (1978) Contrast sensitivity in amblyopia: a preliminary report. Metabol. Ophthal. 2: 135-137

134. Hoekstra J., Van der Groot D.P.J., Van der Brink G. and Bilsen F.A. (1974) The influence of the number of cycles upon the visual contrast threshold for spatial sine wave patterns. Vis. Res. 14: 365-368

135. Rovamo J., Virsu V. and Nasenen R. (1978) Cortical magnification factor predicts the photopic contrast sensitivity. Nature 271: 54-56

136. Rovamo J., and Virsu V. (1979) An estimation and application of the human cortical magnification factors. Exp. Brain Res. 37: 495-510

137. Bodis-Wollner I. (1980) Detection of visual defects using the contrast sensitivity function. Int. Ophthalmol. Clinic 20: 135-155

138. Kulilowski J.J. (1971) Some stimulus parameters affecting spatial and temporal resolution of human vision. Vis. Res. 11: 83-93

139. Kelly D.H. (1975) How many bars makes a grating? Vis. Res. 15: 625-626

140. Banks M.S. and Salapatek P. (1976) Contrast sensitivity function of the infant visual system. Vis. Res. 16: 867-869

141. Savoy R.L. and McCann J.J. (1975) Visibility of low spatial frequency targets: dependence on number of cycles. J. Opt. Soc. Am. 65: 343-350

142. Arden G.B. (1978) Visual loss in patients with normal visual acuity. Trans. Ophthal. Soc. UK 98: 219-231

143. Robson J.G. (1966) Spatial and temporal contrast sensitivity functions of the visual system. J. Opt. Soc. Am. 56: 1141-1142

144. Campbell F.W. (1979) The transmission of spatial information through the visual system. In The Neurosciences Ed. Schmitt F.O. and Wordon F.G, M.I.T. Press, Mass., USA

145. Campbell F.W. (1980) Recent advances in visual physiology. Ophthal. Opt 26/4/80 : 301-308

146. Regan D., Silver R. and Murray T.J. (1977) Visual acuity and contrast sensitivity in multiple sclerosis-hidden visual loss. Brain 97: 563-579

147. Bodis-Wollner I. and Diamond S. (1976) The measurement of spatial contrast sensitivity in cases of blurred vision associated with cerebral lesions. Brain. 99: 695-710

148. Maffei L. and Fiorentini A. (1973) The visual cortex as a spatial frequency analyser. Vis. Res. 13: 1255-1267

149. Charman W.N. (1979) Effect of refractive error in visual tests with sinusoidal gratings. Brit. J. Physiol. Opt. 33: 10-20

150. Green D.G. and Campbell F.W. (1965) Effect of focus on the visual response to a sinusidally modulated spatial stimulus. J. Opt. Soc. Am. 55: 1154-1157

151. Campbell F.W. (1957) The depth of field of the human eye. Optica Acta 4: 157-164

152. Fiorentini A. and Maffei L. (1976) Spatial contrast sensitivity of myopic subjects. Vis. Res. 16: 437-438

153. Hilz R., Rentschler I. and Brettel H. (1977) Myopic and strabismic ambhyopia: substantial differences in human visual development. Exp. Brain Res. 30: 445-446

154. Enoch J.M., Ohzu H. and Itoi M. (1979) Contrast (modulation) sensitivity functions measured in patients with high refractive error with emphasis on aphakia: I Theoretical considerations. Docum. Ophthal. 55: 139-145

155. Campbell F.W. and Gregory A.H. (1960) Effect of size of pupil on visual acuity. Nature 187: 1121-1123

156. Woodhouse J.M. (1975) The effect of pupil size on grating detection at various contrast levels. Vis. Res. 15: 645-648

157. Westheimer G. (1960) Modulation threshold for sinusoidal light distributions on the retina. J. Physiol. 152: 67-75

158. Clinical applications of visual psychophysics. Part I. Contrast Sensitivity 1981 Ed. Proenza L.M., Enoch J.M. and Jampolsky A. Cambridge University Press, London, UK

159. Applegate R.A. and Massof R.W. (1975) Changes in the contrast sensitivity function induced by contact lens wear. Am. J. Optom. 52: 840-846

160. Woo G.C. and Hess R. (1979) Contrast sensitivity function and soft contact lenses. Internat. Contact lens Clinic 6: 37-42

161. Mitra S. and Lamberts D.W. (1981) Contrast sensitivity in soft lens wear. Contact and Intraocular lens Medical Journal 7: 315-322

162. Kirkpatrick D.L. and Roggenkamp J.R. (1985) Effects of soft contact lenses on contrast sensitivity. Am. J. Optom. 62: 407-412

163. Tomlinson A. and Mann G. (1985) An analysis of visual performance with soft contact lenses and spectacle correction. Ophthal. Physiol Opt. 5: 53-57

164. Bernstein I.H. and Brodrick J. (1981) Contrast sensitivities through spectacles and soft contact lenses. Am. J. Optom. 58: 309-313

165. Sjostrand J. and Frisen L. (1977) Contrast sensitivity in macular disease. Arch .Ophthal. 55: 507-514

166. Atkin A., Bodis-Wollner I., Wolkstein M.,Moss A. and Podos S. (1979) Abnormalities of central contrast sensitivity in glaucoma. Am. J. Ophthal. 88: 205-211

167. Hess R.F. (1979) Contrast sensitivity assessment of functional amblyopia in humans. Trans. Ophthal. Soc. UK 99: 391-397

168. Skalka H.W. (1980) Effect of age on Arden grating acuity. Br. J. Ophthal. 64: 21-23

169. Vaegan B. and Halliday B.L. (1982) A forced choice test improves clinical contrast sensitivity testing. Br. J. Ophthal. 66: 477-491

170. McGrath C. and Morrison J.D. (1983) The effect of age on spatial frequency perception in human subjects QJ Exp Physiol 66: 253-261

171. Arundale K.L (1978) An investigation into the variation of human contrast sensitivity with age and ocular pathology. Br. J. Ophthal. 62: 213-215

172. Derefeld E.G., Lennerstrand G. and Lundh B. (1979) Age variations in normal human contrast sensitivity. Acta Ophthal. 57: 679-690

173. Owsley C., Sekular R., and Siemsen D. (1983) Contrast sensitivity throughout adulthood. Vis. Res. 23: 689-699

174. Sokol S., Domar A., and Moskowitz A. (1980) Utility of the Arden grating test in glaucoma screening; high false positive rate in normals over 50 years of age. Invest. Ophthal. 19: 1529-1533

175. Ross J.E., Clarke D.D. and Bron A.J. (1985) Effect of age on contrast sensitivity function: uniocular and binocular findings. Br. J. Ophthal. 69: 51-56

176. Wright C.E. and Drasdo N. (1985) The influence of age on the spatial and temporal contras sensitivity function. Doc. Ophthal. 59: 385-395

177. Sekular R. and Hutman L.P. (1980) Spatial vision and ageing. I. Contrast sensitivity. J. Gerontol. 35: 692-699

178. Zuckerman J.L., Miller D., Dyes W. and Keller M. (1973) Degradation of vision through a simulated cataract. Invest. Ophthal. 12: 213-224

179. Hess R.F. and Woo G.C. (1978) Vision through cataracts. Invest. Ophthal. 17: 428-435

180. Ohzu H. (1976) Application of lasers in ophthalmology and vision research. Mem. Sch. Sci. Eng. 40: 1-28

181. Dressler M. and Rassow B. (1982) Neural contrast sensitivity measurements with a laser interference system for clinical and scientific screening application. Invest. Ophthal. 21: 737-744

182. Kayazawa F., Yamamoto T. and Itoi M. (1981) Clinical measurement of contrast sensitivity function using laser generated sinusoidal grating. Jpn. J. Ophthal. 25: 229-236

183. Enoch J.M. and Hope G.M. (1973) Inteferometric resolution determinations in the fovea and parafovea. Doc. Ophthal. 34: 143-156

184. Williams D.R. (1985) Visibility of interference fringes near the resolution limit. J. Opt. Soc. Am.A 2: 1087-1093

185. Kayazawa F., Yamamoto T. and Itoi M. (1982) Contrast sensitivity measurment in retinal diseases by laser generated sinusoidal grating. Acta Ophthal. 60: 511-524

186. Green D.G. (1970) Testing the vision of cataract patients by means of laser-generated interference fringes. Science 168: 1240-1242

187. Green D.G. and Cohen M.M. (1971) Laser interferometry in the evaluation of potential macular function in the presence of opacities of the ocular media. Trans. Am. Acad. Ophthal. Otolary. 75: 629-637

188. Goldmann H. and Lotmar W. (1969) Beitrag zum Problem der Bestimmung der retinalen Sehschafe bei Patientern mit Katarakt. Klinisch. Mld. Augenheilk 171: 643-650

189. Gstalder R.J. and Green D.G. (1971) Laser interferometric acuity in amblyopia. J. Pediatric Ophthal. 8: 251-256

190. Comerford J.P. (1979) Contrast sensitivity functions for clinical optometry. J. Am. Optometric Ass. 50: 683-686

191. Comerford J.P. (1982) Vision evaluation using contrast sensitivity functions. Am. J. Optom. 60: 394-398

192. Woodhouse J.M. (1983) Practical applications of the contrast sensitivity function. Ophthal. Physiol. Opt. 3: 311-314

193. Vaegan B. (1979) The clinical value of printed contrast sensitivity tests. Proc. J Physiol Soc. 300: 76P

194. Yap M., Grey C., Collinge A. and Hurst M. (1985) The Arden Gratings in optometric practice. Ophthal. Physiol Opt 5: 179-183

195. Skalka H.W. (1981) Arden grating test in evaluating 'early' posterior subcapsular cataracts. Southern Med. J. 74: 1368-1370

196. Griffiths S.N., Drasdo N., Barnes D.A. and Sabell A.G. (1986) The effect of epithelial and stromal edema on the light scattering properties of the cornea. Am. J. Optom. (In press)

197. Operation Manual, Nic-Optonics CS 2000, (1982) Contrast Sensitivity Testing System; Nicolet Biomedical Instruments Wisconsin, USA

198. Sekuler R. and Tynan P. (1977) Rapid measurement of Contrast Sensitivity functions. Am. J. Optom. 54: 573-575

199. Ginsburg A.P. and Cannon M.W. (1983) Comparison of 3 methods for rapid determination of threshold contrast sensitivity. Invest. Ophthal. 24: 793-802

200. Griffiths S.N., Barnes D.A. and Drasdo N. (1984) Psychophysical aspects of contrast sensitivity attenuation in the presence of glare light. Ophthal. Physiol. Opt. 4: 180

201. Operation Manual, Rodenstock Retinometer. (1984) Rodenstock instrumente, Munchen 70, Germany.

202. Van den Berg T.J.T.P. (1986) Importance of pathological intraocular light scatter for visual disability. Doc. Ophthal. 61: 327-333

203 Mishima S. and Hedbys B.O. (1968) Measurement of corneal thickness with the Haag-Streit Pachometer. Arch. Ophthal. 80: 710-713

204 Brown V. A. and Woodhouse J.M. (1986) Assessment of techniques for measuring contrast sensitivity in children. Ophthal. Physiol. Opt. 6:165-170

205 Lakowski R. and Oliver K. (1974) Effect of pupil diameter on colour vision test performance. Mod. Probl. Ophthal. 13:307-311

206. Campbell F.W. and Gubisch R.W. (1966) Optical quality of the human eye. J.Physiol. 186: 558-578

207. Weale R.A. (1985) Human lenticular fluorescence and transmissivity, and their effects of vision. Exp. Eye. Res. 41: 457-473

208. Koetting R.A. (1976) The influence of oral contraceptives on contact lens wear. Am. J. Optom. 43: 268-274

209. Arnulf M.A. and Dupuy M.O. (1960) La transmission des contrastes par le systeme optique de L'oeil et les seuils de contrastes retines.C.R. Acad. Sci. Paris 205: 2757-2759